

EXTRACTION OF AUDITORY EVOKED POTENTIALS FROM ONGOING EEG

A THESIS SUBMITTED TO
THE GRADUATE SCHOOL OF NATURAL AND APPLIED SCIENCES
OF
MIDDLE EAST TECHNICAL UNIVERSITY

BY

SERAP AYDIN

IN PARTIAL FULFILLMENT OF THE REQUIREMENTS
FOR
THE DEGREE OF DOCTOR OF PHILOSOPHY
IN
ELECTRICAL AND ELECTRONICS ENGINEERING

SEPTEMBER 2005

Approval of the Graduate School of Natural and Applied Sciences

Prof. Dr. Canan Özgen
Director

I certify that this thesis satisfies all the requirements as a thesis for the degree of Master of Science.

Prof. Dr. İsmet Erkmen
Head of Department

This is to certify that we have read this thesis and that in our opinion it is fully adequate, in scope and quality, as a thesis for the degree of Master of Science.

Prof. Dr. Buyurman Baykal
Co-advisor

Prof. Dr. Nevzat Güneri Gençer
Supervisor

Examining Committee Members

Prof. Dr. Kemal Leblebicioğlu	(METU, EEE)	_____
Prof. Dr. Nevzat Güneri Gençer	(METU, EEE)	_____
Prof. Dr. Buyurman Baykal	(METU, EEE)	_____
Prof. Dr. Pekcan Ungan (Hacettepe Univ., Medical F.)		_____
Ass. Prof. Yeşim Serinağaoğlu	(METU, EEE)	_____

I Nearby declare that all information in this document has been obtained and presented in accordance with academic rules and ethical conduct. I also declare that, as required, I have fully cited and referenced all material and results that are not original to this work.

Name Lastname : SERAP AYDIN

Signature :

ABSTRACT

EXTRACTION OF AUDITORY EVOKED POTENTIALS FROM ONGOING EEG

Aydın, Serap

Ph.D., Department of Electrical and Electronics Engineering

Supervisor: Prof. Dr. Nevzat Güneri Gençer

Co-Advisor: Prof. Dr. Buyurman Baykal

September 2005, 89 pages

In estimating auditory Evoked Potentials (EPs) from ongoing EEG the number of sweeps should be reduced to decrease the experimental time and to increase the reliability of diagnosis. The first goal of this study is to demonstrate the use of basic estimation techniques in extracting auditory EPs (AEPs) from small number of sweeps relative to ensemble averaging (EA). For this purpose, three groups of basic estimation techniques are compared to the traditional EA with respect to the signal-to-noise ratio(SNR) improvements in extracting the template AEP. Group A includes the combinations of the Subspace Method (SM) with the Wiener Filtering (WF) approaches (the conventional WF and coherence weighted WF (CWWF)). Group B consists of standard adaptive algorithms (Least Mean Square (LMS), Recursive Least Square (RLS), and one-step Kalman filtering (KF)). The regularization techniques (the Standard Tikhonov Regularization (STR) and the Subspace Regularization (SR) methods) forms Group C. All methods are tested in simulations and pseudo-simulations which are performed with white noise and EEG measurements, respectively. The same methods are also tested with experimental AEPs. Comparisons based on the output signal-to-noise ratio (SNR) show that: 1) the KF and STR methods are the best methods among the algorithms tested in this study, 2) the SM can reduce the large amount of the background EEG noise from the raw data, 3) the LMS and WF algorithms show poor performance compared to EA. The SM should be used as

a pre-filter to increase their performance. 4) the CWWF works better than the WF when it is combined with the SM, 5) the STR method is better than the SR method. It is observed that, most of the basic estimation techniques show definitely better performance compared to EA in extracting the EPs. The KF or the STR effectively reduce the experimental time (to one-fourth of that required by EA). The SM is a useful pre-filter to significantly reduce the noise on the raw data. The KF and STR are shown to be computationally inexpensive tools to extract the template AEPs and should be used instead of EA. They provide a clear template AEP for various analysis methods. To reduce the noise level on single sweeps, the SM can be used as a pre-filter before various single sweep analysis methods.

The second goal of this study is to present a new approach to extract single sweep AEPs without using a template signal. The SM and a modified scale-space filter (MSSF) are applied consecutively. The SM is applied to raw data to increase the SNR. The less-noisy sweeps are then individually filtered with the MSSF. This new approach is assessed in both pseudo-simulations and experimental studies. The MSSF is also applied to actual auditory brainstem response (ABR) data to obtain a clear ABR from a relatively small number of sweeps. The wavelet transform coefficients (WTCs) corresponding to the signal and noise become distinguishable after the SM. The MSSF is an effective filter in selecting the WTCs of the noise. The estimated single sweep EPs highly resemble the grand average EP although less number of sweeps are evaluated. Small amplitude variations are observed among the estimations. The MSSF applied to EA of 50 sweeps yields an ABR that best fits to the grand average of 250 sweeps. We concluded that the combination of SM and MSSF is an efficient tool to obtain clear single sweep AEPs. The MSSF reduces the recording time to one-fifth of that required by EA in template ABR estimation. The proposed approach does not use a template signal (which is generally obtained using the average of small number of sweeps). It provides unprecedented results that support the basic assumptions in the additive signal model.

Keywords: Auditory Evoked Potential, Adaptive filtering, Tikhonov regularization, Wavelet Transform

ÖZ

SÜREGİDEN EEG SİNYALİNDEN İŞİSEL UYARILMIŞ POTANSİYELLERİNİN ELDE EDİLMESİ

Aydın, Serap

Doktora, Elektrik-Elektronik Mühendisliği Bölümü

Tez Yöneticisi: Prof. Dr. Nevzat Güneri Gençer

Yardımcı Danışman: Prof. Dr. Buyurman Baykal

Eylül 2005, 89 sayfa

Devam eden EEG sinyalinden, az sayıda kayıt kullanılarak örnek Uyarılmış Potansiyel (UP) bilgisinin elde edilmesi, klinik uygulamalarda kayıt süresinin azaltılması ve tanı güvenilirliğinin arttırması için gereklidir. Bu tez çalışmasındaki ilk amaç, az sayıda tekrardan örnek işitsel UP (IUP) elde edilmesinde geleneksel Ortalama Alma (OA) yöntemi ile temel doğrusal tahmin tekniklerinin kıyaslanmasıdır. Bu amaçla yöntemler kavramsal olarak gruplandırılmıştır. Grup A, üç yöntem içerir: 1) Literatürde yeralan ve Wiener Süzgeç (WS) ile Altuzay Yöntemi (AY)'nin birleştirilmesini öneren yöntem, 2) WS ile AY'nin uygulama sırasının değiştirilmesiyle oluşturulan yöntem, 3) Birinci yöntemde WS yerine yinelemeli bir WS kullanılarak oluşturulan yöntem. Grup B, uyarlanır Enküçük Ortalama Kare (EOK) ve Geribeslemeli Enküçük Kareler (GEK) süzgeç ile Kalman süzgeç (KS) uygulamalarını içerir. Yanısıra, EOK süzgeç, AY ile birleştirilerek de uygulanmıştır. Grup C, geriplan EEG gürültüsünün ikinci dereceden istatistiksel bilgisini kullanan Standart Tikhonov Düzenleme (STD) ile Altuzay Düzenleme (AD) yöntemlerini kapsar. Performans ölçütü olarak sinyal-gürültü-oranı (SGO) kullanılmıştır. Yaklaşık - 5 dB civarında olan giriş SGO değeri, AY kullanılarak 20 dB'ye kadar arttırılabilmektedir. AY yönteminin sağladığı bir başka avantaj da tek kayıtlar üzerindeki EEG gürültüsünün karakteristiğini beyaz gürültüye yaklaştırmasıdır. Bu yüzden AY'nin bir

ön-süzgeç olarak kullanılması, WS yaklaşımlarının ve EOK süzgecin performanslarını arttırmıştır. Deneysel ve yapay verilerle sözügeçen üç grup yöntemin kıyaslanması sonucunda deney süresinin KS ya da STD yöntemleri ile yaklaşık dörtte bir oranında kısaltılabildiği görülmüştür.

Tezin ikinci amacı, referans sinyal kullanılmadan tek kayıt IUP bilgisinin elde edilmesinde yeni bir yöntem önerilmesidir. Tek kayıt UP bilgisinin elde edilmesi, tanı için yeni veriler sağlayabilir. Bu amaçla, tek deneyden IUP tahmini için AY ile Değiştirilmiş Ölçek-Uzay Süzgeç (DOUS) ardarda birbirinden bağımsız olarak uygulanmıştır. AY kullanılarak kaba veride SGO artışı sağlanır. Az gürültülü tek kayıtlar DOUS'den geçirilir. Önerilen yeni yaklaşımla elde edilen tek kayıt gerçek IUP tahminleri büyük ortalamayı yakından izler. Sağlıklı kişilerin verileri kullanıldığında, beklenildiği gibi düşük genlik değişimleri gözlenmiştir. Sinyalin ve gürültünün Dalgacık Dönüşümü katsayıları, AY kullanıldığında ayırtebilebilir hale gelir. 50 kaydın ortalamasına DOUS uygulandığında işitsel beyin sapı yanıtı (250 kaydın ortalaması) elde edilebilmiştir. DOUS kullanılarak beyin sapı yanıtının elde edilmesinde kayıt süresi OA yöntemine göre beşte biri oranında azaltılmıştır. Önerilen yeni yaklaşım, tek kayıt IUP tahmininde etkili bir yöntemdir ve bir referans sinyal (genelde az sayıda deneyin ortalaması alınarak elde edilir) bilgisine ihtiyaç duymaz. Elde edilen yeni sonuçlar, toplanırlık sinyal UP modelinde kabul edilen varsayımları doğrular.

Anahtar sözcükler: İşitsel uyarılmış potansiyel, uyarlanır süzgeç, Tikhonov düzenleme yaklaşımı, dalgacık dönüşümü.

ACKNOWLEDGMENTS

I would like to thank my advisor Prof. Dr. Nevzat Güneri Gençer for his encouragement and support to me during all phases of this work. I would also like to thank my co-advisor Prof. Dr. Buyurman Baykal for his support to this work.

I wish to express my thanks to Prof. Dr. Pekcan Urgan and Ass. Prof. Dr. Süha Yağcıoğlu from Hacettepe University for providing me with the real data and valuable suggestions.

Special thanks also go to my family for giving me the motivation to work on this thesis. They helped me keep my confidence level high.

TABLE OF CONTENTS

PLAGIARISM	iii
ABSTRACT	iv
ÖZ	vi
ACKNOWLEDGEMENTS	viii
TABLE OF CONTENTS	ix
LIST OF TABLES	x
LIST OF FIGURES	xi
CHAPTER	
1 INTRODUCTION	1
1.1 Characteristics of EEG and EPs	1
1.2 Extraction of EPs from ongoing EEG	4
1.3 The Scope of the Thesis	9
1.4 The Significance of the Thesis	9
1.5 The Thesis Organization	9
2 COMPARISON OF BASIC ESTIMATION TECHNIQUES IN EX- TRACTING TEMPLATE AUDITORY EP	11
2.1 The Subspace Method	12
2.2 Group A: The Subspace Method in combination with Wiener Filtering Approaches	13
2.2.1 Conventional Wiener Filtering	14
2.2.2 Coherence Weighted Wiener Filtering	15
2.3 Group B: Standard Adaptive Filtering Algorithms	16

2.3.1	Least Mean Square Filtering	17
2.3.2	Recursive Least Squares Filtering	18
2.3.3	One-step Kalman Filtering Algorithm	19
2.4	Group C: Regularization Techniques	20
2.4.1	Standard Tikhonov Regularization Method	21
2.4.2	Subspace Regularization Method	22
2.5	Results	23
2.5.1	Performance Evaluation	23
2.5.2	Experimental data	23
2.5.3	Simulated data	26
2.5.4	Results with the SM in combination with Wiener Filtering Approaches (Group A)	30
2.5.5	Results with Standard Adaptive Filtering Algorithms (Group B)	33
2.5.6	Results with Regularization Methods (Group C)	38
2.5.7	Computational Complexity	42
3	SINGLE SWEEP AUDITORY EP EXTRACTION	44
3.1	The Modified Scale Space Filtering	44
3.2	Results	52
3.2.1	Pseudo-Simulation Study	52
3.2.2	Experimental Study	62
4	CONCLUSION AND DISCUSSION	72
	REFERENCES	75
	VITA	88

LIST OF TABLES

1.1	The general characteristics of EPs and ERPs	3
1.2	The literature review on <i>template EP estimation</i>	6
1.3	The literature review on <i>single sweep EP extraction</i>	7
1.4	The brief summary on literature review	8
2.1	The filter parameters chosen for the algorithms in Group B . .	34
2.2	The computational complexities of the algorithms	43
3.1	The algorithm of the WTDF (adapted from [127])	47
3.2	The algorithm of the WTSSF (adapted from [131])	50

LIST OF FIGURES

1.1	The international 10-20 electrode placement system for EEG recording [96].	2
1.2	Typical ABR waveform (adapted from [36]). Five general response categories of the ABR waveform are also shown (I-Fast response occur between 2 and 12 <i>ms</i> , II-Slow wave response occur about 12 <i>ms</i> , III- Middle responses occur 12 to 50 <i>ms</i> , IV-Slow responses occur 50 to 300 <i>ms</i> , V-Late responses occur 250 to 600 <i>ms</i>).	4
2.1	The EP can be estimated from a small number of sweeps . . .	11
2.2	The Wiener Filtering model	14
2.3	The Adaptive Filtering model	17
2.4	For experimental data (input SNR = -5 dB), a) the waveforms and b) frequency contents of the grand average EP and single noisy response.	25
2.5	The waveforms of the single sweeps for simulations (the known EP + white noise) for a) input SNR = 0 dB, b) input SNR = -5 dB.	27
2.6	a) The waveforms and b) frequency contents of the known AEP and the noisy sweep (EP + EEG). (input SNR = -5 dB)	28
2.7	a) The known EP and average of 20 noisy sweeps corresponding to simulations and pseudo-simulations	29
2.8	The simulation results for Group A: (a) Output SNR versus the number of sweeps, (b) output SNR versus the input SNR for 20 sweeps	31
2.9	The pseudo-simulation results for Group A: (a) Output SNR versus the number of sweeps, (b) the output SNR versus the input SNR for 20 sweeps	32
2.10	The waveforms of the estimations corresponding to the (a) simulation, (b) pseudo-simulation for 20 sweeps. The letters A, B and C refer the SMCWWF, SMWF and WFSM, respectively	32

2.11	The experimental results for Group A: a) The output SNR versus the number of sweeps, b) The waveforms of the estimations for 64 sweeps. The letters A, B and C refer the SMCWWF, SMWF and WFSM, respectively.	33
2.12	The simulation results for Group B: (a) Output SNR versus the number of sweeps, (b) output SNR versus input SNR for 20 sweeps	35
2.13	The pseudo-simulation results for Group B: (a) The output SNR versus the number of sweeps, (b) the output SNR versus input SNR for 20 sweeps	36
2.14	The waveforms of the estimations corresponding to the (a) simulations and, (b) pseudo-simulations for 20 sweeps. The letters A, B, C and D refer the RLS filtering, KF, SMLMS and LMS filtering, respectively.	37
2.15	The experimental results for Group B: The output SNR versus the number of sweeps using (a) the LMS and SMLMS algorithms, (b) the other methods in Group B	37
2.16	The waveforms of the estimations for experimental 64 sweeps The letters A, B, C and D refer the RLS filtering, KF, SMLMS and LMS filtering, respectively.	38
2.17	Selected basis vectors of \mathbf{H}	40
2.18	The simulation results for Group C: (a) Output SNR versus the number of sweeps, (b) output SNR versus input SNR for 20 sweeps	40
2.19	The pseudo-simulation results for Group C:(a) Output SNR versus the number of sweeps, (b) output SNR versus input SNR for 20 sweeps	41
2.20	The waveforms of the estimations corresponding to a) the simulation study and b) the pseudo-simulation study. The letters A and B refer the STR and SR methods, respectively	41
2.21	The experimental results for Group C: a) The output SNR versus the number of sweeps, b) the waveforms of the estimations for 64 sweeps	42
3.1	The proposed approach for single sweep AEP estimation	44
3.2	An example of detecting sharp edges using WTDF: dyadic WT coefficients at 8 scales of a large boxcar, (adapted from [127])	48

3.3	Graphical illustration of the WTSSF algorithm: WT coefficients at the first scale before filtering, the <i>scf</i> for the WT coefficients at the first and second scales, the spatially selective filter mask and WT coefficients at the first scale after filtering (shown from top to bottom)(adapted from [127]). . .	49
3.4	(a) The waveform, (b) image of the WT coefficients (c) and the MM spectrum corresponding to the generated EP signal. .	54
3.5	(a) The waveform, (b) image of the WT coefficients (c) and the MM spectrum corresponding to the projected data.	55
3.6	The output SNR improvements versus iteration number	56
3.7	The sequences related to the MSSF with <i>si</i>	57
3.8	The sequences related to the WTSSF with <i>fi</i>	58
3.9	The <i>si</i> is performed 14 times in the MSSF and, <i>fi</i> is performed 3 times in the WTSSF.	59
3.10	The waveforms of 6 sweeps used in the pseudo-simulations: a)raw data, b)the noiseless sweeps with amplitude/latency variations, c)the projected data and, d)estimations obtained by using the MSSF after 14 <i>si</i>	61
3.11	The output SNR improvements versus iteration number for experimental data after MSSF and WTSSF.	63
3.12	a) The grand average EP, b) image of the real WT coefficient and, c) the plot of the related MMs.	64
3.13	The waveforms of the grand average and estimations. (<i>si</i> is performed 18 times in the MSSF)	65
3.14	The real WT coefficients associated with a) the average of 32 raw sweeps, b) the grand average EP, c) the projected sweep and d) outputs of the MSSF (<i>si</i> is performed 18 times)	66
3.15	Plots of MMs associated with a) the average of 32 raw sweeps, b) the grand average EP, c) the projected sweep and d) the outputs of the MSSF (<i>si</i> is performed 18 times)	67
3.16	The estimations of experimental ABR data using the a) MSSF and b) WTSSF.	69
3.17	The waveform of the estimation (a), real WT coefficients (b) and their MM spectrums (c) corresponding to the MSSF.	70
3.18	The waveform of the estimation (a), real WT coefficients (b) and their MM spectrums (c) corresponding to the WTSSF.	71

CHAPTER 1

INTRODUCTION

The brain is probably the most complex structure in the known universe. The brain possesses many highly specialized component parts each associated with specific tasks, for example memory and vision. While these parts work together, each part is responsible for a specific function. To understand the functional status of the brain such as in sleep, anesthesia, hypoxia (lack of oxygen) and in certain nervous diseases, e.g. epilepsy, the brain's recordable neuro-electric signals, called electroencephalogram (EEG), are processed and analyzed [90]. The brain electrical activity, that occurs in association with an external stimulus (auditory, visual or somatosensory), is called Evoked Potential (EP). If the experiment is relevant to a cognitive activity, the response signal is frequently called as either event-related-potential (ERP) or cognitive EP in a wide range of cognitive paradigms. EPs are important diagnostic tools in investigation of physiological and psychological situation of subjects. In general, EPs or ERPs are not recognizable by visual inspection since they are buried in spontaneous Electroencephalogram (EEG) with signal-to-noise ratio (SNR) as low as -5 dB considering stimulus-unrelated background EEG as the noise in the measurements [90]. The separation of the EP (the signal) and the ongoing EEG (the noise) in the measurements have been very attractive research area. This requires use of powerful signal processing tools and several methods have been proposed for this purpose. In this chapter, first the general characteristics of the EEG and EP signals are presented. Next, various methods studied for EP estimation will be reviewed.

1.1 Characteristics of EEG and EPs

The EEG recording was first announced by a German psychiatrist named Hans Berger in 1929. The EEG signals are commonly measured from the scalp surface by using scalp electrodes according to the international 10-20 electrode system (1.1). EEG recordings are also obtained from 64, 128, or 256 channel EEG electrode systems for source localization purposes.

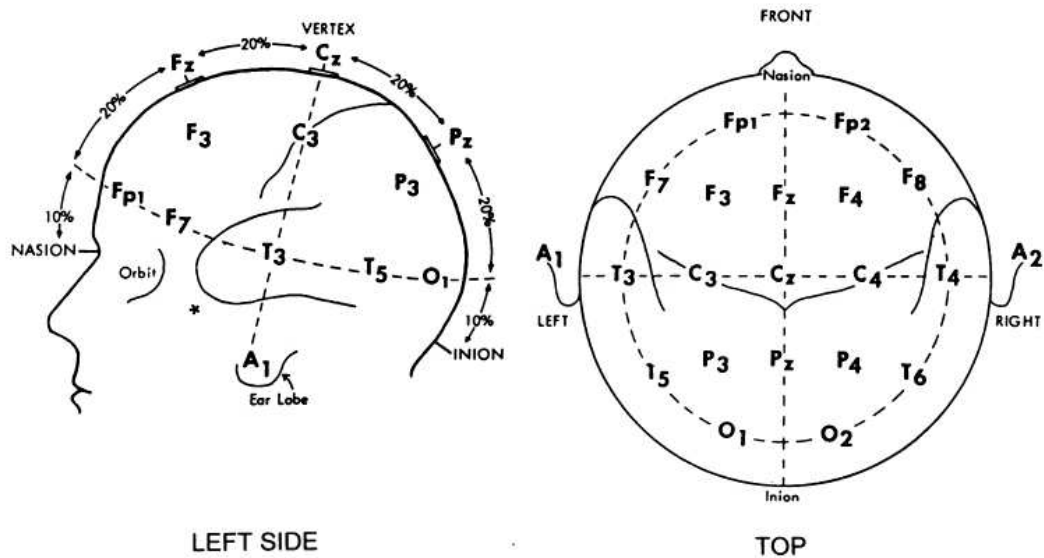


Figure 1.1: The international 10-20 electrode placement system for EEG recording [96].

The spectral classification of the EEG consists of four bands [4]:

δ activities vary from 0.5 to $3.5Hz$. They are rare and are often considered pathological when observed in the normal waking adult with high amplitude.

θ activities vary from 3 to $8Hz$. During sleep, these waves are usually more prominent in the temporal areas of the brain.

α activities vary from 8 to $13Hz$. They are prominent in the occipital region of the brain when the person is relaxed with eyes closed.

β activities vary from 14 to $30Hz$. Their amplitudes range from $5\mu Volt$ to $20\mu Volt$. They are commonly seen in the frontal and central regions of the brain. Each type of EP looks at a different neurological pathway: The auditory evoked potentials (AEPs) help evaluate the auditory nerve pathways from the ears through the brainstem, the visual EP (VEP) evaluates the visual nervous system from the eyes to the occipital cortex of the brain and the somatosensory EP (SEP) assesses pathways from nerves in the arms or legs, through the spinal cord, to the brainstem or cerebral cortex. In this thesis, we deal with AEPs that are valuable tools for some clinical application

areas such as audiometry, psychiatry [11, 45], nervous system disorders [23, 100].

EPs are interpreted in terms of the wave components such as magnitudes and latencies. EPs have no special characteristics like ECG signals. Their components changes depending on 1) stimulus type, 2) individual differences, 3) psychophysiological factors for a given individual [90, 96]. The general characteristics of EPs are briefly summarized in Table 1.1 [4, 46].

Table 1.1: The general characteristics of EPs and ERPs

Type	Specific for recording	Amplitude	Frequency
AEP	on vertex	$0.5 - 10\mu\text{Volt}$	$10\text{Hz} - 3\text{KHz}$
SEP	somatosensory cortex	$1 - 10\mu\text{Volt}$	$2\text{Hz} - 3\text{KHz}$
VEP	occipital cortex	$1 - 20\mu\text{Volt}$	$1\text{Hz} - 300\text{Hz}$
General ERP	(e.g. P300)	$1 - 50\mu\text{Volt}$	$0.2\text{Hz} - 100\text{Hz}$

The auditory brainstem response (ABR) is a subclass of AEPs. ABR is the brain wave activity starting in the inner ear that travels through the auditory nerve and to the auditory nuclei of the brain stem. It does not affected by the mental state of the subject and has very small amplitudes, ranging from 0.001 to 2 $\mu Volt$ [90]. The typical ABR waveform is shown in Figure 1.2 [32]. The brainstem links the brain to the spinal cord. It controls many functions vital to life, such as heart rate, blood pressure and breathing. This area is also important for sleep. Therefore, ABR is used to help diagnose hearing loss, acoustic neuroma and some nervous system abnormalities.

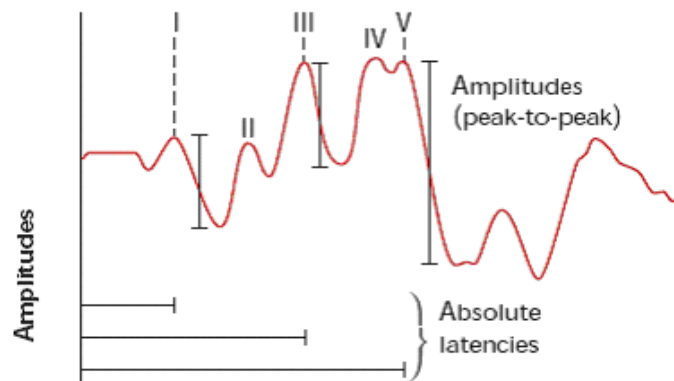


Figure 1.2: Typical ABR waveform (adapted from [36]). Five general response categories of the ABR waveform are also shown (I-Fast response occur between 2 and 12 ms , II-Slow wave response occur about 12 ms , III- Middle responses occur 12 to 50 ms , IV-Slow responses occur 50 to 300 ms , V-Late responses occur 250 to 600 ms).

1.2 Extraction of EPs from ongoing EEG

The ultimate goal in the field of EP research is to recover the response to each stimulus. However, not only the psychophysiological factors [90, 96] but also the recording problems [15, 56] makes the extraction of single sweep

EP from ongoing EEG difficult. Traditionally, a large number of repetitive measurements are ensemble-averaged (EA) to decrease the noise level and find a *template* EP signal, assuming the stimulus-induced changes in the EEG are small [1, 19, 38, 43]. This approach is based on an additive model to describe the background EEG noise and an uncorrelated EP signal [111, 2, 65, 66, 60, 91, 48, 17, 19, 18, 62, 85, 28, 128, 12, 39, 71]. For clinical evaluations, either the template EP signal or possible amplitude/latency variations on single sweeps (with respect to a template EP signal) are used [90]. The use of EA is impractical, however in cases where there are relatively tight constraints related to the available recording time or cooperativity of the subject. This has led to the development of the alternative SNR improvement methods based on the additive model. Therefore, researchers have studied on powerful signal processing techniques associated with either *template EP estimation* or *single trial EP estimation*. In this thesis, three groups of linear filtering algorithms (combinations of the SM with WF approaches, standard adaptive filtering algorithms, Tikhonov regularization techniques) are compared with traditional EA dealing with *template EP estimation*. In addition, a new approach is presented dealing with the *single trial EP estimation*.

Considering the first topic, various methods are suggested as either an alternative to EA to reduce the number of sweeps, or as a post-processing step to remove the noise remaining on average signal. These methods are applied to different types of EPs as summarized in Table 1.2. Some of them may be listed as follows: the weighted averaging approach [17], the subspace averaging method [18, 19], the parametric filtering [52], the adaptive filtering [6, 66, 69, 71, 75, 112, 113, 102], Wiener filtering [12, 24, 91, 126], the transform based algorithms [129, 103, 109], Bayesian estimation [110], and Tikhonov regularization [60]. In these studies, the background EEG noise is assumed to be independent of the stimulus. Among them, the weighted averaging technique is introduced to preserve the high frequency information that may be lost by EA, for both constant noise variances [17] and, non-constant noise variances [18] on noisy sweeps. Most of the adaptive algorithms commonly use the least-mean-square (LMS) algorithm due to its low computational complexity. However, since the estimation performance of LMS algorithm is sensitive to the step-size, different approaches have been studied in EP research area to reduce this sensitivity utilizing the Wavelet Transform (WT) [6, 49, 74], higher order statistics [112] or, moving window technique [69, 102]. The EP signal is commonly assumed to be stationary in post-processing methods based on various estimation techniques dealing

with several types of EPs. For instance, 2^{nd} order statistical information about the signal and the noise [28], least square lattice algorithm [75], adaptive filtering approaches [102] and WT [109] is used for BAEP estimation. Another WT based post-processing method is presented to enhance the SNR for SEP and VEP signals [129]. A group of basic estimation techniques are compared to traditional EA such that the Bayesian estimation and Kalman filtering (KF), which is based on mean square estimation technique, are found to better than the others in template AEP estimation regarding as the SNR enhancement[62]. In literature, the state-space modeling concept is also used for template EP estimation from a relatively small number of sweeps [30, 50, 92, 111]. The SNR improvement methods require either a reference signal or prior knowledge about the signal or noise. A set of measurements must be available for both of these requirements. To overcome these drawbacks, a few studies evaluate the measurement dividing into two part: the EP signal corrupted with the noise is estimated by filtering of the post-stimulus interval after characterizing of the noise from the pre-stimulus interval [70, 72, 75, 111]. Either signal or noise is assumed to be stationary in linear SNR improvement algorithms. However, such assumptions are being questioned in some reports describing the EPs or ERPs as superposition of some phase modulated rhythmic activities which may be related to different cognitive processes of the brain [80, 20, 67, 93, 55].

Table 1.2: The literature review on *template EP estimation*

	MS	B	LS	TB
actual AEP	[69]	[110]		
simulation	[121, 12, 102]	[110]	[111]	
actual SEP/VEP	[121, 28, 69] [75, 109, 91] [102]		[111]	[129, 21]

The template EP is widely consulted in literature associated with the second topic (*single sweep EP estimation*) for several EPs as summarized in Table 1.3. The possible variations, which may important in some clinical

Table 1.3: The literature review on *single sweep EP extraction*

	MS	B	LS	TB
actual AEP				[103, 47]
simulation	[113, 66]	[60]	[2, 105]	[105, 103]
actual SEP/VEP		[65, 66]	[105, 72]	[115]
P300		[60]		

evaluations [3, 98, 118, 84], are obtained by evaluating a small number of sweeps in wide range of EP research area. In that case, the specific features are identified from a template EP by using various algorithms such as an adaptive algorithm for VEPs [113], a specified model for movement related EPs [71, 72, 111], a neural network approach (training based algorithm) for either SEPs [47], maximum likelihood approach [51], moving window technique for intracranially ERP [25] or, the multi-resolution-decomposition approximation for auditory ERP signals [105, 103]. The template EP signal is computed by averaging small number of sweeps in these studies. Therefore, validity of the feature selection is highly influenced by the noise remaining on the template EP. In this thesis, we propose a new approach that combines the SM and a wavelet domain filtering named as modified scale space filter (MSSF) for single sweep auditory EP estimation. The proposed approach does not require a template EP. In EP research area, researchers have also dealt with the analysis of ERPs or EEG itself. The literature may be summarized in Table 1.4 with respect to relevant topics ((i) template EP estimation, ii) single sweep EP estimation, iii) ERP analysis, iv) EEG/ERP analysis) and estimation techniques (least square (LS), mean square (MS), Bayesian (B), transform based (TB), model based (MB), neural network (NN) approach, independent component analysis (ICA)).

Table 1.4: The brief summary on literature review

	i	ii	iii	iv
MS	[12, 28, 69] [75, 91, 109] [102, 113, 121]	[66, 113]	[30]	[114]
LS	[111, 120, 128]	[2, 72]	[72]	
B	[110, 60]	[65, 60, 66]	[30]	
TB	[25, 129, 21] [8, 109, 128] [129, 9]	[103, 47, 105] [115]	[5, 21, 25] [85, 118]	[55, 99]
MB	[50, 92, 19, 95]		[122]	
NN	[116, 33]	[47]	[73, 132, 34]	
ICA			[80]	[57, 58, 80] [59]

In this thesis, the SM that is usually proposed to filter the noise components in image processing [97, 104], has been applied solely to estimate EPs. We apply the SM as presented by Moor [82]. The SM is proposed as a secondary filtering process following the conventional WF in a simulation study [12]. We change the application order of the filtering and the SM in this thesis. We also use an iterative WF approach, called the Coherence Weighted WF (CWWF) that is introduced for SEP estimation [91], instead of conventional WF. These combination methods form the Group A among the basic linear estimation techniques to be compared for template auditory EP estimation as a first contribution of this thesis. The basic adaptive algorithms (LMS, RLS and one-step KF) and the Tikhonov regularization techniques form Group B and Group C, respectively. Standard Tikhonov regularization (STR) method has not been applied to extract the EPs whereas a special case of the STR so called Subspace Regularization (SR) method is proposed to single trial EP estimation [60]. In this thesis, we use both the STR and SR methods as post-processing steps for template AEP estimation. The above listed three groups of algorithms are introduced in Chapter 2. As a result of the comparison study, it is concluded that the SM is a useful pre-filter to reduce the large amount of the background EEG noise from the raw data. Then, less-noisy sweeps are filtered in wavelet domain with MSS in the second contribution of the thesis. The theoretical basis of the filtering algorithm

are given in Chapter 3.

1.3 The Scope of the Thesis

The objectives of this study are as follows:

- 1) to compare a group of linear filtering algorithms relative to traditional EA for template AEP estimation from a small number of sweeps,
- 2) to present a new approach for single sweep AEP extraction.

1.4 The Significance of the Thesis

As a first contribution of this thesis, we compare a group of basic linear estimation techniques to forms a reference for future studies on auditory EP extraction using all possible data sets (i.e, simulations, pseudo-simulations and experimental data). The SM, which was used as a post-processing step for EP extraction, is shown to be an effective pre-processing step to improve the performance of different algorithms. The STR method was not applied before for auditory EP estimation. It is shown to be better than the SR method and found among the best in this case.

Corresponding to the second goal of this study, a wavelet domain filter, namely modified scale-space filter MSSF is applied to the projected data. This new approach provides new results that support additivity model assumption.

1.5 The Thesis Organization

The thesis is organized as follows: In Chapter 2, the comparison study was given on the estimation of template AEP from small number of sweeps. The algorithms corresponding to the three groups of methods, the Subspace Method in combination with Wiener Filtering approaches, standard Adaptive Filtering approaches, Tikhonov regularization techniques, were given in section 2.2, 2.3 and 2.4, respectively. The results corresponding to the actual and simulated data sets were given in section 2.5.

In Chapter 3, a new approach was presented to single trial auditory EP estimation. For this purpose, two independent methods, the SM and MSSF in this thesis, were applied consecutively. The SM and MSSF algorithm were

introduced in section 2.1 and section 3.1, respectively. The new approach was tested in both simulations and experimental studies in template AEP estimation. The related results were given in section 3.2.2 and 3.2.1. The MSSF was used for estimation of template ABR, as well. The MSSF was applied to average small number of sweeps as a post-filter to obtain the template ABR. For this purpose, MSSF was tested for actual ABR data recorded from rats and the results were given in section 3.2.2.

CHAPTER 2

COMPARISON OF BASIC ESTIMATION TECHNIQUES IN EXTRACTING TEMPLATE AUDITORY EP

In this chapter, a group of algorithms were assessed to obtain a template auditory EP from a relatively small number of sweeps (Figure 2.1).

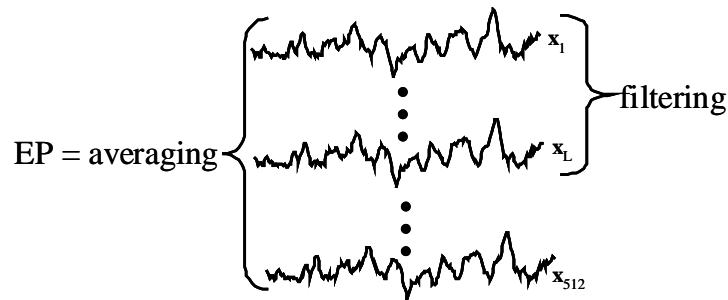


Figure 2.1: The EP can be estimated from a small number of sweeps

Here, each noisy sweep denoted by \mathbf{x}_i .

The additive signal model was commonly considered to estimate different types of EPs, such as somatosensory EP [2, 65, 66, 60, 91, 111], visual EP [18, 19, 48], auditory EP [12, 17, 62], cognitive EP [39, 85] or, brainstem auditory EP [28, 128]. In this comparison study, the same model was adopted for auditory EP estimation. Mathematically, this can be expressed as follows:

$$\mathbf{x}_i(n) = \mathbf{s}(n) + \mathbf{w}_i(n) \quad 0 \leq n \leq N - 1, \quad 1 \leq i \leq L \quad (2.1)$$

where \mathbf{s} and \mathbf{w}_i respectively represent the true EP signal (the grand average EP in experimental case and the known EP in simulations) and the noise components of the response \mathbf{x}_i to the i^{th} stimulus. Here n is the time index and N denotes the number of samples per response. L represents the number of repetitions.

In experimental studies, the EP signal $\hat{\mathbf{s}}$ (grand average AEP) was computed by

$$\hat{\mathbf{s}}(n) = \frac{1}{L} \sum_{i=1}^L \mathbf{x}_i(n). \quad (2.2)$$

where L represents the overall number of sweeps.

In addition to the additive signal model, we assume the following: 1) the EP signal is stationary, and 2) the EP signal and the background EEG noise are uncorrelated.

Below, the mathematical basis of the algorithms studied in this work, shall be briefly introduced. The matrices and vectors were given with boldfaced lowercase and uppercase letters, respectively. The scalar variables were given in regular type.

2.1 The Subspace Method

It was shown that, it is not possible to reconstruct the exact data matrix \mathbf{S} from the noisy version \mathbf{X} [82]. Thus, estimates of \mathbf{S} should be explored. In this study, the noise matrix \mathbf{X} is approximated by a matrix of rank r in the least squares sense [36]. Note that, it is possible to obtain a minimum variance estimate or a whole set of data matrices \mathbf{S} that could have generated the observation matrix \mathbf{X} under certain assumptions [82]. The least squares estimates or the minimum variance estimate can simply be obtained using the singular value decomposition (SVD) of \mathbf{X} . In this section, we shall briefly describe the SVD and the least squares estimate of \mathbf{S} .

The SVD of $\mathbf{X} \in \mathbf{R}^{N \times L}$ is any factorization of the form,

$$\mathbf{X} = \mathbf{U}\mathbf{\Sigma}\mathbf{V}^T \quad (2.3)$$

where $\mathbf{U} \in \mathbf{R}^{N \times N}$ and $\mathbf{V} \in \mathbf{R}^{L \times L}$ are orthogonal matrices. The columns of \mathbf{U} and \mathbf{V} are called as left and right singular vectors which span the column space and row space of \mathbf{X} , respectively. The entries of the diagonal matrix

Σ indicates the singular values of \mathbf{X} such as $\lambda_1 > \dots > \lambda_{p-1} > \lambda_p$ where $p = \min(N, L)$ [36].

The SVD of \mathbf{X} can be expressed as

$$\mathbf{X} = \begin{pmatrix} \mathbf{U}_{m1} & \mathbf{U}_{m2} \end{pmatrix} \begin{pmatrix} \Sigma_{m1} & \mathbf{0} \\ \mathbf{0} & \Sigma_{m2} \end{pmatrix} \begin{pmatrix} \mathbf{V}_{m1}^t \\ \mathbf{V}_{m2}^t \end{pmatrix} \quad (2.4)$$

For $r = \text{rank}(\mathbf{S})$ then $\Sigma_{m1} = \text{diag}(\lambda_1, \dots, \lambda_r)$, $\lambda_r \gg \lambda_{r+1}$ [36].

The least squares estimate \mathbf{S}_{LS} can be computed by projecting \mathbf{X} onto the signal subspace as follows [36]:

$$\mathbf{Y} = \mathbf{U}_{m1} \mathbf{U}_{m1}^t \mathbf{X} = \mathbf{U}_{m1} \Sigma_{m1} \mathbf{V}_{m1}^T \quad (2.5)$$

Note that, the original column space of \mathbf{S} can not be recovered since $\mathbf{U}_{m1} \neq \mathbf{U}_{s1}$ where \mathbf{U}_{s1} consists of the largest r left-singular vectors of the original signal matrix \mathbf{S} [82]. However, as the SNR increases, the canonical angles between \mathbf{U}_{m1} and \mathbf{U}_{s1} decrease [42].

In an EP experiment, possible amplitude variations on single sweeps will not change the rank of \mathbf{S} whereas latency variations will be effective. The number of sweeps having different latencies determine the number of basis which spans the signal subspace. If we assume that the EP signal is stationary, then only the first left singular vector spans the signal subspace of interest and $r = 1$.

2.2 Group A: The Subspace Method in combination with Wiener Filtering Approaches

In a simulation study, to improve the performance of conventional Wiener filtering (WF), filter outputs are projected onto the signal subspace by using the SM [12]. In this study, we apply the same method to extract auditory EPs. In addition, we explore the use of changing the application order of filtering and the projection process. We also use the Coherence Weighted Wiener Filter (CWWF), which was presented for estimation of somatosensory EPs [91], instead of conventional WF to filter out the noise remaining on the projected version the data. Thus, these three mentioned methods are chosen as the first group of algorithms used for the performance assessment. The algorithms in Group A can be listed as follows:

- Projection after WF (WFSM)
- WF after projection (SMWF)
- CWWF after projection (SMCWWF)

Wiener Filtering is a linear discrete-time filtering operation as shown in Figure 2.2. Here \mathbf{x}_i and $y_i(n)$ are the input and output sequences of the filter, $d_i(n)$ is the desired signal, and i is the trial index. The desired signal can be calculated as

$$d_i(n) = \frac{1}{L-1} \sum_{j=1, j \neq i}^L x_j(n) \quad (2.6)$$

The estimation error $e_i(n)$ is expressed as

$$e_i(n) = d_i(n) - y_i(n) \quad (2.7)$$

The elementary properties of WF can be found elsewhere [44]. We give the basic mathematical descriptions about the weight vector of both WF and CWWF in the following sub-sections.

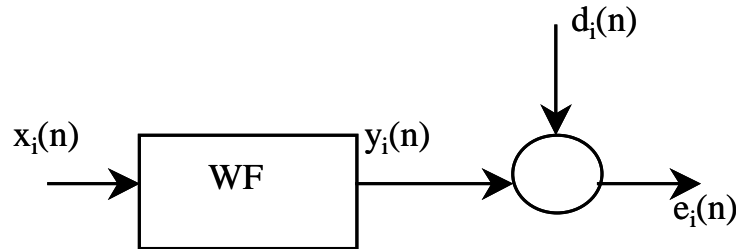


Figure 2.2: The Wiener Filtering model

2.2.1 Conventional Wiener Filtering

Assume that the i^{th} noisy sweep, namely \mathbf{x}_i and the desired response \mathbf{d}_i are jointly wide-sense stationary stochastic processes as given with Equation 2.1 and Equation 2.6, respectively.

WF converge the optimum weight vector \mathbf{w}_{oi} based on Mean Square (MS) estimation without any need of an algorithm. The optimum weight vector is computed by minimizing the mean square error as follows:

$$\frac{\partial J_i(n)}{\partial w_i} = 0, \quad J_i(n) = E|e_i(n)|^2 \quad (2.8)$$

$$\mathbf{w}_{oi} = \mathbf{R}_i^{-1} \mathbf{p}_i. \quad (2.9)$$

Here \mathbf{R}_i denotes the $N \times N$ correlation matrix of the i^{th} input noisy sweep \mathbf{x}_i and \mathbf{p}_i is the cross-correlation vector between the input noisy sweep \mathbf{x}_i and the desired signal \mathbf{d}_i . Then the corresponding WF output vector (\mathbf{y}_i) is obtained as follows

$$y_i(n) = \sum_{m=0}^M w_{oi}(m)x_i(n-m), \quad n = 1, \dots, N \quad (2.10)$$

where \mathbf{w}_{oi} refers the i^{th} optimum weight vector. Here M refers the filter length.

2.2.2 Coherence Weighted Wiener Filtering

The weight vector, namely the Wiener filter coefficient vector is also estimated in an iterative way [91]. For this purpose, the filter transfer function $\mathbf{H}(\omega)$ is defined by

$$\mathbf{H}(\omega) = \frac{\mathbf{S}_s(\omega)}{\mathbf{S}_s(\omega) + \mathbf{S}_z(\omega) \frac{1}{L-1}} \quad (2.11)$$

where ω is the frequency index, $\mathbf{S}_s(\omega)$ and $\mathbf{S}_z(\omega)$ denote the power spectral densities (squared magnitude of the Fourier Transform) corresponding to the signal \mathbf{s} and the noise \mathbf{z} . The power spectral densities are defined for L consecutive sweeps as follows,

$$\mathbf{S}_s(\omega) = \frac{L}{L-1} \mathbf{S}_{\bar{x}}(\omega) - \frac{1}{L-1} \mathbf{S}_x(\omega) \quad (2.12)$$

$$\mathbf{S}_z(\omega) = \frac{L}{L-1} [\mathbf{S}_x(\omega) - \mathbf{S}_{\bar{x}}(\omega)] \quad (2.13)$$

Here, $\mathbf{S}_x(\omega)$ and $\mathbf{S}_{\bar{x}}(\omega)$ are the power spectral densities corresponding to the input noisy signal \mathbf{x}_i and averaged L number of noisy sweeps. These

spectrums are calculated iteratively by using a coherence function γ_{xz} . The coherence function reflects the degree of correlation between the different frequency components of two stationary time sequences $x(n)$ and $z(n)$ as

$$\gamma_{xz} = \frac{\mathbf{S}_{xz}(\omega)}{\sqrt{\mathbf{s}_{xx}(\omega)\mathbf{S}_{zz}(\omega)}} \quad (2.14)$$

where the $\mathbf{S}_{xz}(\omega)$ is the cross spectrum between $\mathbf{x}(n)$ and $\mathbf{z}(n)$. Here, $\mathbf{S}_{xx}(\omega)$ and $\mathbf{S}_{zz}(\omega)$ are the auto-power spectra of each signal. The filter transfer function is then expressed for the i^{th} response as

$$\mathbf{H}(\omega, i) = \frac{\mathbf{S}_{\bar{x}}(\omega, i)}{\mathbf{S}_{\bar{x}}(\omega, i) + \mathbf{S}_{\bar{z}}(\omega, i)\frac{1}{L}} \quad (2.15)$$

where

$$\mathbf{S}_{\bar{x}}(\omega, i) = \frac{i-1}{i}\mathbf{S}_{\bar{x}}(\omega, i-1) + \frac{1}{i}\gamma(\omega, i)\mathbf{S}_x(\omega, i) \quad (2.16)$$

and

$$\mathbf{S}_{\bar{z}}(\omega, i) = \frac{i-1}{i}\mathbf{S}_{\bar{z}}(\omega, i-1) + \frac{1}{i}[1 - \gamma(\omega, i)]\mathbf{S}_x(\omega, i). \quad (2.17)$$

Here, $\gamma(\omega, i)$ refers the spectral coherence between $\mathbf{S}_x(\omega, i)$ and $\mathbf{S}_{\bar{x}}(\omega, i-1)$. Thus, the filter impulse response is obtained by taking the inverse Fourier Transform of the transfer function $\mathbf{H}(\omega)$ [91].

2.3 Group B: Standard Adaptive Filtering Algorithms

The standard LMS and RLS algorithms are based on the Wiener filter theory and the theory of least squares and Kalman filters, respectively. In the present study, the LMS filtering, the RLS filtering and, one-step Kalman filtering algorithms are applied. The block diagram representation of the adaptive filters is illustrated in Figure 2.3 [44].

Here, $\mathbf{x}_i(n)$ and $\mathbf{w}_i(n)$ denotes respectively the input noisy sequence and weight vector of the filter at time n . The filter output sequence $\mathbf{y}_i(n)$ is given by

$$y_i(n) = \mathbf{w}_i^H(n)\mathbf{x}_i(n). \quad (2.18)$$

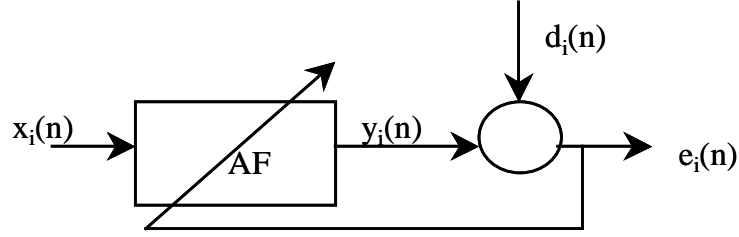


Figure 2.3: The Adaptive Filtering model

where superscript H denotes Hermitian transposition. Since the noise on the desired signal and the input signal are assumed uncorrelated, the desired signal sequence $d_i(n)$ is calculated from the average of $L - 1$ sweeps as given with Equation 2.6. The estimation error $e_i(n)$ is computed by using Equation 2.7.

2.3.1 Least Mean Square Filtering

The LMS algorithm is a stochastic gradient search algorithm that is an alternative way of finding the optimum weight vector \mathbf{w}_{oi} . In this algorithm, the mean square error is minimized by moving along the negative gradient direction with a constant learning rate (step-size) symbolized by μ . In this algorithm, iterative search algorithm is used as follows:

$$\hat{\mathbf{w}}_i(n+1) = \hat{\mathbf{w}}_i(n) + \frac{\mu}{2} (-\nabla J_i(n)) \quad (2.19)$$

where $J_i(n) = E|e_i(n)|^2$. Here, the error $e_i(n)$ is computed as a posteriori that is based on the current weight vector. Its expression is given in Equation 2.7. By solving above equation the weight vectors $\hat{\mathbf{w}}_i$ are computed in the following formula:

$$\hat{\mathbf{w}}_i(n+1) = \hat{\mathbf{w}}_i(n) + \mu \mathbf{x}_i(n) e_i^*(n) \quad (2.20)$$

The entries of $\hat{\mathbf{w}}_i$ are initially set to zero. In case, the weight error between $\hat{\mathbf{w}}_i$ and the optimum weight vector is defined by

$$e(n) = \hat{\mathbf{w}}_i(n) - \mathbf{w}_{oi}. \quad (2.21)$$

This weight error can be rewritten in terms of the estimation error $e_{oi}(n)$ produced in the optimum Wiener filtering algorithm:

$$e(n+1) = [\mathbf{I} - \mu \mathbf{x}_i(n) \mathbf{x}_i^H(n)] e(n) + \mu \mathbf{x}_i(n) e_{oi}^*(n) \quad (2.22)$$

where $e_{oi}(n) = d_i(n) - \mathbf{w}_{oi}^H \mathbf{x}_i(n)$. $[\mathbf{I} - \mu \mathbf{x}_i(n) \mathbf{x}_i^H(n)] = \mathbf{I}$, the step-size parameter μ should be selected as

$$0 < \mu < \frac{2}{\sum_{n=1}^N |\mathbf{x}_i(n)|^2} \quad (2.23)$$

2.3.2 Recursive Least Squares Filtering

In adaptive RLS algorithm, the weight vector is computed by minimizing the exponentially weighted errors based on Least Squares estimation approach as follows:

$$\frac{\partial J_i(n)}{\partial w_i} = \frac{\partial}{\partial w_i} E \left\{ \sum_{j=1}^n \lambda^{n-j} |e_i(j)|^2 \right\} = 0 \quad (2.24)$$

where i indicates the number of sweeps ($i = 1, \dots, L$). Here, the error function is in form

$$e_i(n) = d_i(n) - \widehat{\mathbf{w}}_i^H(n) \mathbf{x}_i(n) \quad (2.25)$$

Then, the resulting solution of Equation 2.24 is obtained as

$$\left[\sum_{i=1}^n \lambda^{n-i} \mathbf{x}_i \mathbf{x}_i^H \right] \widehat{\mathbf{w}}_i(n) = \sum_{i=1}^n \lambda^{n-i} \mathbf{x}_i d_i^*(n) \quad (2.26)$$

We can rewrite the above equation in matrix form as follows:

$$\Phi_i(n) \widehat{\mathbf{w}}_i(n) = \mathbf{z}_i(n) \quad (2.27)$$

where $\sum_{i=1}^n \lambda^{n-i} \mathbf{x}_i \mathbf{x}_i^H = \Phi_i(n)$ and $\sum_{i=1}^n \lambda^{n-i} \mathbf{x}_i d_i^*(n) = \mathbf{z}_i(n)$.

When the exponentially weighting factor (λ) is set to 1, the problem becomes an ordinary least squares problem. By applying the matrix inversion Lemma to the matrix Φ_i , the weight vector is computed by using the resulting update equation as follows:

$$\widehat{\mathbf{w}}_i(n) = \widehat{\mathbf{w}}_i(n-1) + \mathbf{k}_i(n) \xi_i^*(n) \quad (2.28)$$

$$\xi_i(n) = d_i(n) - \widehat{\mathbf{w}}_i^H(n-1) \mathbf{x}_i(n) \quad (2.29)$$

$$\mathbf{k}_i(n) = \frac{\mathbf{P}_i(n-1)\mathbf{x}_i(n)}{\lambda + \mathbf{x}_i^H(n)\mathbf{P}_i(n-1)\mathbf{x}_i(n)} \quad (2.30)$$

$$\mathbf{P}_i(n) = \lambda^{-1}\mathbf{P}_i(n-1) - \lambda^{-1}\mathbf{k}_i(n)\mathbf{x}_i^H(n)\mathbf{P}_i(n-1) \quad (2.31)$$

where \mathbf{P}_i is the input correlation matrix. The error $\xi_i^*(n)$ is defined as a priori that is based on the old weight vector. The algorithm requires an initial setting as given below:

$$\hat{\mathbf{w}}_i(0) = 0 \quad \text{and} \quad \mathbf{P}_i(0) = \delta^{-1}\mathbf{I} \quad \delta : \text{a small positive constant}$$

It is recommended based on practical experience that δ should be selected smaller than $0.01\sigma_{\mathbf{x}}^2$ where $\sigma_{\mathbf{x}}^2$ is the variance of the input sequence $\mathbf{x}_i(n)$. If $\lambda = 1$, the RLS filter converge to the optimum solution, namely $E\{\hat{\mathbf{w}}_i(n)\} = \mathbf{w}_{oi}$ for $n \geq M$.

The RLS algorithm is a special case of the KF. The relations between these algorithms are given in the literature [107]. The RLS algorithm has more computational complexity over LMS algorithm since it requires vector multiplications for each weight update.

2.3.3 One-step Kalman Filtering Algorithm

The KF solves the minimum mean square estimation problem based on the state-space concept in recursive manner. It is the linear minimum variance estimator for finite duration data records. In the literature, it is stated that the KF provides a smaller mean square error than does the WF [108]. However, the KF requires more computational effort.

In one-step adaptive KF algorithm, the weight vector is updated as follows

$$\hat{\mathbf{w}}_i(n+1) = \hat{\mathbf{w}}_i(n) + \mathbf{g}_i(n)e_i^*(n) \quad (2.32)$$

where $e_i(n)$ denotes the estimation error which is computed by using Equation 2.7 and $\mathbf{g}_i(n)$ denotes the Kalman gain which is computed in form

$$\mathbf{g}_i(n) = \frac{\mathbf{K}_i(n-1)\mathbf{x}_i(n)}{\mathbf{x}_i^H(n)\mathbf{K}_i(n-1)\mathbf{x}_i(n) + \mathbf{Q}_m} \quad (2.33)$$

KF leads to minimization of the trace of the $N \times N$ state error correlation matrix $\mathbf{K}_i(n)$ which is calculated as below

$$\mathbf{K}_i(n) = \mathbf{K}_i(n-1) - \mathbf{g}_i(n)\mathbf{x}_i^H(n)\mathbf{K}_i(n-1) + \mathbf{Q}_p \quad (2.34)$$

Here \mathbf{Q}_m and \mathbf{Q}_p are $N \times N$ autocorrelation matrices associated with the measurement noise sequence and the process noise sequence, respectively. H

denotes the hermitian transposition. Both these noise sequences are assumed to be zero mean white noise sequences. Thus, \mathbf{Q}_m and \mathbf{Q}_p are initially selected as follows,

$$\mathbf{Q}_m = q_m \mathbf{I}_{N \times N}, \quad \mathbf{Q}_p = q_p \mathbf{I}_{N \times N} \quad (2.35)$$

where q_m and q_p are used to denote the noise variance of the measurement and the process noises, respectively. These noise processes are assumed to be statistically independent and uncorrelated. The initial settings of the KF algorithm are given by,

$$\hat{\mathbf{w}}_i(0) = 0 \quad \text{and} \quad \mathbf{K}_i(0) = k_0 \mathbf{I} \quad (2.36)$$

where the initial weight vector is assumed to be independent of the both q_m and q_p . If there is a correlation between the states, the KF works as a RLS filter.

2.4 Group C: Regularization Techniques

Tikhonov regularization is a technique that is largely used to solve ill-posed linear problems and linear least squares problems in various areas. In addition to the standard Tikhonov regularization (STR) approach [117] there are also special cases, one of them which is the subspace regularization (SR) method presented in [119]. The SR method was already applied for single trial EP estimation in the literature [60]. In the present study, both the SR and the STR methods are applied as post-processing steps after EA.

Let the EP signal be modeled with respect to the additive model (see Equation 2.1) as follows:

$$\mathbf{s} = \mathbf{H}\theta \quad (2.37)$$

where $\mathbf{H} \in \mathbf{R}^{N \times p}$ is the known *observation* matrix. The columns of \mathbf{H} are the basis vectors modeling the EP signal. The model parameters denoted by $\theta \in \mathbf{R}^p$ can be obtained by solving the ordinary least squares (LS) problem

$$\min\{\|\mathbf{H}\theta - \mathbf{x}\|^2\} \quad (2.38)$$

The ordinary LS solution $\hat{\theta}_{LS}$ of this problem is

$$\hat{\theta}_{LS} = (\mathbf{H}^T \mathbf{H})^{-1} \mathbf{H}^T \mathbf{x} \quad (2.39)$$

Since $N > p$, the system can be called over-determined. To model the signal appropriately, the basis vectors should overlap enough. Thus, the matrix $\mathbf{H}^T\mathbf{H}$ in Equation 2.39 becomes ill conditioned yielding unstable solution. Then, the problem becomes an ill-posed problem that should be solved by using regularization techniques to obtain stable solution. The theoretical basis of these techniques are summarized in the following sections.

2.4.1 Standard Tikhonov Regularization Method

The general form of the Tikhonov solution is obtained by minimizing the weighted least-squares problem:

$$\min\{\|\mathbf{H}\theta - \mathbf{x}\|^2 + \alpha^2\|\mathbf{L}(\theta - \theta^*)\|^2\} \quad (2.40)$$

where $\mathbf{L} \in \mathbf{R}^{p \times n}$ is non-negative semi-definite matrix for $n \geq p$. θ^* refers to the initial estimate of the solution. α is the regularization parameter which regularizes the minimization of the side constraint relative to the minimization of the residual norm. α^{-1} is proportional to the bound of perturbations in \mathbf{H} and \mathbf{x} . The regularization matrix \mathbf{L} is either the identity matrix or approximation of the derivative operators based on the smoothness assumption about the solution. In this case, \mathbf{L} has the null space that are not contaminated by the noise [41].

The solution of the weighted least squares problem is called as the standard Tikhonov regularized solution [37, 117] and expressed as

$$\hat{\theta}_\alpha = (\mathbf{H}^T\mathbf{H} + \alpha^2\mathbf{L}^T\mathbf{L})^{-1}(\mathbf{H}^T\mathbf{x} + \alpha^2\mathbf{L}^T\mathbf{L}\theta^*) \quad (2.41)$$

where $\mathbf{L} \in \mathbf{R}^{p \times n}$ is non-negative semi-definite matrix for $n \geq p$. α is the regularization parameter which regularizes the minimization of the semi norm relative to the minimization of the residual norm. α^{-1} is proportional to the bound of perturbations in \mathbf{H} and \mathbf{x} .

The Tikhonov solution denoted by $\hat{\theta}_\alpha$ consist of both a regularized part ($\hat{\theta}_{reg}$) and an un-regularized part ($\hat{\theta}_{null}$) lying in the null space as follows

$$\hat{\theta}_\alpha = \hat{\theta}_{reg} + \hat{\theta}_{null}. \quad (2.42)$$

The null space of the second term in Equation 2.40 (so called the semi norm) is determined by the regularization matrix \mathbf{L} . The null space contributes to the solution of Equation 2.42. When $\mathbf{L} = \mathbf{I}$, the Tikhonov solution reminds of the truncated singular-value-decomposition solution as follows [41]

$$\hat{\theta}_k = \sum_{i=1}^k \mathbf{u}_i^t \mathbf{x} \mathbf{v}_i / \sigma_i \quad (2.43)$$

where k is the truncation index. Here, \mathbf{u}_i and \mathbf{v}_i refer the left and right singular vectors of \mathbf{H} , respectively. σ_i denotes the i^{th} singular value of \mathbf{H} .

In various application areas, the regularization matrix has been constructed in different ways [119]. One of them is described in the following subsection which assumes an inhomogeneous solution with sharp variations.

2.4.2 Subspace Regularization Method

In the SRM, the original least squares problem is modified as follows:

$$\min\{\|\mathbf{L}_1(\mathbf{x} - \mathbf{H}\theta)\|^2 + \alpha^2\|\mathbf{L}_2(\theta - \theta^*)\|^2\} \quad (2.44)$$

where \mathbf{L}_1 and \mathbf{L}_2 are the regularization matrices. The matrix \mathbf{L}_1 is selected utilizing the prior information about the noise

$$\mathbf{L}_1^T \mathbf{L}_1 = \mathbf{C}_w^{-1} \quad (2.45)$$

where \mathbf{C}_w is the covariance matrix of the background EEG noise sequences. The 2^{nd} order statistical information about the background EEG noise is obtained from a set of measurements collected before the experiments.

Assuming the measurements are jointly Gaussian, the regularization matrix \mathbf{L}_2 is determined for a special case such that $\mathbf{H}^T \mathbf{H} = \mathbf{I}$ [60]. Then the LS solution is expressed in terms of random coefficients as

$$\hat{\theta}_{LS} = \mathbf{H}^T \mathbf{x} = \sum_{i=1}^p \psi_i c_i \quad (2.46)$$

where the coefficients, c_i are uncorrelated to model the EP with minimum number of basis. The autocorrelation matrix of these coefficients is obtained from the correlation matrix of data as follows:

$$E\{\mathbf{c}\mathbf{c}^T\} = E\{\mathbf{H}^T \mathbf{x} \mathbf{x}^T \mathbf{H}\} = \mathbf{H}^T \mathbf{R}_x \mathbf{H} \quad (2.47)$$

This expression is largely used in PCA to solve the Equation 2.46 if the basis vectors are formed with the eigenvectors of \mathbf{R}_x . If the distance between the model and the signal subspace spanned by the eigenvectors of

\mathbf{R}_x , the norm $\|\mathbf{H}\theta - \mathbf{H}_s\mathbf{H}_s^T\mathbf{H}\theta\| = \|(\mathbf{I} - \mathbf{H}_s\mathbf{H}_s^T)\mathbf{H}\theta\|$ must be minimum. Here, \mathbf{H}_s consists of the r largest eigenvectors of the autocorrelation matrix corresponding to input of the estimator. Thus, this norm is used as a side constraint of the problem (Equation 2.44) such that $\mathbf{L}_2 = (\mathbf{I} - \mathbf{H}_s\mathbf{H}_s^T)\mathbf{H}$.

Then, the estimated solution can be expressed in the following form:

$$\hat{\theta}_\alpha = (\mathbf{H}^T\mathbf{L}_1^T\mathbf{L}_1\mathbf{H} + \alpha^2\mathbf{L}_2^T\mathbf{L}_2)^{-1}(\mathbf{H}^T\mathbf{L}_1^T\mathbf{L}_1\mathbf{x} + \alpha^2\mathbf{L}_2^T\mathbf{L}_2\theta^*) \quad (2.48)$$

2.5 Results

2.5.1 Performance Evaluation

In this study, we use the SNR in evaluating the performance of the algorithms. The input and output SNRs are defined as follows:

$$inputSNR = 10\log \left[\frac{\sum_{i=1}^N \mathbf{s}(i)^2}{\sum_{i=1}^N (\mathbf{s}(i) - \mathbf{x}(i))^2} \right] \quad (2.49)$$

$$outputSNR = 10\log \left[\frac{\sum_{i=1}^N \mathbf{s}(i)^2}{\sum_{i=1}^N (\mathbf{s}(i) - \mathbf{y}(i))^2} \right] \quad (2.50)$$

where \mathbf{s} , \mathbf{x} and \mathbf{y} denote the signal, i.e., the grand average auditory EP (or known EP in simulations), input noisy sequence of the estimator and the output of the estimator, respectively.

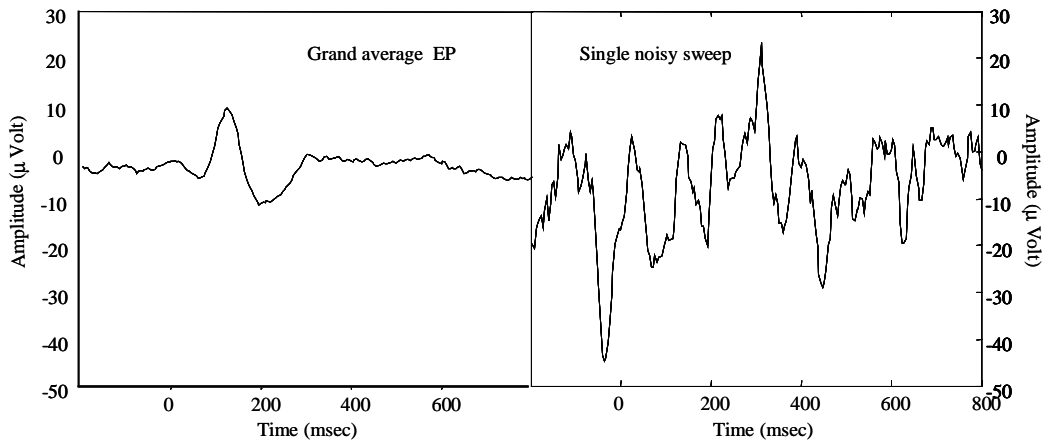
To understand the effect of the number of sweeps for a specified input SNR, the output SNR improvements are calculated after each additional sweep. In addition, the effects of the input SNR are explored, for a specific number of sweeps, by changing the input SNR and calculating the corresponding output SNR. In experimental studies, the output SNR values are calculated after each additional sweep using the empirically found optimum parameters of each algorithm. Since it is not possible to analyze all the output waveforms recovered under different SNR conditions for all methods, a series of plots are shown to represent the effect of the input SNR.

2.5.2 Experimental data

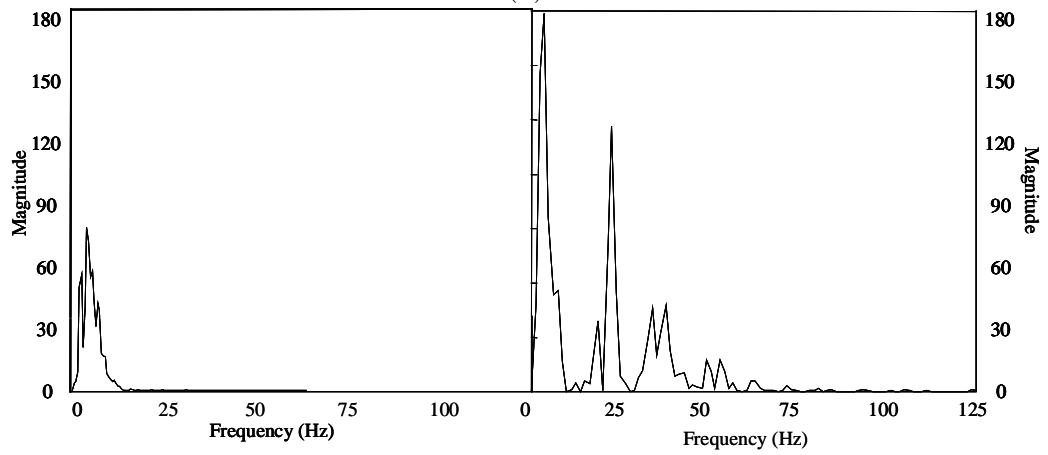
The experimental data was provided from the EEG Research Laboratory of Biophysics Department at the Hacettepe University Medical Faculty. Single sweeps were recorded from the left mastoid of eight subjects listening to

binaurally delivered stimuli via headphones. Vertex electrode was used as the reference. The pass-band of the amplifier was 0.3-70 Hz and the amplifier noise was $2 \mu V$. During the experiments, the subject was sitting on a chair in an electrically and acoustically shielded room. The stimuli were 1 *kHz* tones of 100 *msec* duration and 80 *dB* HL (Hearing Level) intensity, presented with an inter-stimulus interval of 2 sec. 512 single sweeps were acquired with a sampling rate of 250 samples/sec. The epoch length was 1 *sec* including a 200 *msec* pre-stimulus part. The SNR of a single sweep was found to be about -5 *dB*. To generate the pseudo-simulations, spontaneous EEG recordings were obtained from the same subject under the same experimental conditions but without using any stimulation.

The waveforms and power spectra of the grand average EP and a single sweep are shown in Figure 2.4. Note that, the EP is not visible in the single sweep and the power spectra overlap.



(a)



(b)

Figure 2.4: For experimental data (input SNR = -5 dB), a) the waveforms and b) frequency contents of the grand average EP and single noisy response.

2.5.3 Simulated data

A realistic auditory EP signal is generated by using the following EP model [121]:

$$s(n) = \sum_{r=1}^M [a_r \cos(\frac{2}{\pi}Trn) + b_r \sin(\frac{2}{\pi}Trn)] \quad (2.51)$$

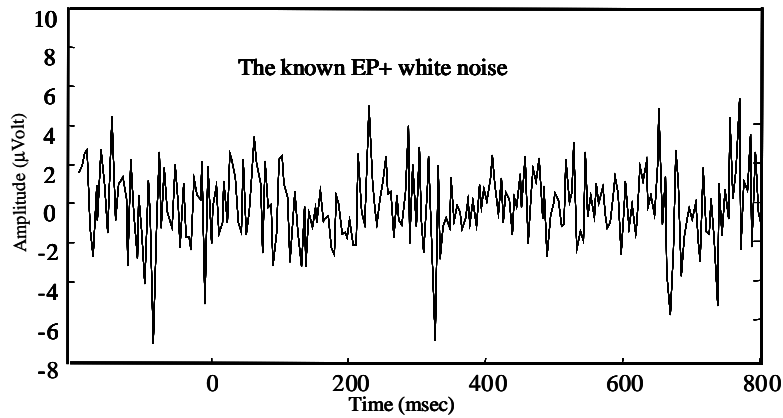
where n is the time index, T denotes the number of samples and M is the model order. To obtain a typical auditory EP signal, the model parameters are chosen for $T = 250$ and, $M = 4$, as follows:

$$\begin{aligned} a_1 &= 62, a_2 = -44, a_3 = -10, a_4 = 12, \\ b_1 &= -10, b_2 = -5, b_3 = 14, b_4 = -2 \end{aligned}$$

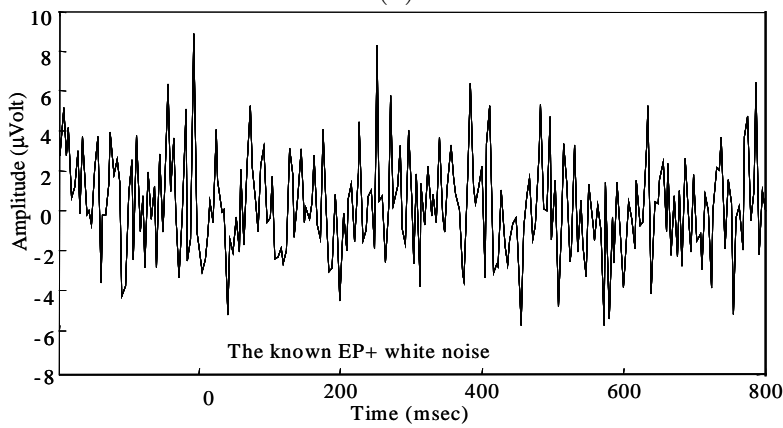
In the simulation studies, white noise sequences with different variances are added to the known auditory EP signal to obtain 40 noisy sweeps with a specific SNR. Examples of the generated noisy sweep waveforms are shown in Figure 2.5 (a) and (b), for SNR values of -5 dB and 0 dB, respectively. Note that, the auditory EP signal is not visible for both SNR conditions.

In the pseudo-simulation studies, spontaneous EEG sequences are added on the known auditory EP. The waveforms and power spectra of the simulated EP signal and the single noisy sweep (SNR is -5 dB) are shown in Figure 2.6. Note that, the EP signal is not visible in the single sweep and the power spectra overlap.

Figure 2.7 shows different waveforms of ensemble averages to illustrate the effect of the SNR on the EP signals. The noise fluctuations are apparent as the SNR decreases.

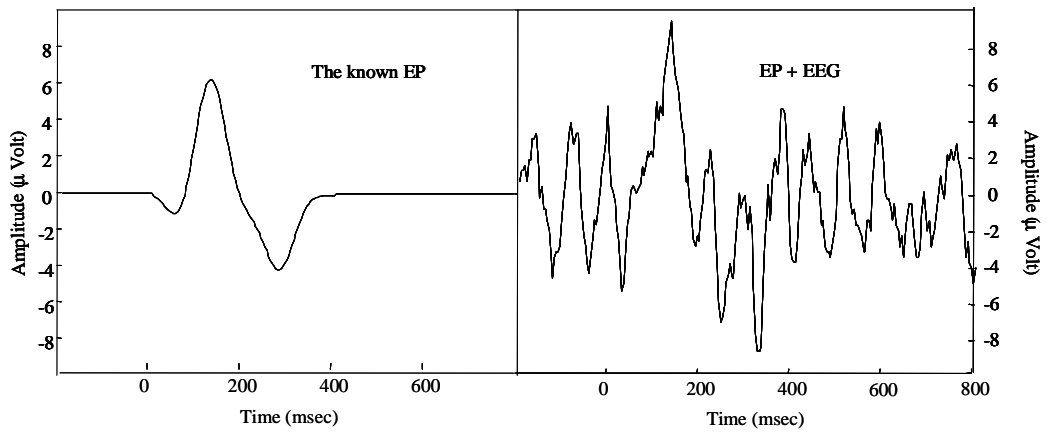


(a)

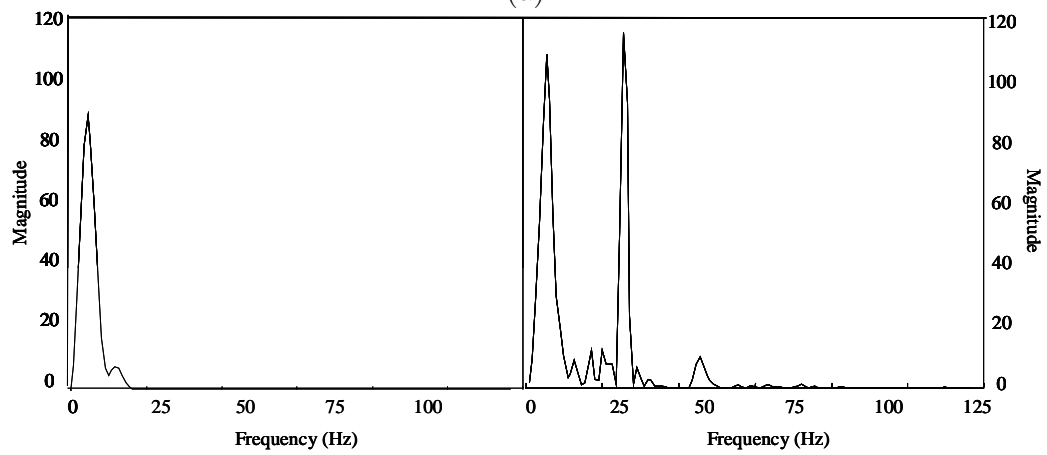


(b)

Figure 2.5: The waveforms of the single sweeps for simulations (the known EP + white noise) for a) input SNR = 0 dB, b) input SNR = -5 dB.



(a)



(b)

Figure 2.6: a) The waveforms and b) frequency contents of the known AEP and the noisy sweep (EP + EEG). (input SNR = -5 dB)

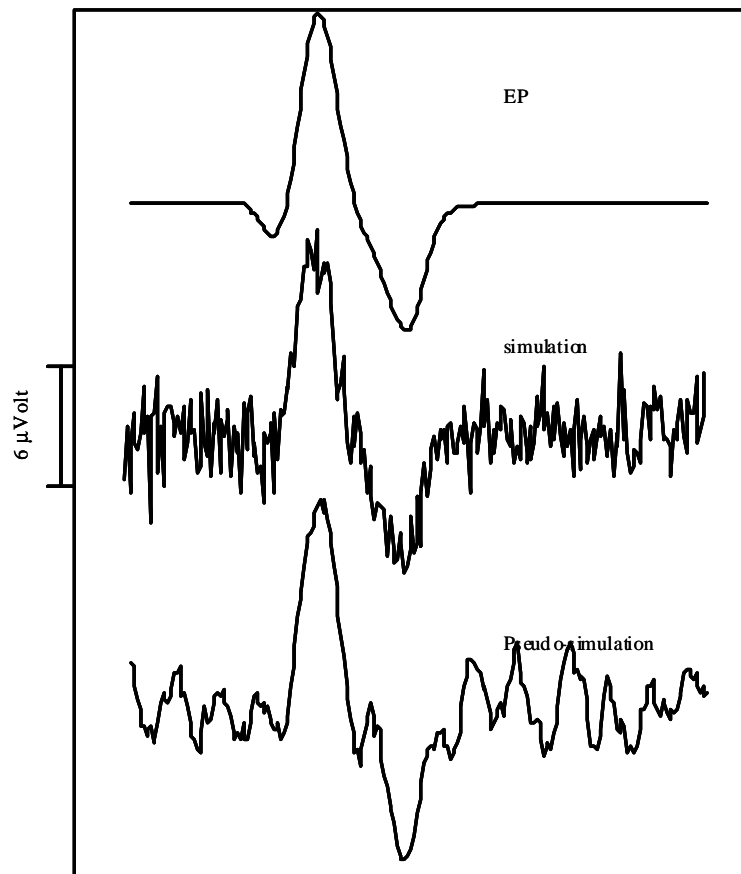


Figure 2.7: a) The known EP and average of 20 noisy sweeps corresponding to simulations and pseudo-simulations

2.5.4 Results with the SM in combination with Wiener Filtering Approaches (Group A)

Figure 2.8 (a) shows changes in the output SNR values for different number of sweeps used in the simulation study. It is observed that the SMCWWF provides superior results compared to EA. WF, WFSM and SMWF provide only a marginal improvement. No SNR improvements are observed for CWWF alone, thus the results are not given in these figures. Figure 2.8 (b) presents the output SNR versus input SNR plots for 20 sweeps. SMCWWF provides an output SNR which is about 13 dB above the values of the EA for all input SNR values. WF, WFSM and SMWF again provide only a marginal improvement. When input SNR is adjusted to 0 dB, the performances of the WF and EA are nearly the same. In addition, WFSM and SMWF provides almost the same performance under 0 dB SNR condition.

Figure 2.9 (a) shows changes in the output SNR values for different number of sweeps used in the pseudo-simulation studies. No SNR improvements are observed for WF. For 40 sweeps, the SMCWWF provides 45 dB of output SNR, whereas a 33 dB of output SNR is obtained by using the EA. For the first 20 sweeps, the algorithms in Group A do not have good performance. For more than 20 sweeps, both the SMWF and SMCWWF provide more SNR enhancement compared to the EA. Therefore, we adjust the input SNR for 20 sweeps and then the output SNR improvements are shown in Figure 2.9 (b). Both SMWF and SMCWWF are superior to the EA, whereas the WF and WFSM show poor performances. As the number of sweeps used in projections increases the output SNR of the single sweeps increases.

Figure 2.10 shows the waveforms of the estimated EPs in the simulation and pseudo-simulation studies when the input SNR is -5.5 dB and only 20 sweeps are used. Among the methods of Group A, the WFSM provides the most clear waveform in the simulation studies, whereas SMCWWF result is better in the pseudo-simulations.

Figure 2.11 (a) shows the changes in the output SNR values for different number of sweeps when experimental data are used. Both SMWF and SMCWWF provide higher SNR improvements compared to EA. In the case of WFSM, an SNR improvement is observed when the number of sweeps are increased up to 64. The waveforms of the estimations for 64 sweeps are given in Figure 2.11 (b). There are undesired noise fluctuations in both pre-stimulus and post-stimulus intervals when the methods in Group A are used. The main positive and negative peaks of the grand average are ob-

tained without distortion by using the SMCWWF and SMWF. However, the same estimation performance can not be observed by applying the WF and WFSM.

To find the maximum SNR that a method can achieve in the experimental studies, the number of sweeps is increased from 32 to 511 (the average of 512 sweeps is considered as the signal). The ensemble average yields an SNR of 68 dB for 511 sweeps and the methods of SMCWWF and SMWF reach to this value when only 128 sweeps are used. No further improvements are observed when the number of sweeps is increased beyond 128 sweeps. When the WFSM is used, the output SNR increases to 45 dB when 100 sweeps are used and remains constant even the number of sweeps is more than 100.

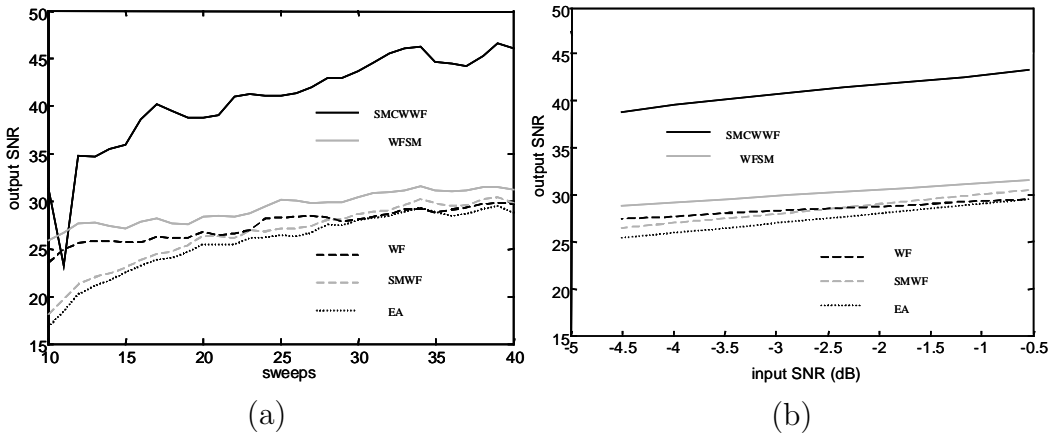


Figure 2.8: The simulation results for Group A: (a) Output SNR versus the number of sweeps, (b) output SNR versus the input SNR for 20 sweeps

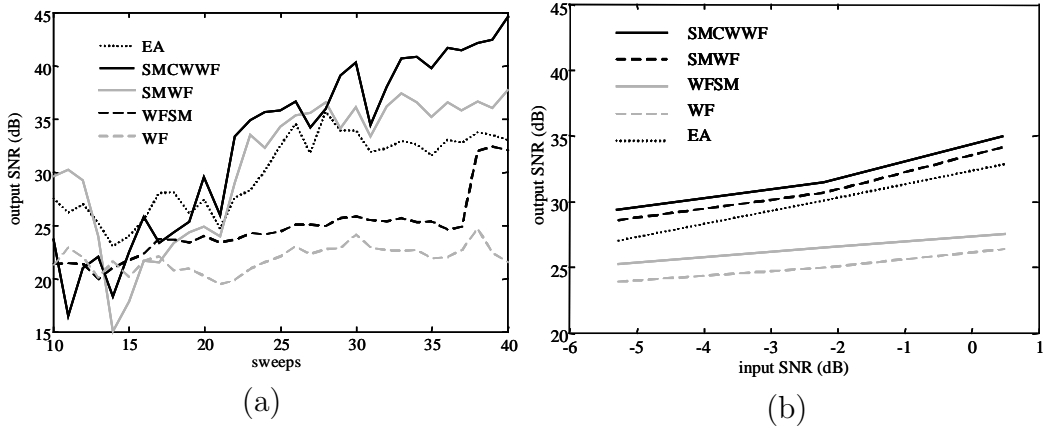


Figure 2.9: The pseudo-simulation results for Group A: (a) Output SNR versus the number of sweeps, (b) the output SNR versus the input SNR for 20 sweeps

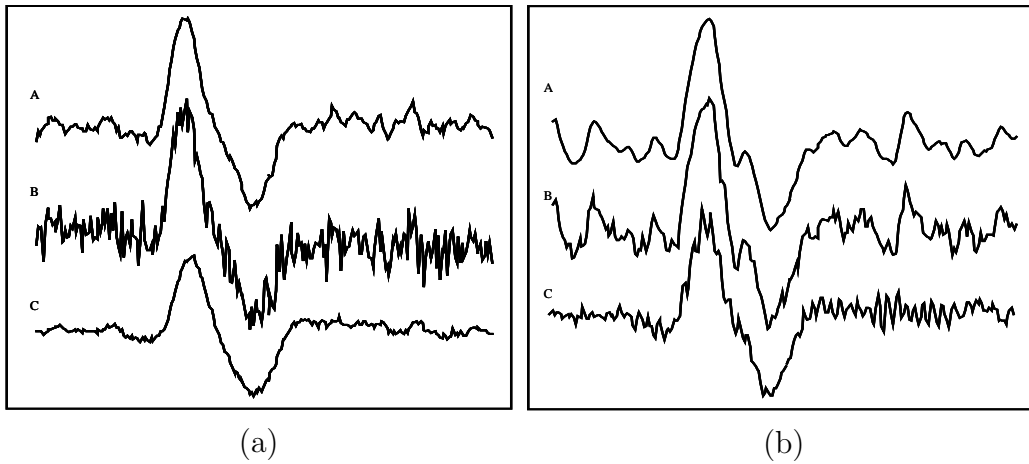


Figure 2.10: The waveforms of the estimations corresponding to the (a) simulation, (b) pseudo-simulation for 20 sweeps. The letters A, B and C refer the SMCWWF, SMWF and WFSM, respectively

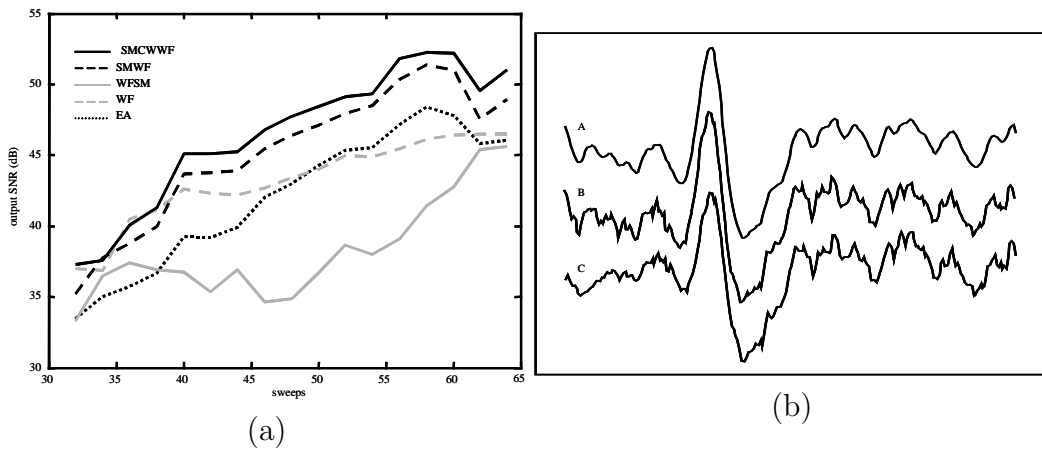


Figure 2.11: The experimental results for Group A: a) The output SNR versus the number of sweeps, b) The waveforms of the estimations for 64 sweeps. The letters A, B and C refer the SMCWWF, SMWF and WFSM, respectively.

2.5.5 Results with Standard Adaptive Filtering Algorithms (Group B)

In this study, the filter parameters are chosen empirically by using actual standard auditory data sets collected from 8 healthy volunteers. To determine the useful parameter sets roughly, two data sets are chosen and the number of sweeps used in the estimation process is increased from 32 to 128. A parameter set that provides maximum output SNR improvement is determined within their theoretical ranges (see Section 2.3). The optimal parameter set is explored by adjusting the parameters around this rough estimate. When a parameter set provides optimal estimation performance for all data sets, it is decided as the *optimal* parameter set. The same filter parameters are used in the simulation and pseudo-simulation studies.

It is observed that a filter length $M = 50$ is appropriate for all experimental data sets. Other filter parameters chosen for different algorithms in Group B are presented in Table 2.1. Note that, the adjusted parameter values may change depending on the variations of stimulus types and experimental conditions.

Table 2.1: The filter parameters chosen for the algorithms in Group B

filter parameters	μ	λ	δ	q_p	q_m	k_o
adjusted values	0.000011	0.001	0.1	100	0.1	0.2

Figure 2.12 (a) shows changes in the output SNR values for different number of simulated sweeps. Three algorithms in Group B, namely the RLS filter, the KF and SMLMS (the LMS filtering after SM), provide better SNR improvements when compared to the EA. When 10 sweeps are used, an SNR enhancement of 16 dB is obtained by using the RLS filtering. This high performance is preserved as the number of sweeps is increased. When 40 sweeps are used, it is possible to obtain an output SNR of 47 dB using the RLS filtering. However, the output SNR can only reach 28 dB with the EA. Figure 2.12 (b) presents the output SNR versus input SNR plots for 20 sweeps. For all algorithms, except the LMS filtering, the output SNR increases linearly for a wide range of input SNR values (-7.5 dB to 4 dB). We observe that there is a linear relationship between input SNR and output SNR improvement corresponding to the algorithms of the RLS, LMS and KF.

Figure 2.13 (a) shows changes in the output SNR values for different number of sweeps used in the pseudo-simulation studies. For all sweep numbers, the RLS filtering provides output SNR values about 5 dB above the corresponding SNRs obtained using the EA. The LMS filtering is found unsuccessful even when it is applied to the projected data. Figure 2.13 (b) shows the output SNR versus input SNR plots for 20 sweeps. The output SNRs obtained using the RLS and KF are above the corresponding ones obtained with the EA and increases linearly for all input SNR values. The slope for the KF is slightly greater than the slope for the RLS. The LMS filtering is found unsuccessful when only 20 sweeps are used (even for a high input SNR of 0 dB). When the LMS filter is applied to the projected version of data, the output SNR improves, yet it remains below the corresponding SNR value obtained using the EA. The improvement in the output SNR values is also influenced by the number of sweeps used for the projection. Increasing sweep number to 32 improves the performance notably.

Figure 2.14 shows the waveforms of the estimations in both simulations and pseudo-simulations obtained from 20 sweeps (the input SNR is -5.5 dB). For both studies, the most clear waveforms are obtained by using the RLS

and KF algorithms.

To understand the effect of step sizes, the LMS and SMLMS methods are applied to the experimental data using three different step sizes ($\mu_1 = 0.000011, \mu_2 = 0.000022, \mu_3 = 0.000044$). The corresponding output SNR improvements for increasing number of sweeps are shown in Figure 2.15 (a). We observe that the performance of the LMS filtering increases when the number of sweeps are increased. In addition, the sensitivity to the step-size decreases when the LMS filtering is applied after the SM. Figure 2.15 (b) shows the changes in the output SNR values for incremental number of sweeps when experimental data are used. The KF appears to have the best performance compared to the EA. When more than 20 sweeps are used, the KF provides an SNR enhancement of 15 dB compared to EA.

Figure 2.16 shows the estimated waveforms obtained by applying the algorithms in Group B to 64 actual sweeps. The KF provides the highest SNR improvement. The RLS filtering and the SMLMS method show nearly the same performance. The maximum SNR value (68 dB) is provided by the RLS filter and KF when only 128 sweeps are used and no further enhancements are observed when the number of sweeps is increased from 128 to 511. The output SNR increases to 45 dB when 100 sweeps are filtered by the LMS filtering and this SNR improvement remains nearly constant beyond 100 sweeps.

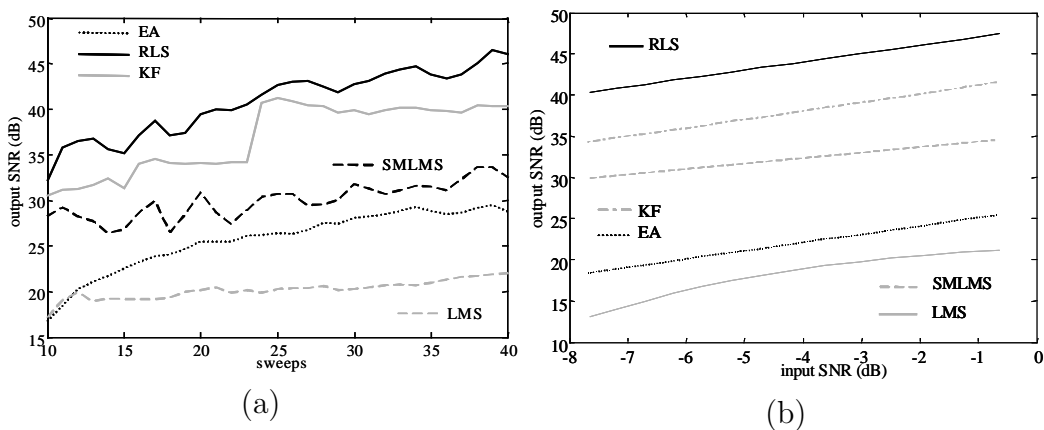


Figure 2.12: The simulation results for Group B: (a) Output SNR versus the number of sweeps, (b) output SNR versus input SNR for 20 sweeps

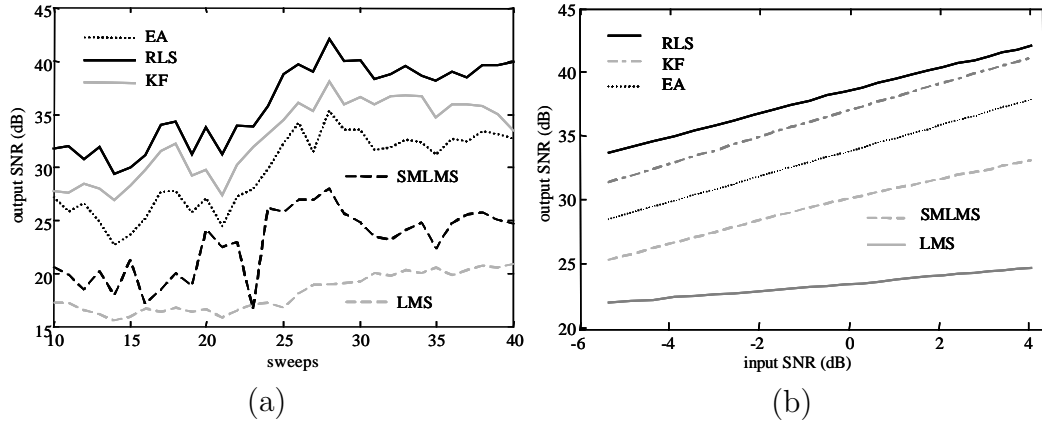


Figure 2.13: The pseudo-simulation results for Group B: (a) The output SNR versus the number of sweeps, (b) the output SNR versus input SNR for 20 sweeps

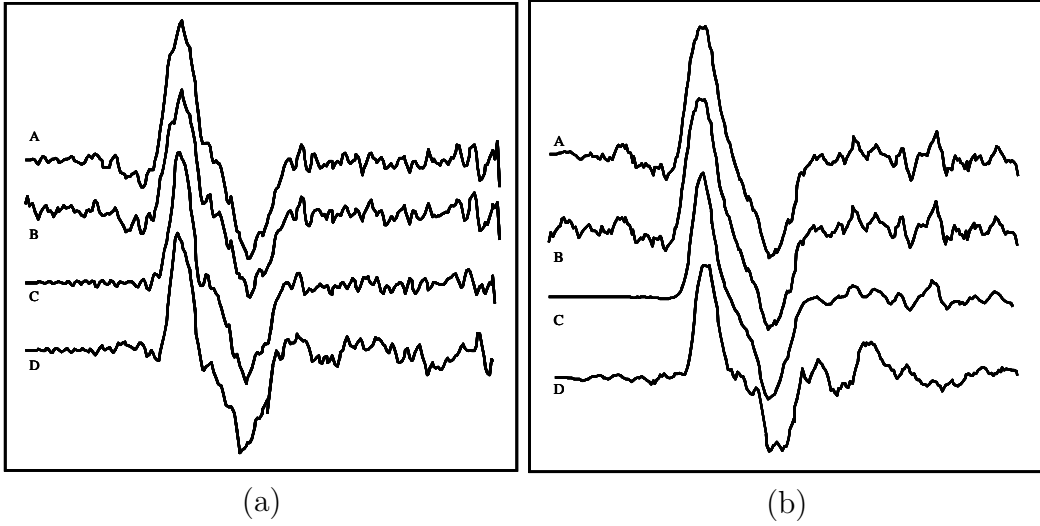


Figure 2.14: The waveforms of the estimations corresponding to the (a) simulations and, (b) pseudo-simulations for 20 sweeps. The letters A, B, C and D refer the RLS filtering, KF, SMLMS and LMS filtering, respectively.

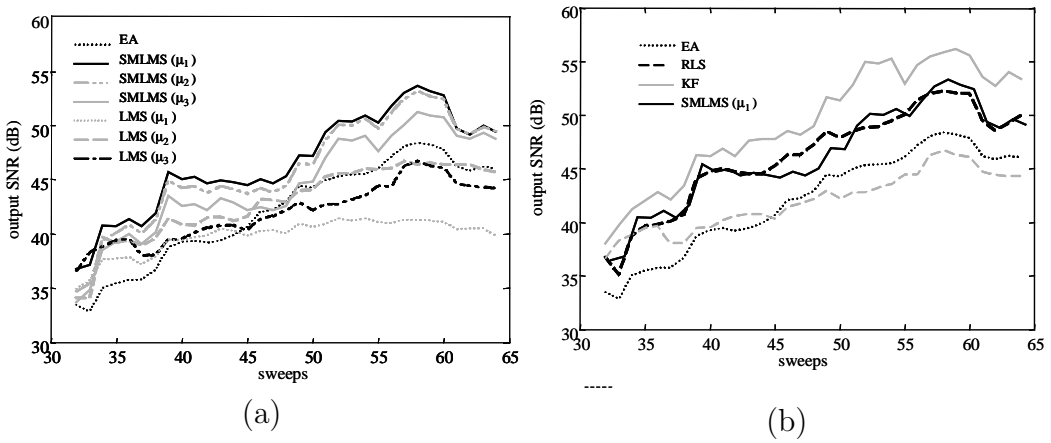


Figure 2.15: The experimental results for Group B: The output SNR versus the number of sweeps using (a) the LMS and SMLMS algorithms, (b) the other methods in Group B

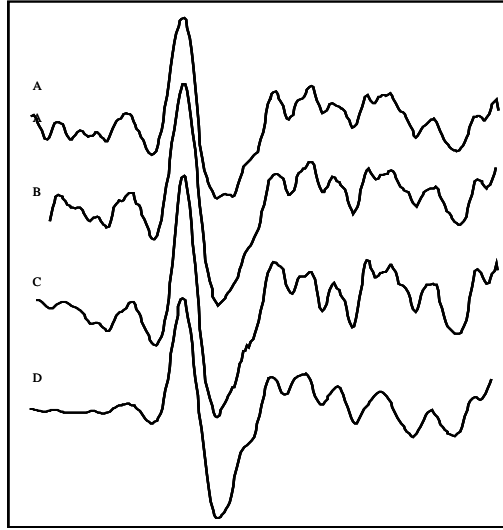


Figure 2.16: The waveforms of the estimations for experimental 64 sweeps. The letters A, B, C and D refer to the RLS filtering, KF, SMLMS and LMS filtering, respectively.

2.5.6 Results with Regularization Methods (Group C)

In the STR and SR methods, the same observation matrix \mathbf{H} is used for all data sets. The basis vectors, namely the columns of \mathbf{H} are chosen as the scaling functions associated with the Meyer wavelets [16]. This selection is based on the known auditory EP waveform. The basis vectors are formed to cover the estimated EP interval. The useful basis set is determined by testing both the STR and SR methods with the experimental data. The basis set is formed by shifting and dilating a reference scaling function (Figure 2.17). Initially 40 basis functions are generated by 10 dilations and 4 shifts (of one sample). Using this basis set, the output SNR improvements are recorded by increasing the number of sweeps from 32 to 128. To determine the optimal number of dilations, the number of dilations is decreased. For each of 8 actual data sets, the same SNR improvement is obtained when only 5 dilations are used. Thus, in simulations, pseudo-simulations and experimental studies 20 basis vectors are used to form \mathbf{H} .

The regularization parameter α is chosen by evaluating the Generalized Cross Validation (GCV) function using the regularization tools presented by Hansen [40].

In the application of the SR, the autocorrelation matrix corresponding to the input of the estimator (the average of small number of sweeps) is analyzed. The two eigenvectors corresponding to the two largest eigenvalues of the autocorrelation matrix form the columns of \mathbf{H}_s .

Figure 2.18 (a) shows changes in the output SNR values for different number of sweeps used in the simulation study. Both the STR and SR methods provide about 20 dB more SNR than the EA for all number of sweeps. Figure 2.18 (b) shows the output SNR versus input SNR for 20 sweeps. Both the STR and SR methods keep the same performance for all input SNR values. Figure 2.19 (a) shows the output SNR versus the number of sweeps for the pseudo-simulation study. Both regularization methods appear to be more successful in comparison with the EA. The difference between the performances of the STR and SR methods get larger in the pseudo-simulations. For 40 sweeps, an output SNR of 49 dB is obtained by the STR method, whereas it is 33 dB when the EA is applied. Figure 2.19 (b) presents the output SNR versus input SNR plots for 20 sweeps. There is a linear relationship between the performance of the methods and input SNR in both simulations and pseudo-simulations. The STR shows better performance in the pseudo-simulation studies whereas the performance of the SR degrades.

The waveforms of the estimations obtained in the simulation and pseudo-simulation studies are given in Figure 2.20. For these estimations, 20 sweeps are used and the input SNR is assumed as -5.5 dB. In the simulation study, almost the same waveforms (which perfectly match the waveform of the known auditory EP) are obtained by using STR and SR whereas they are different in the pseudo-simulations. Some undesired fluctuations on both pre-stimulus and post-stimulus intervals remain when the SR is used whereas almost the whole noise component is perfectly removed when the STR is applied.

Figure 2.21 (a) shows the changes in the output SNR values for different number of sweeps when the experimental data are used. As the number of sweeps increases, the performance of the STR and SR increase rapidly and they perform better than the EA after the first 35 sweeps. The waveforms of the estimations for 64 sweeps are given in Figure 2.21 (b). Almost the same waveforms, very similar in shape to the grand average EP, are estimated by using the STR and the SR methods.

To find the maximum SNR that a method can achieve in the experimental studies, the number of sweeps is increased from 32 to 511. Both methods reach to the maximum output SNR value of 68 dB when only 128 sweeps are used and no major enhancements are observed when the number

of sweeps is increased beyond 128.

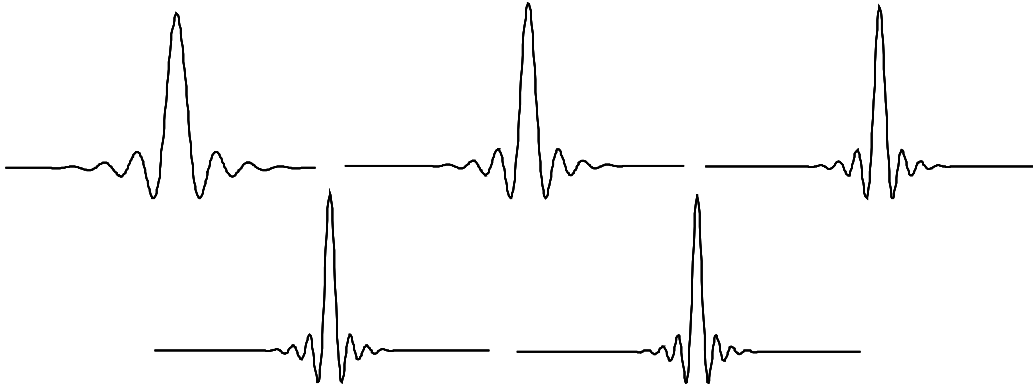


Figure 2.17: Selected basis vectors of \mathbf{H} .

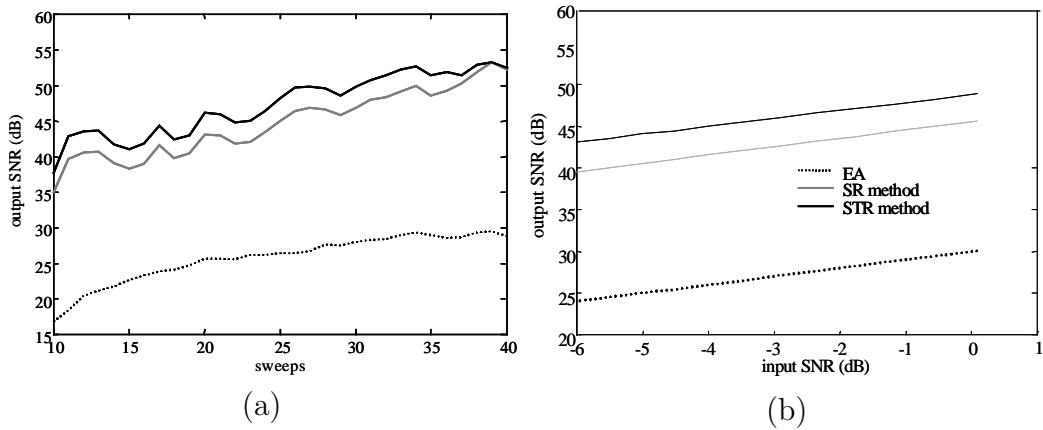


Figure 2.18: The simulation results for Group C: (a) Output SNR versus the number of sweeps, (b) output SNR versus input SNR for 20 sweeps

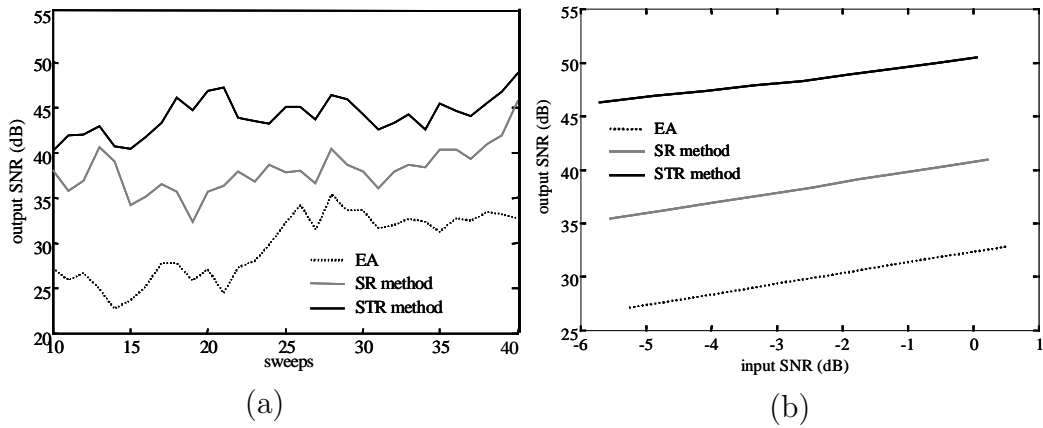


Figure 2.19: The pseudo-simulation results for Group C:(a) Output SNR versus the number of sweeps, (b) output SNR versus input SNR for 20 sweeps

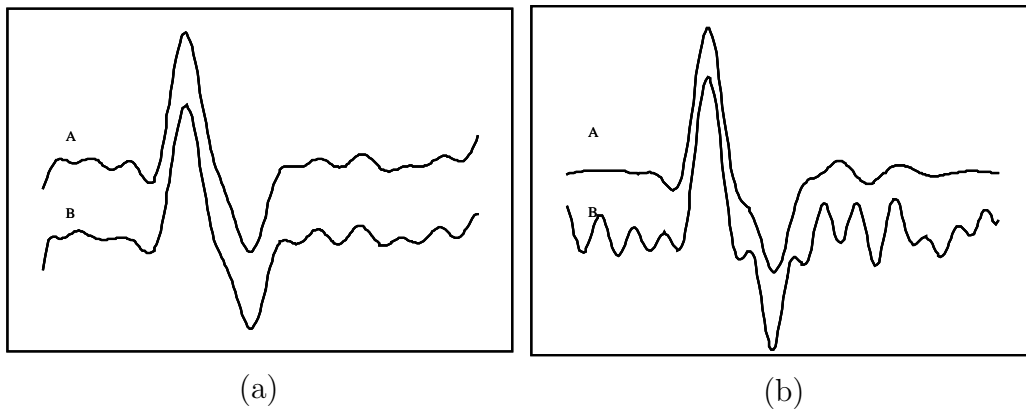


Figure 2.20: The waveforms of the estimations corresponding to a) the simulation study and b) the pseudo-simulation study. The letters A and B refer the STR and SR methods, respectively

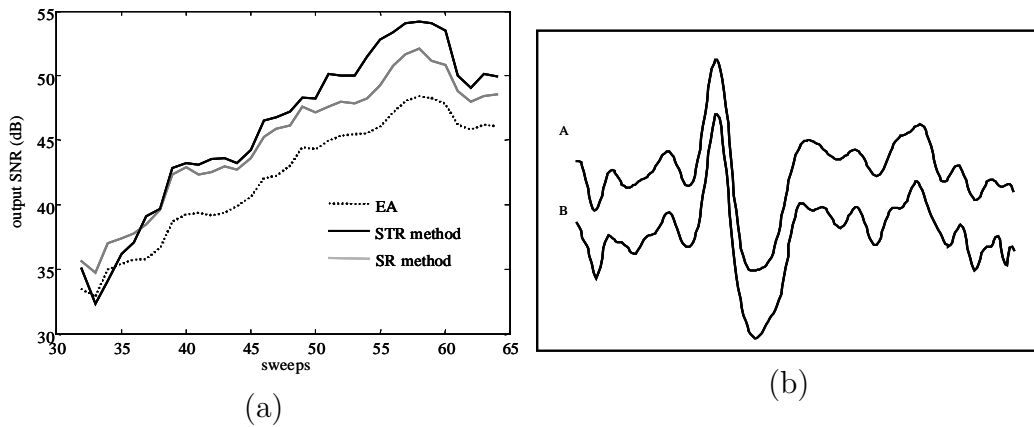


Figure 2.21: The experimental results for Group C: a) The output SNR versus the number of sweeps, b) the waveforms of the estimations for 64 sweeps

2.5.7 Computational Complexity

The computational complexity [14] of the discussed algorithms is investigated from various sources [44, 86, 64]. To compare the algorithms in that respect, the total number of floating point operations is chosen as a complexity measure (O). Table 2.2 presents the corresponding measures for different algorithms. Here N denotes the number of samples at each sweep, M is the number of weights in the related filter, and L is the number of sweeps.

It is observed that, the LMS filtering algorithm and WF have the lowest, whereas Tikhonov Regularization methods has the highest computational complexity. However, for specific parameter values (for example, $N = 250$ $M = 50$ $L = 60$) the computation times in an average personal computer is in seconds. Thus, as long as the number samples N is on the same order, all algorithms can be assumed to be computationally efficient.

Most of the basic estimation techniques show definitely better performance compared to EA in extracting the EPs. The KF or the STR effectively reduce the experimental time (to one-fourth of that required by EA). The SM is a useful pre-filter to significantly reduce the noise on the raw data.

Table 2.2: The computational complexities of the algorithms

method	O
SM	$O(NL^2)$
WF	$O(M^2)$
LMS	$O(M)$
RLS/KF	$O(M^2)$ (each iteration)
STR/SR	$O(N^3)$
CWWF	$O\left(\frac{N}{2}\log_2(N)\right)$ (each iteration)

The significance of this comparison study can be summarized as follows: The KF and STR are computationally inexpensive tools to extract the template auditory EPs and should be used instead of EA. They provide a clear template auditory EP for various analysis methods. To reduce the noise level on single sweeps, the SM can be used as a pre-filter before various single sweep analysis methods.

CHAPTER 3

SINGLE SWEEP AUDITORY EP EXTRACTION

In this thesis study, we propose a new approach for single sweep auditory EP estimation. In the proposed hybrid algorithm, the SM and a wavelet domain filter named as Modified Scale Space Filter (MSSF) are used consecutively (Figure 3.1). Firstly, large amount of EEG noise on the raw data is removed by using the SM as a pre-filter. The WT coefficients corresponding to the signal and noise becomes distinguishable due to SNR improvement after the projection process. Thereafter, less-noisy single sweeps are filtered in the wavelet domain by using MSSF. The new approach is tested with pseudo-simulations and experimental studies. The basic components of the new approach are introduced in the following subsections.

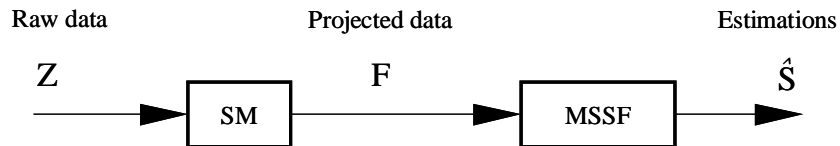


Figure 3.1: The proposed approach for single sweep AEP estimation

3.1 The Modified Scale Space Filtering

Singularities provide important features of signals. In mathematics, a singularity of a function is, in general, a point at which the derivative does not

exist, whereas the function is differentiable at every neighborhood point. The singular structure of a function $f(x) \in \mathbf{L}^2(\mathbf{R})$ is characterized by Lipschitz exponents and can be detected through the WT [78]. The Lipschitz exponent is defined as a generalized measure of the differentiability or regularity of f (If f can be locally approximated by a polynomial, then it is regular.) [16].

The WT of a function $f(x) \in \mathbf{L}^2(\mathbf{R})$ is defined as

$$Wf(s, x) = f(x) \star \psi_s(x) \quad (3.1)$$

where $\mathbf{L}^2(\mathbf{R})$ denotes the vector spaces of measurable, square-integrable one dimensional functions. Here $\psi_s(x)$ is a dilated version of $\psi(x)$ such that $\psi_s(x) = \frac{1}{s}\psi\left(\frac{x}{s}\right)$. x and s indicate the location and scale index. In smaller scales, the high frequency components of f are observed. Thus, the time resolution is high in small scales, the frequency resolution is high in the large scales. The set of couples (s, x) is called the *scale-space* plane. If the function f has N samples, the largest scale is $s = N$ [79].

Any point (s_0, x_0) in the scale-space is called *modulus maximum* (MM) if $|Wf(s_0, x)| < |Wf(s_0, x_0)|$ when x is in either to the right or left neighborhood of x_0 [79]. The chain of MM across scales in the scale-space plane is called *modulus maxima line* [79]. A remarkable property of MMs is their ability to characterize the Lipschitz regularity of f . If Lipschitz exponent of $f(x)$ is negative (positive) at a certain location x , then the amplitudes of the MMs increase (decrease) as the scale decreases. If it is 0, then the maxima values remain constant over a large range of scales.

If the decay behavior of the MMs corresponding to signal and noise singularities are different, then this information can be used for extracting an approximate signal information from a noisy signal [78, 77]. The Lipschitz exponent of White noise is shown to be negative, whereas the signal has singularities with positive Lipschitz exponents. Thus the MMs corresponding to singularities of signal (noise) decrease (increase) as the scale decreases. For low SNR, the MMs in small scales are mostly dominated by noise. Thus, it is difficult to use the MMs at small scales to recover the signal. The original signal corrupted with noise was approximated by using WT and an alternate projection algorithm [78]. This approximation does not require that the noise is white. Another de-noising algorithm (WT scale-space filter (WTSSF)) based on distinguishing signal and noise singularities from the WT MM lines was also presented in [131].

In the EP research area, detecting the WT coefficients created by the EP signal or EEG noise has already been applied for the EP estimation [9, 103,

105, 115]. In those studies, commonly, the WT coefficients corresponding to signal are identified with respect to the WT of a template EP. For single-trial EP estimation, the WT coefficients other than the ones identified from the template EP are set to 0. However, since the template EP is still noisy, the validity of this approach is questionable. In another study, the above given ideas, i.e., the singularity characteristics of the EEG and EP signals were explored. It was shown that the EEG noise has singularities whose Lipschitz exponents are almost negative, whereas the Lipschitz exponents of the EP signal singularities are positive [129]. The EP signal is extracted by the alternate projection algorithm after removing the maxima that do not propagate to larger scales.

In the present study, firstly, the WTSSF is applied to estimate auditory EPs in combination with the SM. Application of the SM identifies the WT coefficients created by the noise more methodologically. Although this approach yields SNR improvement, it does not provide the true EP waveform. The resultant signals in the pre- and post-stimulus intervals carry undesired fluctuations. To distinguish the WT coefficients corresponding to the EP signal and the background EEG noise more accurately, this algorithm is modified. In the WTSSF, a *scale correlation function (scf)* is adopted to enhance the MMs originated by the signal. In fact, this algorithm is originated from a Wavelet Transform domain filter (WTDF) that is introduced to remove the Gaussian distribution white noise from the noisy signal that contains very sharp edges [127]. Since the WT coefficients created by sharp edges have much higher correlation between scales than the WT coefficients created by the noise, the *scf*, that is, the multiplication of wavelet coefficients at adjacent scales, is used to identify the sharp edges in the WTDF citeXu1994. The algorithm of the WTDF, so called an edge extraction technique, is given in Table 3.1. Here, $corr2(m, n)$ refers the *scf* and m and n indicates the scale and time index, respectively. This procedure, which use dyadic WT, is demonstrated for a large boxcar having two sharp edges and two small bumps as shown in Figure 3.2. Since the data has 256 points, dyadic WT is performed for 8 scales. Note that, the WT is correlated across scales since sharp edges creates high amplitude coefficients. The two sharp edges are extracted after the first iteration. The two small bumps are extracted after the second iteration. The first iteration of the filtering algorithm is demonstrated graphically in Figure 3.3 showing how the *scf* highlights the edges.

```

First, Save a copy of  $W(m,n)$  to  $WW(m,n)$ 
Initialize the "spatial filter mask":  $mask(m,n)$  to 0's

Loop for each wavelet scale  $m$ 
{
  Loop for the iteration process
  {
    Compute the power of  $Corr2(m,n)$  and  $W(m,n)$ :
     $PCorr(m) = \sum_n Corr2(m,n)^2$ 
     $PW(m) = \sum_n W(m,n)^2$ 

    Re-scale the power of  $Corr2(m,n)$  to that of  $W(m,n)$ :
    Loop for each pixel point  $n$ 
    {
       $new\ Corr2(m,n) = Corr2(m,n) * \sqrt{\frac{PW(m)}{PCorr(m)}}$ 
    } end loop  $n$ 
    Loop for each pixel point  $n$ 
    {
      Compare pixel values in new  $Corr2(m,n)$  and  $W(m,n)$ :
      if  $|Corr2(m,n)| > |W(m,n)|$ 
      {
        Extract edge information from  $W(m,n)$  and  $Corr2(m,n)$ ,
        and save it in the "spatial filter mask":
         $Corr2(m,n) = 0.0$ 
         $W(m,n) = 0.0$ 
         $mask(m,n) = 1$ 
      } end if
    } end loop  $n$ 
  } iterate until  $PW(m) \leq$  the noise threshold at scale  $m$ 
  Apply the "spatial filter mask" to the saved copy,  $WW(m,n)$ ,
  at scale  $m$ . Save the filtered data to  $Wnew(m,n)$ :
  Loop for each pixel point  $n$ 
  {
     $Wnew(m,n) = mask(m,n) * WW(m,n)$ 
  } end loop  $n$ 
} end loop  $m$ 

```

Table 3.1: The algorithm of the WTDF (adapted from [127])

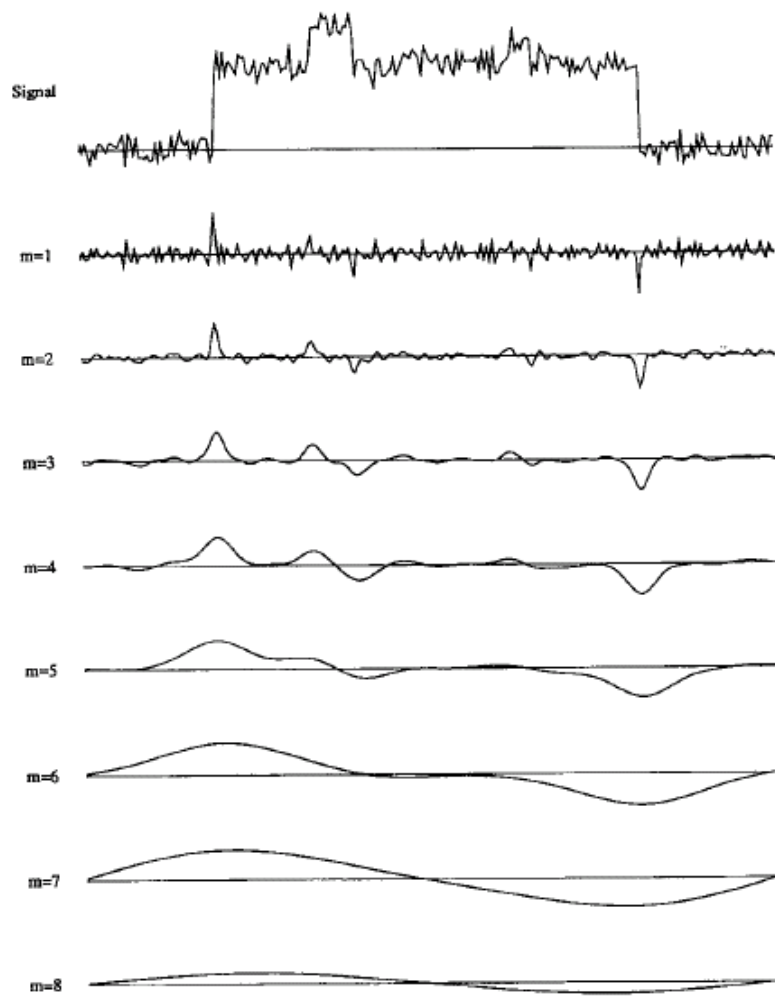


Figure 3.2: An example of detecting sharp edges using WTDF: dyadic WT coefficients at 8 scales of a large boxcar, (adapted from [127])

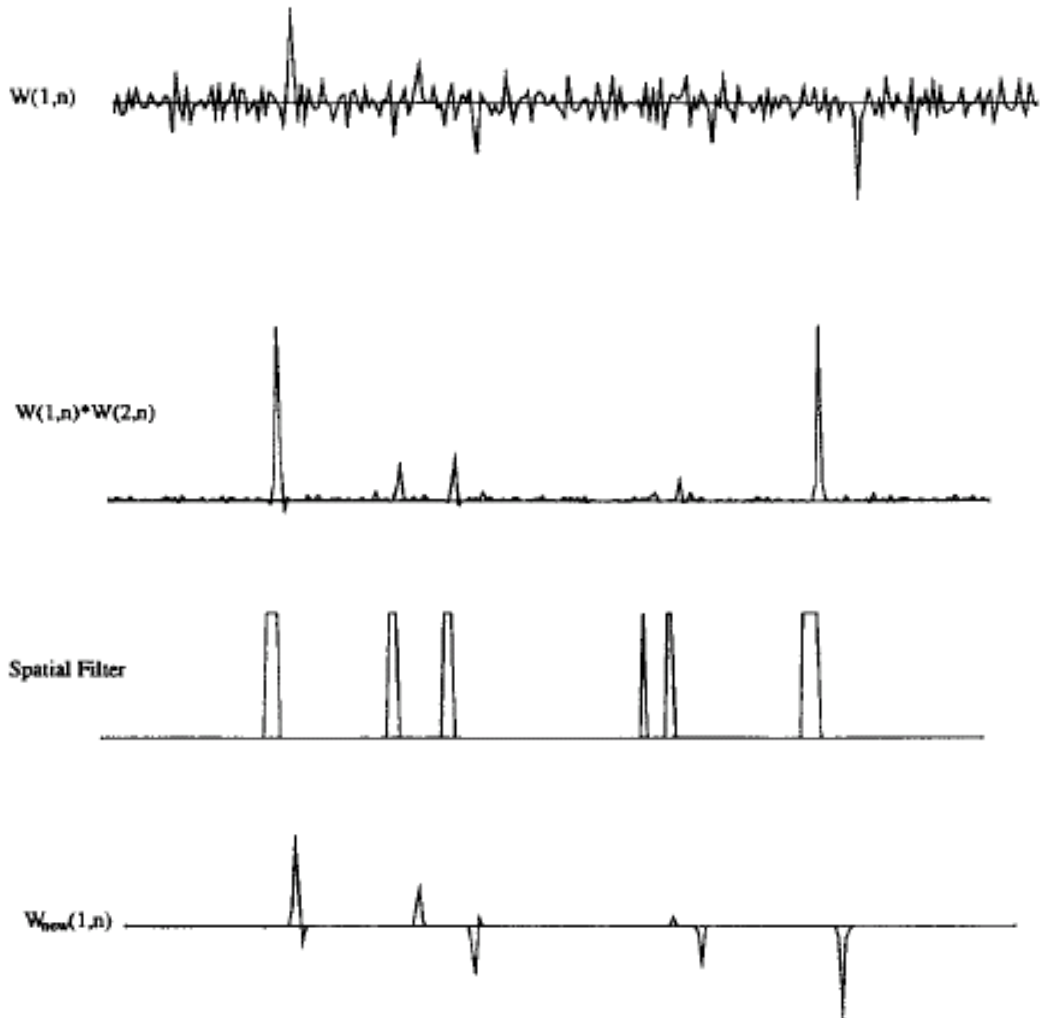


Figure 3.3: Graphical illustration of the WTSTF algorithm: WT coefficients at the first scale before filtering, the *scf* for the WT coefficients at the first and second scales, the spatially selective filter mask and WT coefficients at the first scale after filtering (shown from top to bottom)(adapted from [127]).

```

Initialize:
  wb(m, n) = wc(m, n)
  scale filter: sfilter(m,n) = [0]
  scr2(m, n) = wc(m, n) × wc(m + 1, n) m ≤ J, n = 1, 2, ... N
Loop for signal modulus maxima extraction:
  loop for iteration
  {
    loop for scale m
    {
      if m ≤ S
        mscr(m) = max1 ≤ n ≤ N (|scr2(m, n)|)
        mwc(m) = |wc(m, n)|, where |scr2(m, n)| = mscr(m)
        loop for sample n
        {
          scr2b(m, n) = scr2 (m, n) × (mwc/mscr)
        } end loop n
      else
        pscr(m) = ∑n scr2(m, n)^2
        pwc(m) = ∑n wc(m, n)^2
        loop for sample n
        {
          scr2b(m,n) = scr2(m,n) × √(pwc(m)/pscr(m))
        } end loop n
      end if
    } end loop m
  } end iteration
Scale space filtering:
  loop for scale m
  loop for sample n
  {
    Wnew(m, n) = sfilter(m, n) × wb(m, n)
  }
  end loop n
  end loop m

```

Table 3.2: The algorithm of the WTSSF (adapted from [131])

In the algorithm of WTSSF, a re-scaling scheme was proposed to remove the WT coefficients created by the noise within an algorithm as given in Table 3.2. Here M denotes the small scale limit where the noise power is assumed relatively high. Such scales correspond to the high frequency components in the Fourier domain. M is determined using the following formula [131]:

$$M = \log_2 \frac{f_m}{f_u} - 1$$

where f_m is the sampling frequency and f_u is the maximum frequency in the frequency range of the signal which is roughly estimated from the power spectral density of the noisy data.

In this thesis study, we attempt the WTSSF for single sweep auditory EP extraction by using real WT instead of dyadic WT to obtain time/frequency resolution as high as possible. As well, the WTSSF is modified and the adopted filter is named as the *modified* scale-space filter (MSSF). In the MSSF, we utilize the ratio between the WT coefficients at adjacent scales. Correspondingly, we define a ratio function rf instead of the scale correlation function scf used in the WTSSF to select the WT coefficients created by the EEG noise more accurately. Thus, the algorithm is as follows:

1 computation of the ratio function rf :

$$rf(x, s) = \frac{Wf(x, s+1)}{Wf(x, s)}, \quad s = 1, \dots, S, \quad x = 1, \dots, N$$

2 normalization of the ratio function:

$$nrf(s, x) = cf(s, x) \sqrt{P_{Wf}(s) / P_{rf}(s)}, \quad s = 1, \dots, M$$

$$nrf(x, s) = cf(x, s) \frac{M_{Wf}(s)}{M_{rf}(s)} \quad s = M+1, \dots, S$$

where

$$\begin{aligned} M_{Wf}(s) &= \max |Wf(x, s)| \\ M_{rf}(s) &= \max |rf(x, s)| \end{aligned}$$

3 selection of the WT coefficients originated by the noise:

$$Wf(s, x) = 0 \quad |Wf(s, x)| \leq |nrf(s, x)|$$

4 return to step (1) and perform re-filtering iteratively.

Both the WTSSF and the MSSF can be applied iteratively. In this study, we use *frame iteration (fi)* (i.e., starting a new iteration after each scale is filtered) and *scale iteration (si)* (i.e., repeating the filtering operation for each scale) for both algorithms.

3.2 Results

In this study, the proposed scale space filtering approaches are tested with pseudo-simulations and experimental data.

3.2.1 Pseudo-Simulation Study

In the pseudo-simulations, the recorded EEG sequences are added to the known data sets. The performance of the scale space approaches are tested for two data sets: 1) with no latency and amplitude variations in single sweeps, 2) with latency and amplitude variations.

In the first case, two small bumps are placed on the pre- and post-stimulus intervals of the reference EP signal. These are generated to avoid similarity between the waveforms of the wavelet function and a typical auditory EP signal. In the second case, an ideal waveform is generated.

Case 1: Estimating single-sweeps when there is no latency and amplitude variations

The template EP signal is obtained by using the EP model (see Equation 2.51) which is represented by a dynamic Fourier series [121]. To obtain a typical auditory EP signal, the model parameters are chosen as follows:

$$\begin{aligned} a_1 &= 2.72, a_2 = -3.4, a_3 = -0.34, a_4 = 0.034, \\ b_1 &= 0.068, b_2 = -0.34, b_3 = 0.68, b_4 = -0.068 \\ T &= 250, M = 4, k = 1, \dots, 250 \end{aligned}$$

Since no latency variations are assumed on single sweeps, only the first largest eigenvector can be used in the SM to project the raw data. Figure

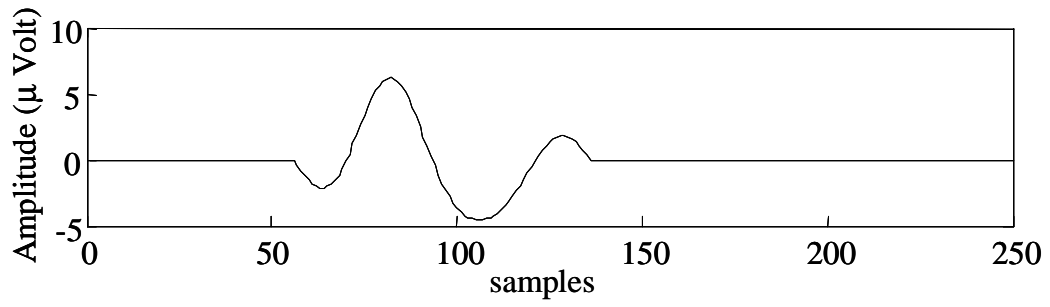
3.4 and 3.5 shows the waveforms, real WT coefficients and their MM spectrums corresponding to the generated EP signal and the projected sweep, respectively. Since the projected data contains noise fluctuations, large number of MMs are observed besides three main MM lines created by the signal edges. In the small scales (first 20 scales), there are a large number of non-zero coefficients associated with the projected data, whereas those coefficients are zero for the generated EP signal.

Both MSSF and WTSSF are applied to the projected data using scale iterations and frame iterations. The resulting output SNR improvements are shown in Figure 3.6. As the number of iterations increases, the best performance is obtained for the MSSF when the frame iterations are used. It is observed that, the performance of MSSF increases linearly as the iteration number is increased. The WTSSF shows a peak at the 4th iteration when the frame iterations are used.

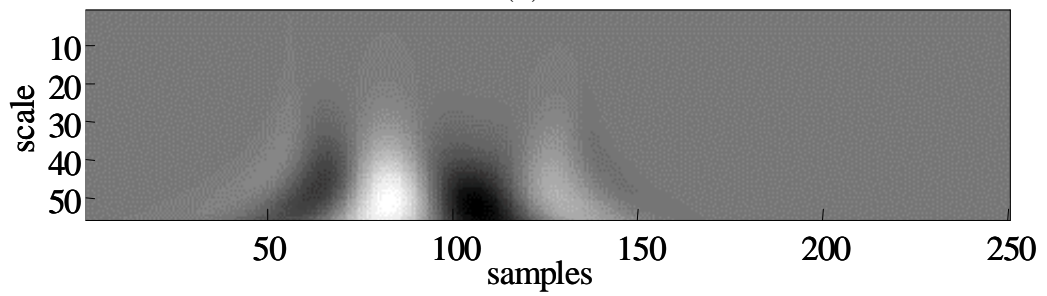
The sequences related to the MSSF and the WTSSF after two iterations are demonstrated in Figure 3.7 and 3.8, respectively. It is seen that, different coefficients are set to zero in these algorithms. This led to different estimation performances.

The waveforms of the estimations are shown in Figure 3.9. Each single sweep in the projected data is filtered by the WTSSF and the MSSF (si is performed 14 times in the MSSF and, fi is performed 3 times in the WTSSF).

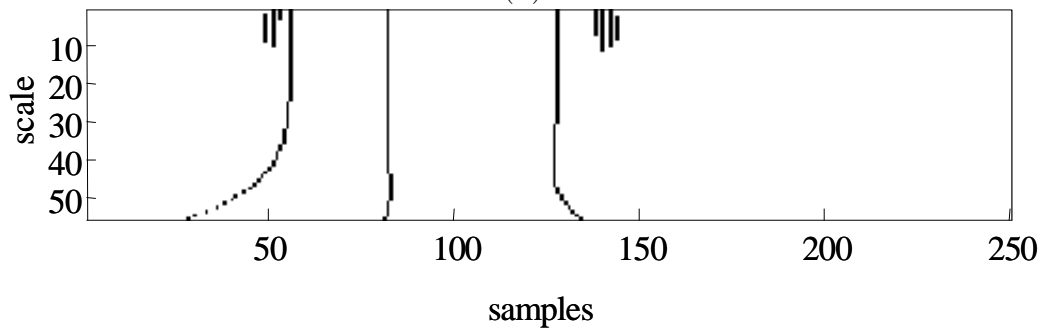
Another filtering approach may be setting the coefficients of small scales lower than a threshold to zero. For this purpose, average of 10 sweeps (template EP) is transformed in the wavelet domain and the threshold is estimated from that real WT coefficients. Similarly, a threshold is obtained from the wavelet coefficients of the projected single sweep. The signals reconstructed using the remaining coefficients are compared with the ones obtained using the scale space filtering approaches discussed in this study. The most clear and adequate signal waveform is obtained by using the MSSF. The other estimations contain undesired fluctuations in the pre- and post-stimulus intervals of the recovered signal.



(a)

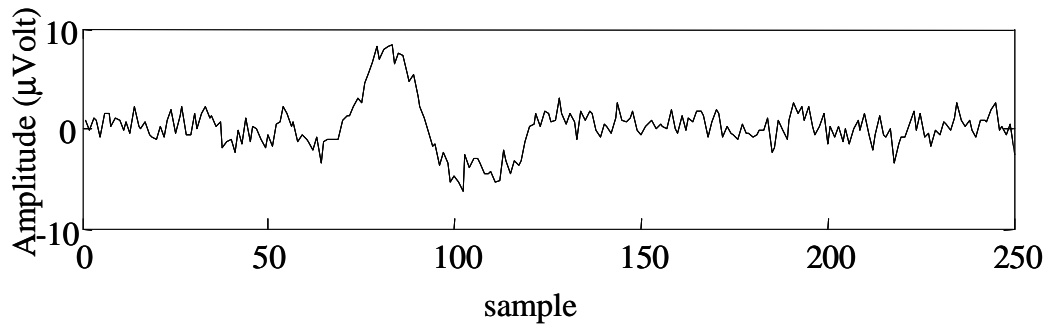


(b)

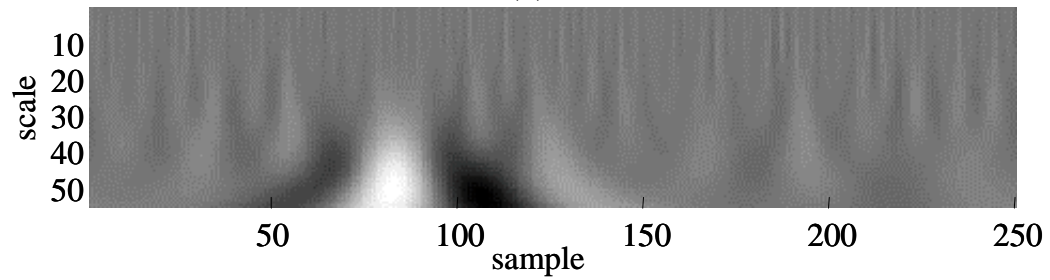


(c)

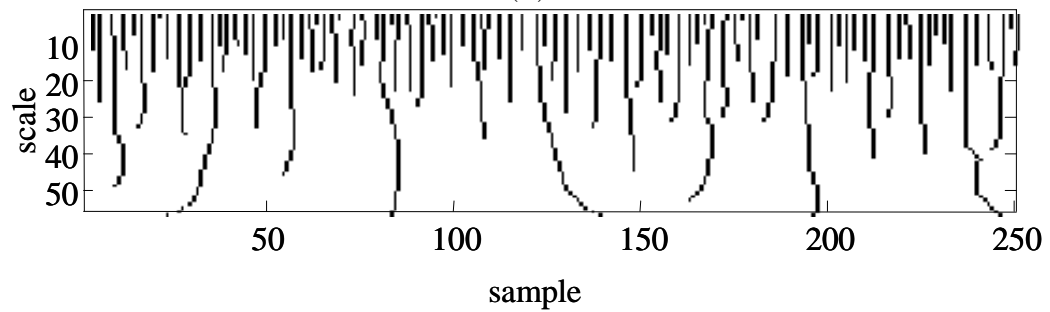
Figure 3.4: (a) The waveform, (b) image of the WT coefficients (c) and the MM spectrum corresponding to the generated EP signal.



(a)



(b)



(c)

Figure 3.5: (a) The waveform, (b) image of the WT coefficients (c) and the MM spectrum corresponding to the projected data.

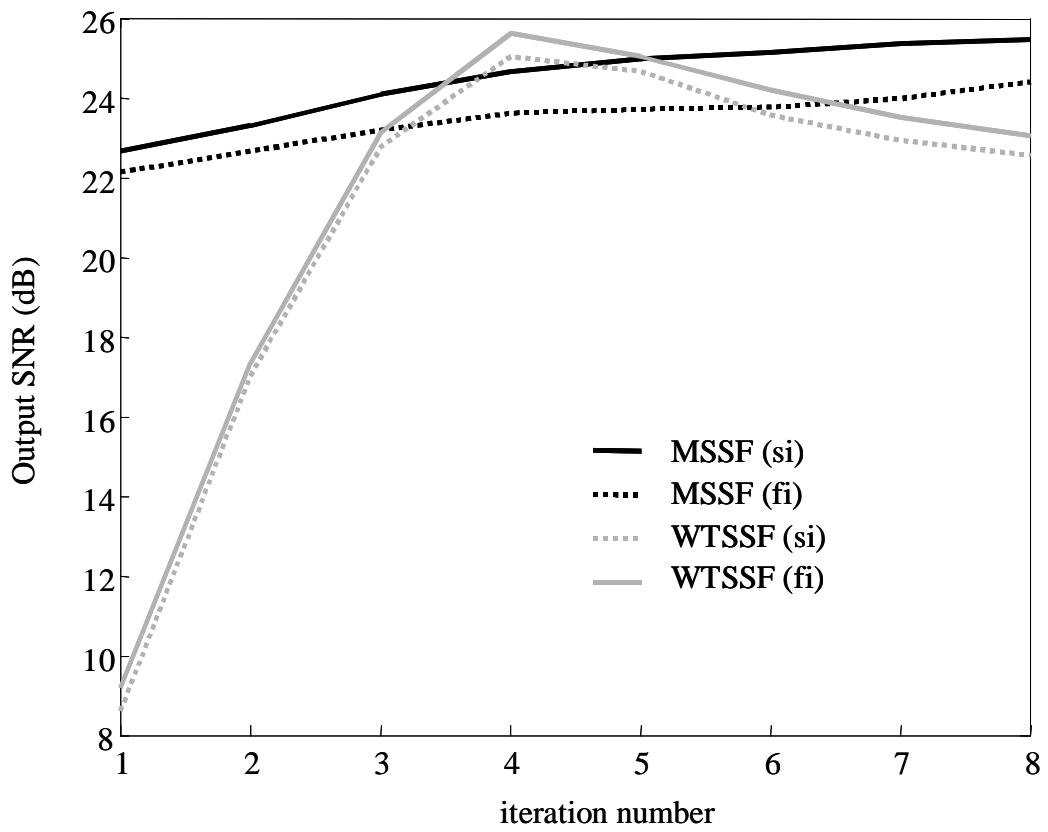


Figure 3.6: The output SNR improvements versus iteration number

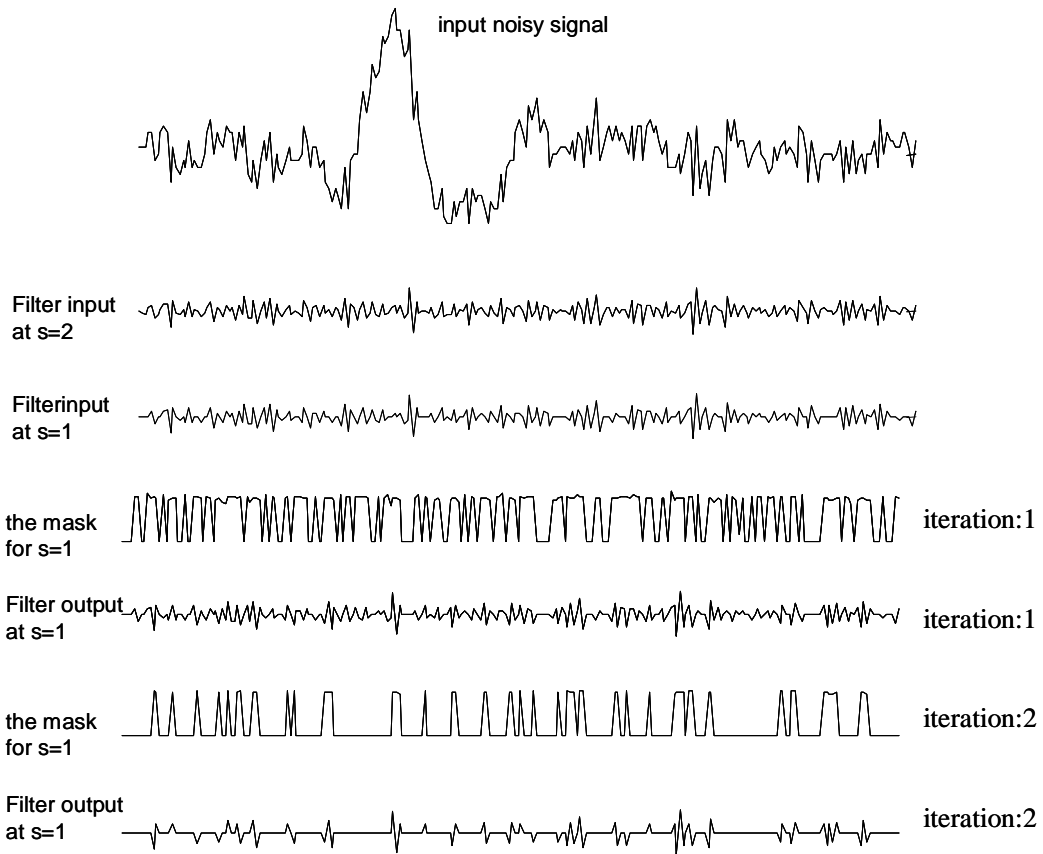


Figure 3.7: The sequences related to the MSSF with s_i

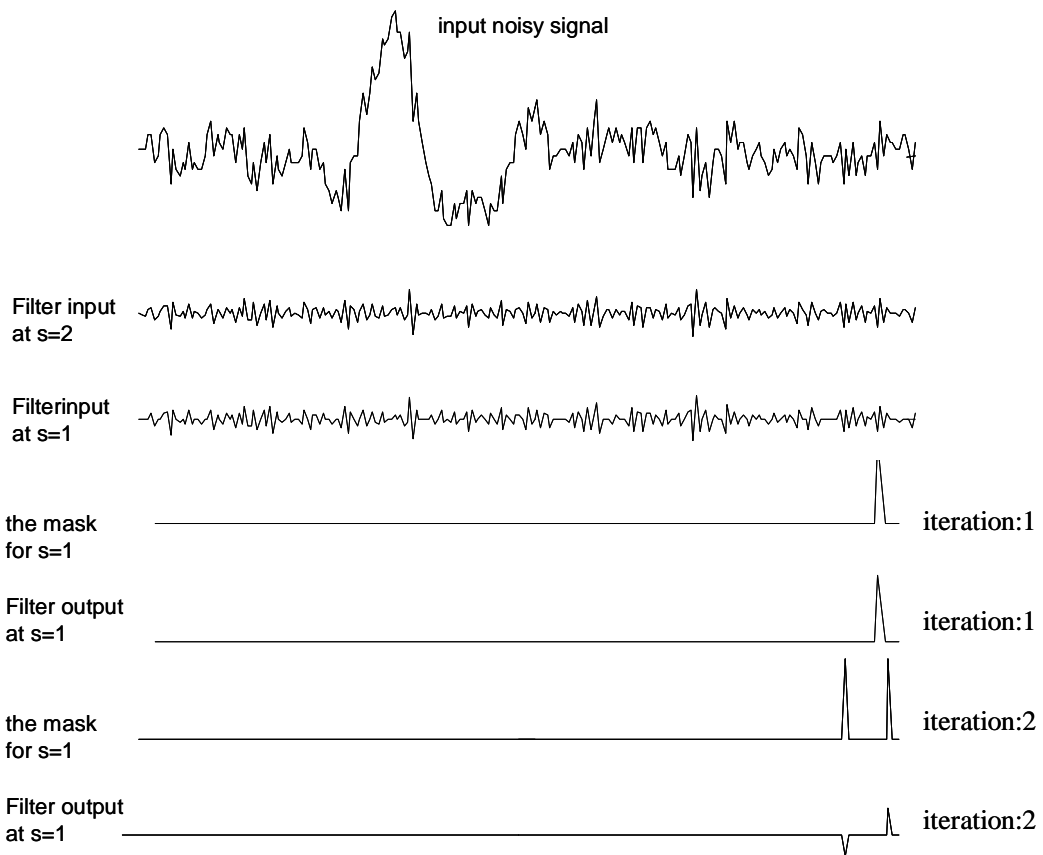


Figure 3.8: The sequences related to the WTSSF with f_i

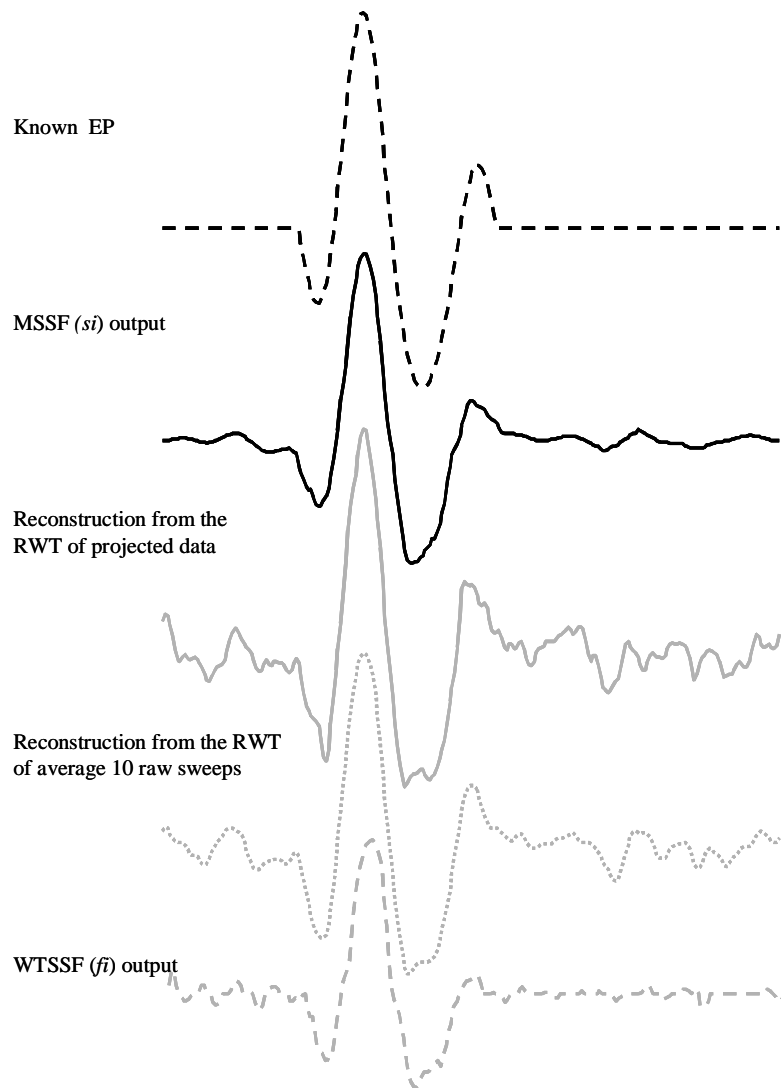


Figure 3.9: The *si* is performed 14 times in the MSSF and, *fi* is performed 3 times in the WTSSF.

Case 2: Estimation of single-sweeps having amplitude and/or latency variations

To observe the performance of scale space filtering approaches in the case of latency/amplitude variations, a pseudo-simulation study is performed with 6 sweeps. The template AEP signal is obtained by using the EP model given by Equation 2.51. The model parameters are chosen as follows:

$$\begin{aligned}a_1 &= 120, a_2 = -64, a_3 = -10, a_4 = 12, \\b_1 &= -1, b_2 = -15, b_3 = 14, b_4 = -1, \\T &= 250, M = 4, k = 1, \dots, 250\end{aligned}$$

Synthetic latency and amplitude variations are generated on the known EP signal. In two sweeps latency variations are assumed. In two other sweeps, the amplitude of the known EP is modified. The remaining two sweeps have no amplitude or latency variations. The recorded EEG sequences are added to the known data with -5 dB of input SNR. Since there is a latency variation among raw data, two largest eigenvectors are selected in the SM.

Figure 3.10 shows waveforms of the 6 sweeps: the raw data, noiseless EP signals with amplitude and latency variations, EP signals after SM, and the MSSF outputs obtained after 8 *si*. Note that, the waveforms of the single noise-less sweeps are not visible in the raw data. They become roughly distinguishable after the SM. Small ripples are observed on the waveforms of the estimations.

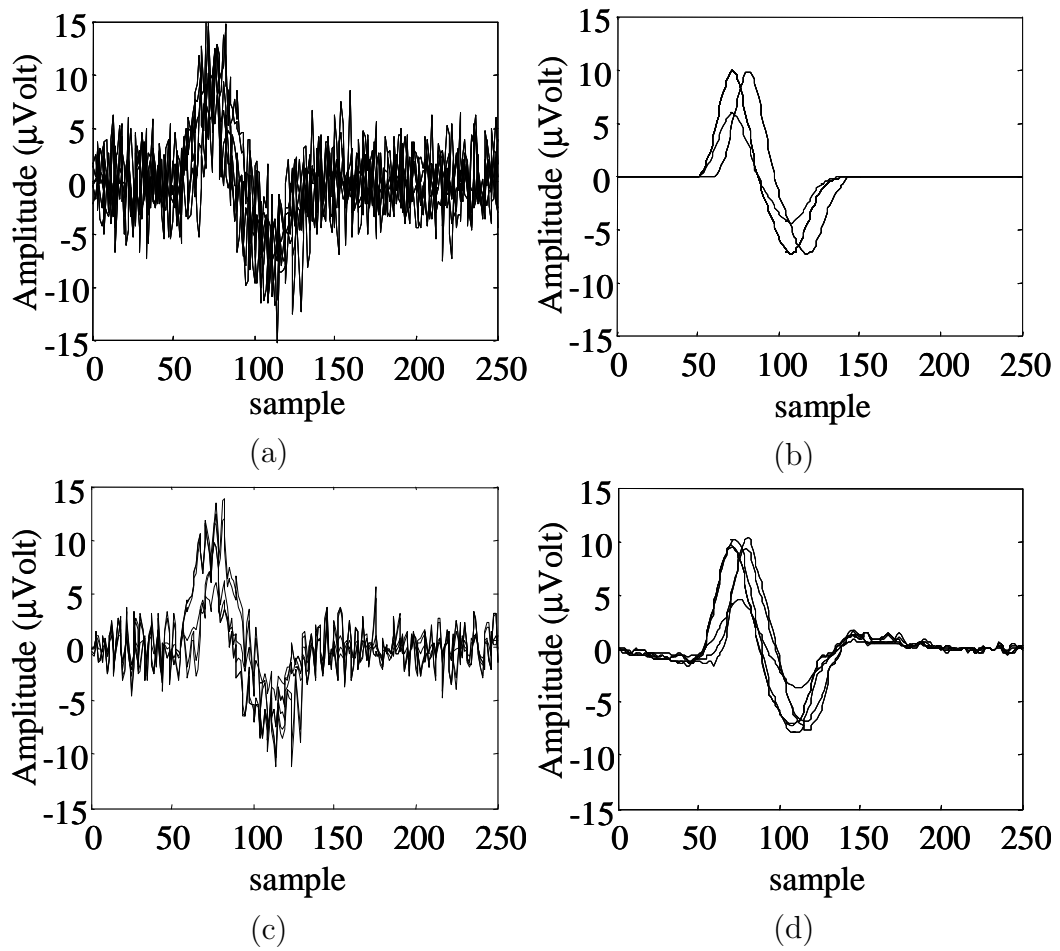


Figure 3.10: The waveforms of 6 sweeps used in the pseudo-simulations: a)raw data, b)the noiseless sweeps with amplitude/latency variations, c)the projected data and, d)estimations obtained by using the MSSF after 14 *si*

3.2.2 Experimental Study

Chapter 2.5, section 2.5.2 presents the related information about the experimental studies with auditory stimuli.

Figure 3.12 shows the waveform of the reference EP (average of 512 sweeps), the corresponding WT coefficients and the MM points of a specific experiment. Since the characteristics of the background EEG noise is different from that of the white noise, there is still noise on the average signal even though the large number of sweeps are averaged. The noise remaining on the grand average, however, becomes similar to white noise. Thus, a large number of MMs are observed at finer scales as shown in Figure 3.12.

The raw data (32 single-sweeps) are projected onto the signal space by using the SM with respect to the first eigenvector since latency variations are not expected for handled data. In this way, the output SNR is increased to 25 dB and then, the waveform of the EP (the grand average) becomes distinguishable.

The output SNR improvements obtained by filtering of the projected data with MSSF and WTSSF are shown in Figure 3.11. It is observed that, the estimation performances of these filters do not change when the scale iteration is performed instead of the frame iteration. Initially (after a few iterations), the performance of WTSSF is better. However, as the number of iterations increases, its performance decreases. Whereas, the performance of the MSSF increases as the number of iterations increases. Figure 3.13 shows the waveform of the reference EP and estimations obtained using MSSF (after 18 iterations). The results obtained with scale truncation (i.e., reconstruction using the scales of only low frequency components) are also presented. For that study, both the average of 32 sweeps and projected sweep are used to determine the threshold in the scales. It is observed that, the MSSF provides the most clear waveform providing less noisy pre- and post-stimulus intervals.

The images related to the real WT coefficients corresponding to average of 32 sweeps, grand average EP, projected sweep and, the output of the MSSF are presented in Figure 3.14. The corresponding MM spectrums are shown in 3.15. Note the similarity between the WT coefficients associated with the average of 32 single-sweeps and the projected sweep: in small scales, a large number of coefficients are non-zero. These non-zero coefficients are set to zero by filtering (Figure 3.14 (d)). Thus, MMs becomes more sparse via the MSSF (Figure 3.15 (d)).

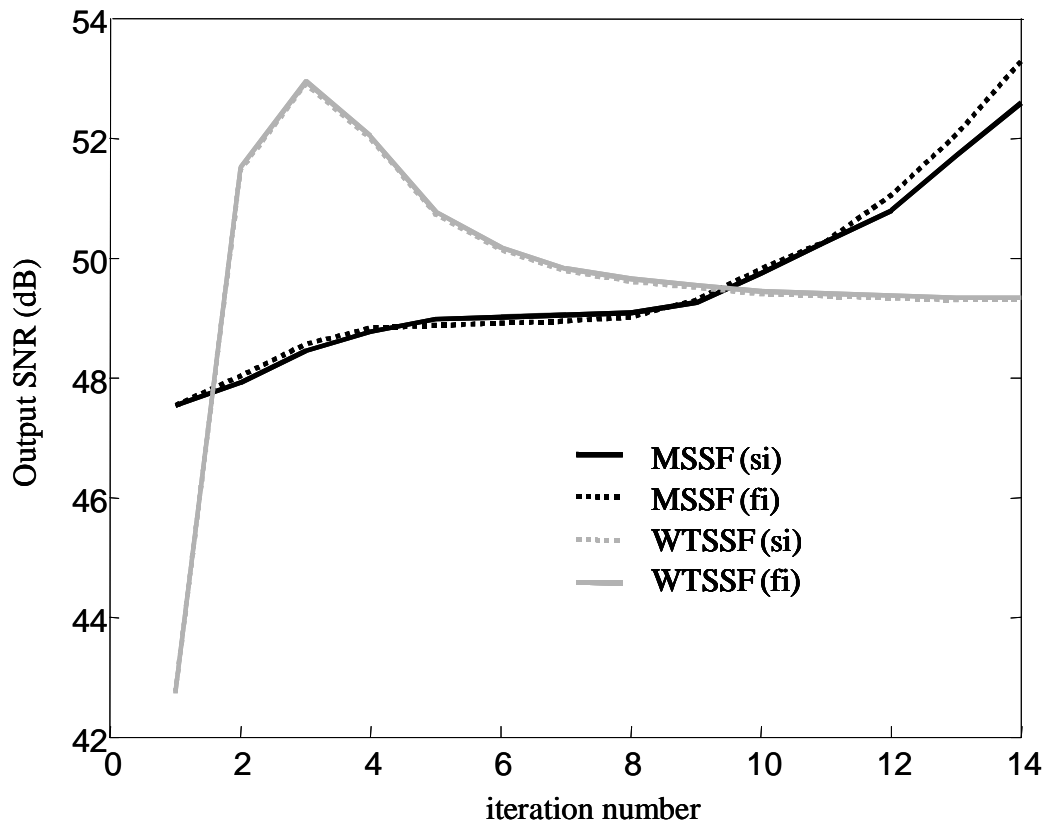
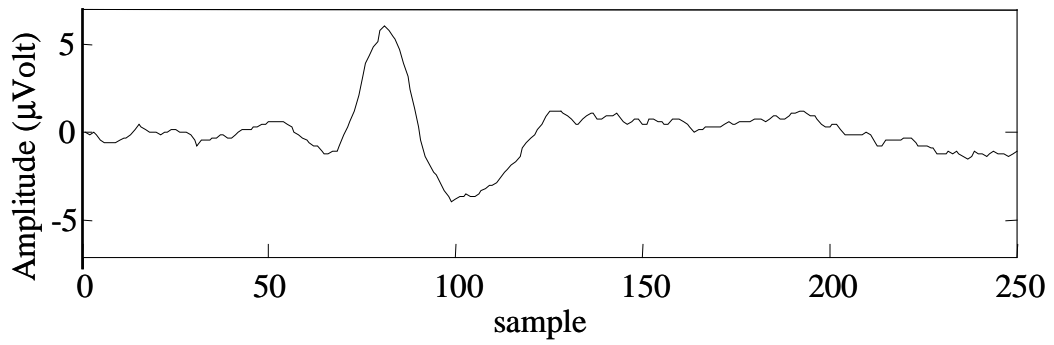
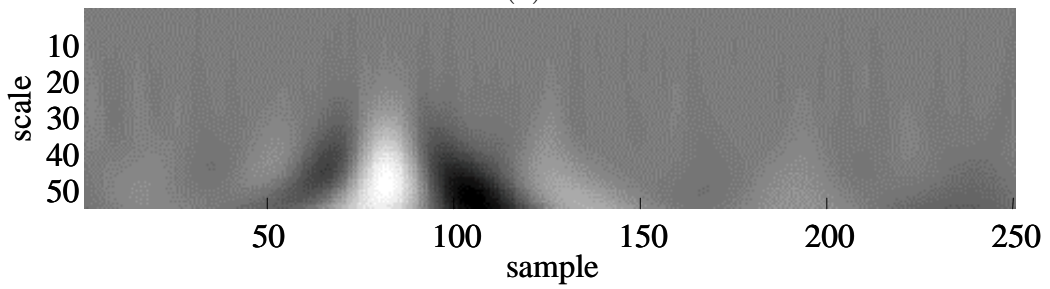


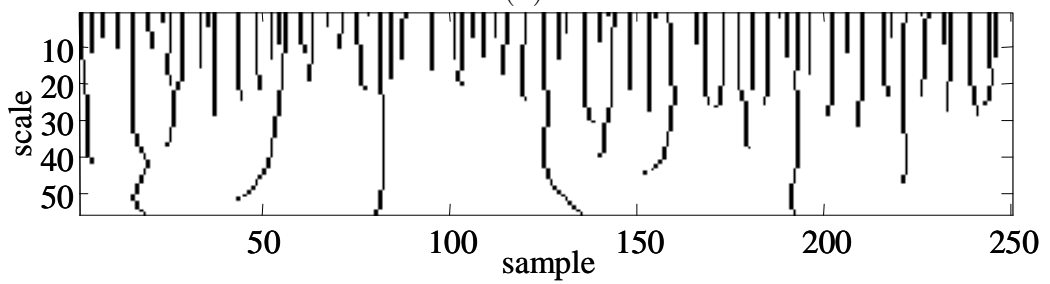
Figure 3.11: The output SNR improvements versus iteration number for experimental data after MSSF and WTSSF.



(a)



(b)



(c)

Figure 3.12: a) The grand average EP, b) image of the real WT coefficient and, c) the plot of the related MMs.

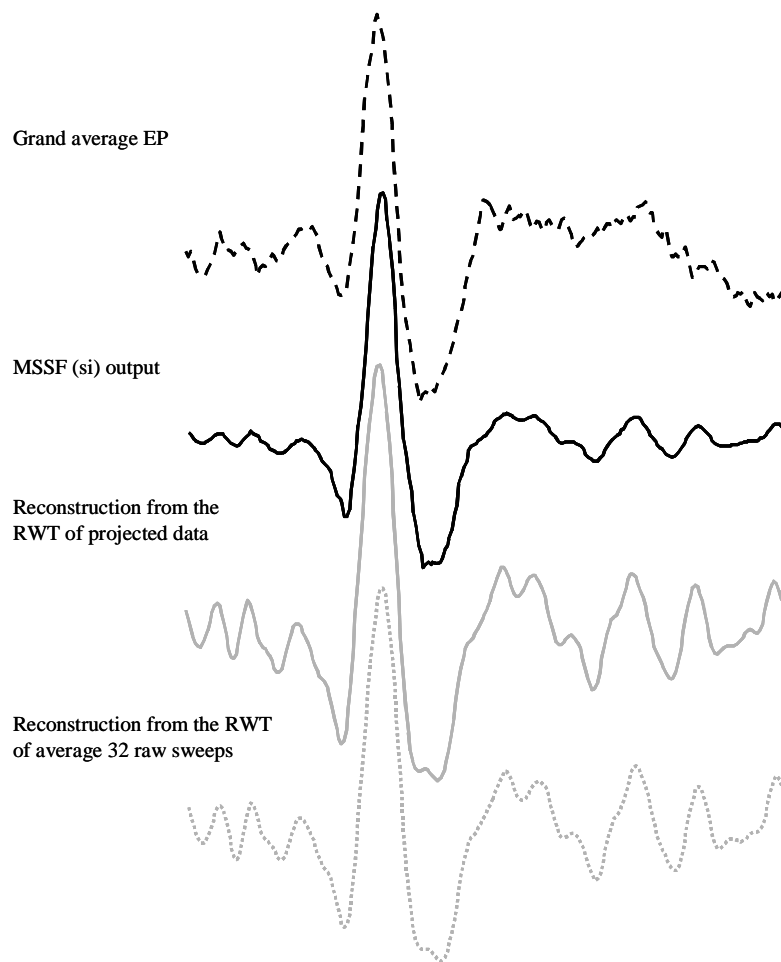


Figure 3.13: The waveforms of the grand average and estimations. (*si* is performed 18 times in the MSSF)

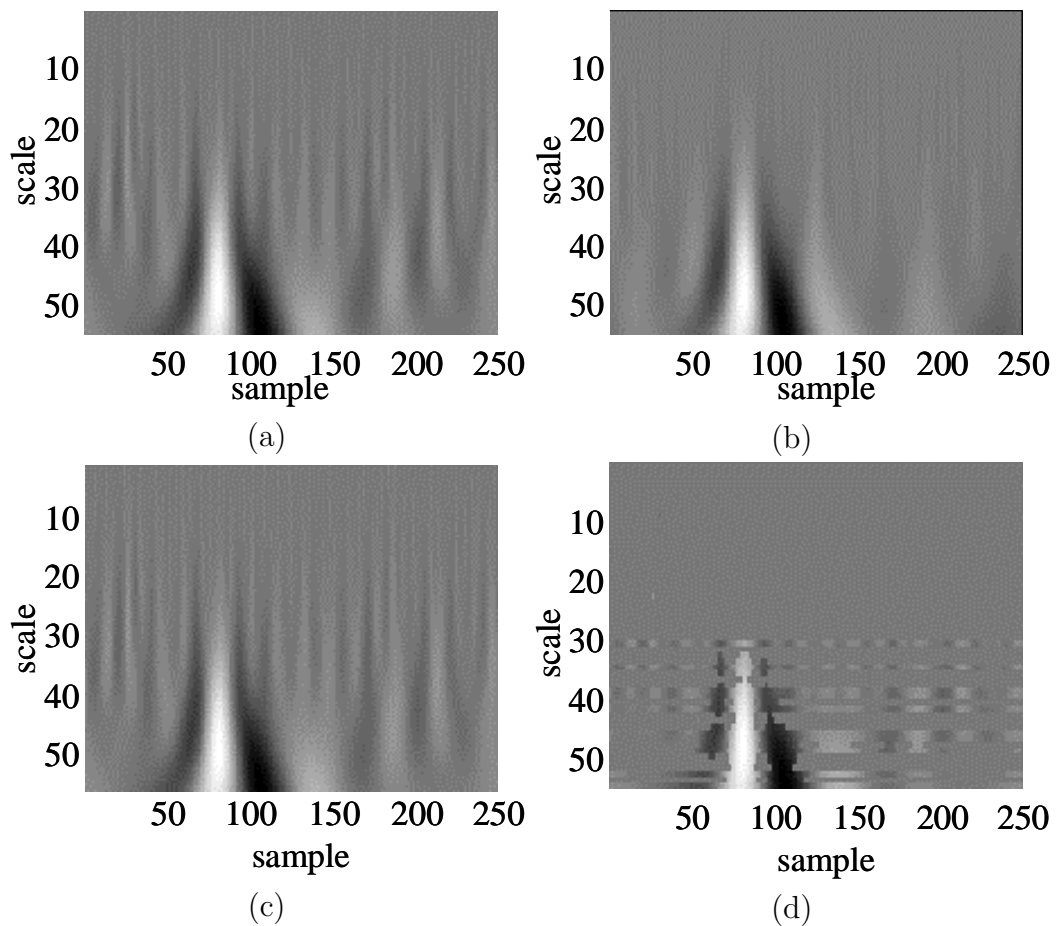


Figure 3.14: The real WT coefficients associated with a) the average of 32 raw sweeps, b) the grand average EP, c) the projected sweep and d) outputs of the MSSF (si is performed 18 times)

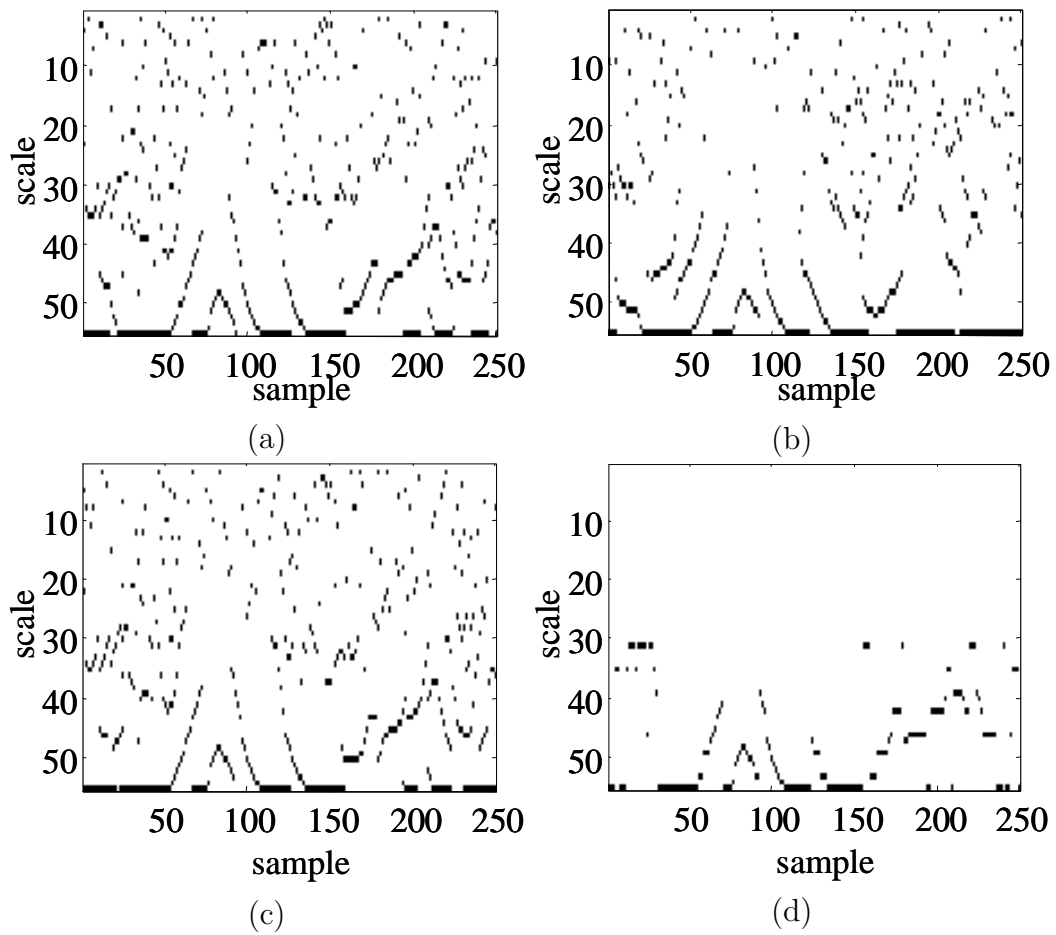


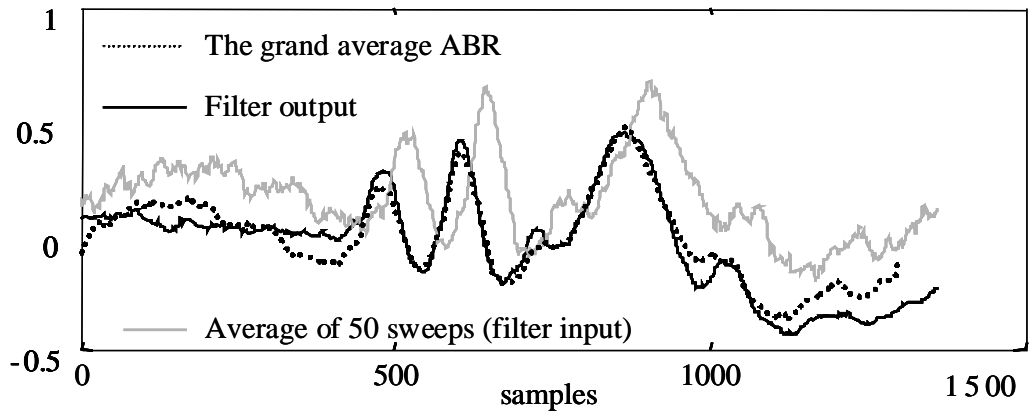
Figure 3.15: Plots of MMs associated with a) the average of 32 raw sweeps, b) the grand average EP, c) the projected sweep and d) the outputs of the MSSF (*si* is performed 18 times)

Template ABR estimation

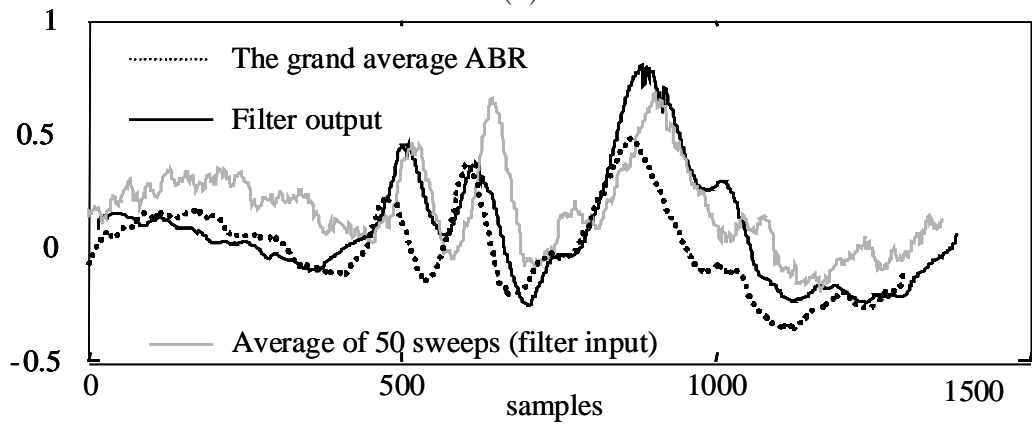
The proposed filter is also tested with experimental ABR data obtained from six rats under auditory stimuli. The data are recorded with a sampling frequency of 96 KHz and filtered with 1^{st} order Butterworth filter ($100 - 2500\text{ Hz}$). The recording period is 15 msec , so 1440 samples are acquired during each experiment.

To estimate the template ABR, namely the average of 250 sweeps, the average of 50 noisy sweeps is filtered using both MSSF and WTSSF. The waveforms of the estimations corresponding to the MSSF and WTSSF are respectively given in Figure 3.16 (a) and (b). The singularity behavior of the ABR waveform is dominated by a number of oscillations, providing five distinguishable peaks. When the MSSF is used, the estimated peaks match the ones obtained by the grand average. Moreover, the pre-stimulus intervals are closer to zero. However, the same performance can not be obtained by the WTSSF.

To test the performances of MSSF and WTSSF, another actual ABR data set is used. For this case, the input SNR is increased to about 3 dB when 50 single-sweeps are averaged. In addition, the waveform of the reference ABR (the grand average ABR signal) becomes distinguishable after averaging process. The waveform of the estimation, filtered real WT coefficients and their MM spectrums corresponding to the MSSF and WTSSF are shown in Figure 3.17 and 3.18, respectively. The waveform of the estimation obtained by using the MSSF closely matches the reference ABR signal and the output SNR is increased to 28 dB . However, the WTSSF provides 20 dB of output SNR. Note that, a number of coefficients, which may be created by ABR peaks, are set to zero at various scales when WTSSF is used. Thus, it can be said that the MSSF shows better performance in extracting the template ABR. The usage of the MSSF reduces the recording time to one-fifth of that required by EA.

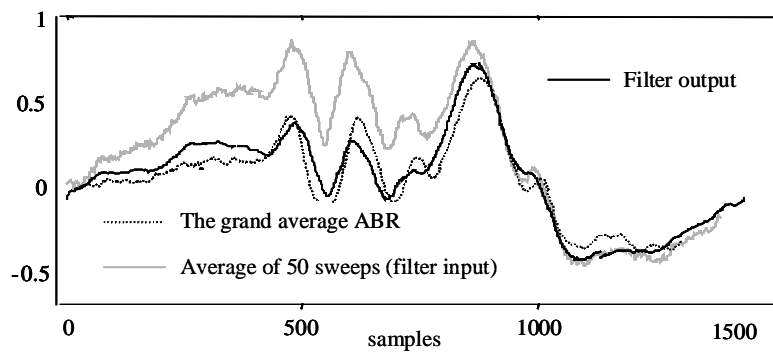


(a)

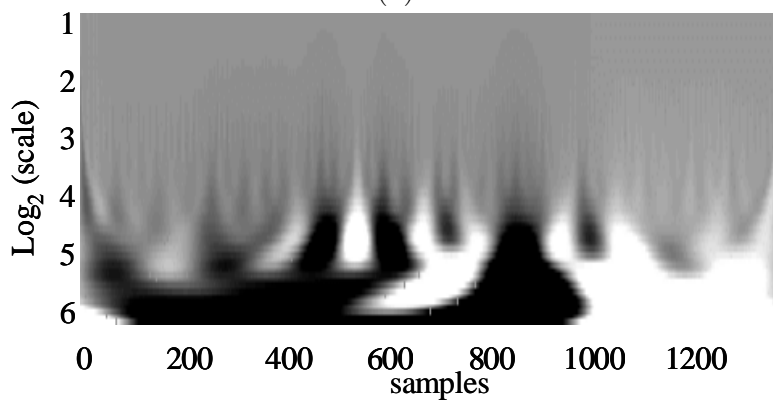


(b)

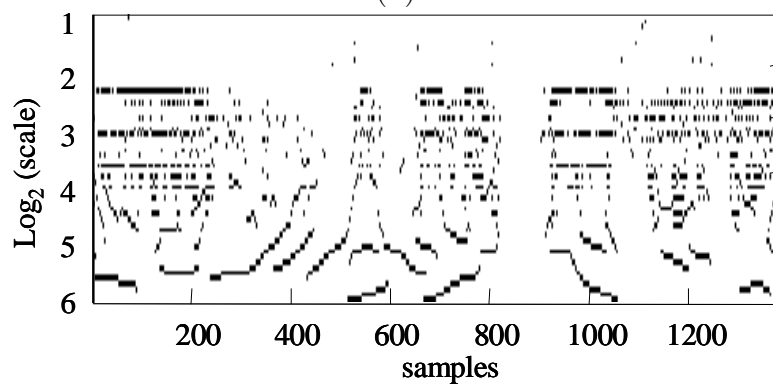
Figure 3.16: The estimations of experimental ABR data using the a) MSSF and b) WTSSF.



(a)

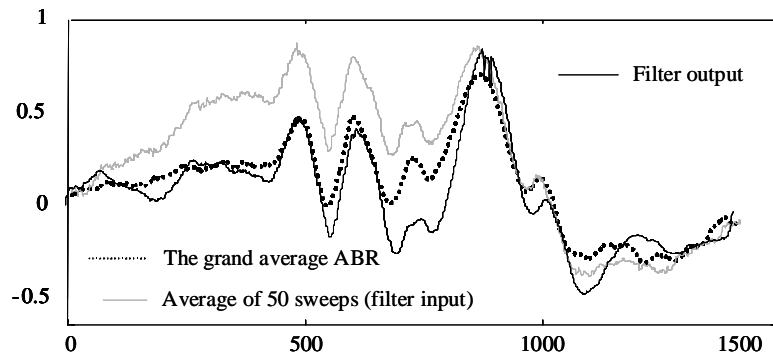


(b)

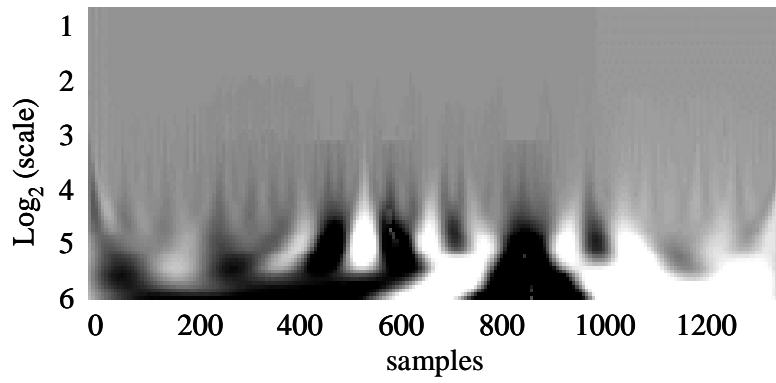


(c)

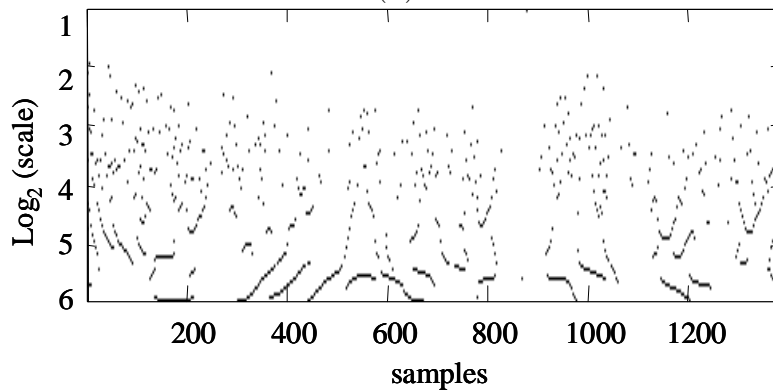
Figure 3.17: The waveform of the estimation (a), real WT coefficients (b) and their MM spectrums (c) corresponding to the MSSF.



(a)



(b)



(c)

Figure 3.18: The waveform of the estimation (a), real WT coefficients (b) and their MM spectrums (c) corresponding to the WTSSF.

CHAPTER 4

CONCLUSION AND DISCUSSION

The conclusion part of this thesis study is presented in the following two subsections:

I-Comparison of Basic Linear Estimation Techniques in Extracting Template Auditory Evoked Potentials

The performance of the basic estimation techniques (WF approaches, standard adaptive filtering algorithms and Tikhonov regularization techniques) were assessed in estimating the template auditory EP compared to the traditional EA. The algorithms were tested with simulations, pseudo-simulations and experimental studies dealing with standard auditory EPs. The SNR was used as the performance criteria. To obtain simulated data, white noise sequences were added to the known auditory EP signals generated by using the Fourier series model. In pseudo-simulation studies, actual EEG recordings were used instead of white noise sequences.

Among the first group of methods, the SMWF seems to provide better performance compared to WFSM in both pseudo-simulations and experimental cases. This result shows that a large amount of EEG noise can be removed by using the SM as a pre-filter. After application of the SM, the characteristic of the remaining EEG noise renders closer to that of white noise which can be removed optimally by conventional WF. The SMCWWF was found better than the SMWF for all data sets. Thus, the CWWF in combination with SM appears to be a better alternative to both the conventional WF and EA. However, CWWF has more computational complexity than conventional WF, since it is computed iteratively depending on the fast Fourier Transform computations.

In the second group of algorithms, the RLS filtering and KF show better performances compared to EA. The RLS filtering has the best performance in both simulation and pseudo-simulation tests, whereas the KF provides the highest performance in experimental studies. In this study, we have selected an initial filter parameters set according to experimental data sets. When

we analyze the KF after 128 sweeps, it shows a low-pass filter characteristics which has a narrower bandwidth compared to the RLS filter. This indicates the relatively better performance of the KF in the experimental studies. However, with the same initial settings, it has wider a low-pass filtering characteristics after 40 sweeps in the simulation and pseudo-simulation studies.

The LMS filter performance depends on 1) the number of sweeps to be filtered, 2) the step size parameter μ , 3) the filter length, and 4) the input SNR of single sweeps. It is, in general, found unsuccessful for low input SNR (-5 dB) cases. The selection of step size parameter is assumed to be the crucial factor in the performance. To obtain a better performance with the LMS filtering, various methods were proposed which explore an optimum step-size at each iteration [68, 124]. In another study, the optimum value was determined methodologically considering the filter length, input signal variance and the desired signal [13]. In the present study, these approaches are not attempted, instead the performance of the SMLMS algorithm is tested. The SMLMS algorithm appears to be relatively less sensitive to the step size and showed better performance compared to the EA in both experimental and simulation trials. However, its performance in the pseudo-simulations proves again unsatisfactory. In conclusion, we leave the following matters for future work: 1) the use of optimal step size in LMS algorithms, 2) exploring further properties of the SMLMS algorithm for a better performance.

The regularization methods (the third group of algorithms; i.e., STR and SR), show better performance compared to EA. It is observed that, the STR is marginally better than SR in all cases. Note that the STR method is optimum for smooth solutions whereas the SR allows sharp variations in the solutions. The basis vectors of \mathbf{H} are chosen from the dilated and shifted forms of a mother wavelet which resemble the waveform of the auditory evoked potential. The linear combination of these smooth vectors models the EP. In line with the fact that a sharp variation in the coefficients of this combination is not expected, we have not observed the superiority of SR compared to STR. In addition, the STR method has less computational complexity than the SR method. Thus, we propose the use of STR method instead of SR for template auditory EP estimation.

We propose the use of basic estimation techniques to obtain a template EP instead of traditional EA to reduce the recording time. The performances of these techniques in extracting the signal, i.e., the grand average EP from small number of sweeps are investigated. If there are amplitude/latency

variations in single sweeps, than the grand average signal would change correspondingly. In such a case, we would again expect a better performance compared to EA. We have not explored the performance of these methods assuming such variations in single trials. However, we propose the use of STR and KF to obtain a high quality template EP signal used in single sweep analysis methods [113, 66, 71, 72, 111, 47, 51, 25, 103, 105, 85].

In conclusion, most of the basic estimation techniques show definitely better performance compared to EA in extracting the EPs. Both KF and the STR effectively reduce the experimental time (to one-fourth of that required by EA). The SM, based on the LS estimation technique, proves to be a useful pre-filter that can significantly reduce the noise in the raw data.

II-A Modified Scale Space Filter to extract single-sweep AEPs

A new approach was presented to observe the possible amplitude and/or latency variations on single sweep auditory EPs without using a template signal. The proposed approach uses the SM as a pre-process to increase the SNR from about -5 dB to 0 dB. Consequently, the WT coefficients corresponding to the signal and the noise becomes distinguishable. Then, the less-noisy sequences (projected sweeps) are filtered individually in wavelet domain with MSSF. The new algorithm was tested in both pseudo-simulations and experimental studies. In pseudo-simulation studies, EEG noise measurements were added to the artificial data sets that consist of either unchanged single-sweeps or amplitude/latency variations. For both cases, noise remaining on the projected data were removed successfully by using the MSSF. In experimental studies, small amplitude variations were observed as expected. The MSSF was also tested for actual ABR data sets recorded from rats in extracting of a template ABR from less number of sweeps. For this purpose, MSSF was applied to the average of 50 single-sweeps. Then, a clear template ABR was obtained from 50 sweeps instead of 250 sweeps. Thus, the experimental time was reduced five times when the MSSF was used.

The results show that the MSSF is an efficient filter to remove the actual EEG noise when the input SNR is higher than 0 dB. We propose the usage of the SM as a primary process for auditory EPs to enhance the SNR when the input SNR is very low.

REFERENCES

- [1] Aunon J I. Evoked potentials research. *IEEE Engineering in Medicine and Biology Magazine*. 1992: 11(1); 67-68.
- [2] Bai O, Nakaruma M, Nagamine T and Shibasaki H. Parametric Modeling of Somatosensory Evoked Potentials Using Discrete Cosine Transform. *IEEE Transaction on Biomedical Engineering* 2001: 48; 1347-1351
- [3] Barrett P T, Eysenck H J. The relationship between evoked potential component amplitude, latency, contour length, variability zero crossing and psychometric intelligence. *ELSEVIER Personality and Individual Differences*. 1994: 16(1); 3-32.
- [4] Basar E. Relation Between EEG and Brain Evoked Potentials. *EEG Brain Dynamics*, Elsevier/North-Holland Biomedical 1980: 34; 97-107.
- [5] Basar E, Schurmann M, Demiralp T, Eroglu C B, Ademoglu A. Event related oscillations are Real brain responses-wavelet analysis and new strategies. *Int. Journal of Psychophysiology* 2001: 92-123.
- [6] Beigi M, Erfanian A and Elkhani M. Multi-resolution Adaptive Filter for Estimating Brainstem Auditory Evoked Potential. *Proc. 20th Annual Int. Conf. IEEE/EMBS* 1998: 20; 1474-1477.
- [7] Bernat M E, William J, William J G. Decomposing ERP timefrequency energy using PCA. *ELSEVIER Clinical Neurophysiology*. 2005: 116(6); 1314-1334.
- [8] Bertrand O, Bohorquez J, Pernier J. Time-frequency digital filtering based on an invertible wavelet transform: an application to evoked potentials. *IEEE Transactions on Biomedical Engineering*. 1994: 41(1); 77 - 88.
- [9] Bradley A P, Wilson W J. On wavelet analysis of auditory evoked potentials. *ELSEVIER Clinical Neurophysiology*. 2004: 115(5); 1114-1128.
- [10] Brandt M E, Jansen B H, Carbonari J P. Pre-stimulus spectral EEG patterns and the visual evoked response. *ELSEVIER Electroencephalography and Clinical Neurophysiology*. 1991: 80(1); 16-20.

- [11] Boutros N, Nasrallah H, Leighty R, Torello M, Tueting P, Olson S. Auditory evoked potentials, clinical vs. research applications. *ELSEVIER Psychiatry research*. 1997: 69; 183-195.
- [12] Cichocki A, Gharieb R and Hoya T. Efficient Extraction of Evoked Potentials By Combination of Wiener Filtering and Subspace Methods. *Proc. Int. Conf. IEEE/CASSP Acoustics, Speech, and Signal Processing 2001*: 5; 3117-3120
- [13] Chen R Y, Wang C L. On the optimum step size for the adaptive sign and LMS algorithms. *IEEE Transactions on Circuits and Systems*. 1990: 37(6); 836-840.
- [14] Cormen, T.H., Leiserson, C.E. and Rivest, R.L. *Introduction to Algorithms*, The MIT Press, 1990.
- [15] Cutmore TR H, James D A. Identifying and reducing noise in psychophysiological recordings. *ELSEVIER International Journal of Psychophysiology*. 1999: 32; 129-150
- [16] Daubechies I. *Ten lectures on Wavelets*. Society for Industrial and Applied Mathematics, Philadelphia, PA: SIAM. 1992.
- [17] Davila C E and Mobin M S. Weighted Averaging of Evoked Potentials *IEEE Transaction on Biomedical Engineering* 1992: 39; 338-345
- [18] Davila C E, Welch A J and Rylander H G. Improved Signal Subspace Method for EP Estimation. *Proc. 10th Annual Int. Conf. IEEE/EMBS* 1988: 4; 1175-1176
- [19] Davila C E, Srebro, R. Subspace averaging of steady-state visual evoked potentials. *IEEE Transactions on Biomedical Engineering*. 2000: 47(6); 720-728
- [20] Delorme A, Makeig S, Fabre-Thorpe M, Sejnowski T. From single-trial EEG to brain area dynamics. *Neurocomputing*. 2002: 44-46; 1057-1064.
- [21] Demiralp T, Ademoğlu A, Istefanopulos Y, Başar E, Eroğlu C B. Wavelet analysis of oddball P300. *ELSEVIER International Journal of Psychophysiology* 1999: 221-227

- [22] Demiralp T, Ademoglu A, Istefanopulos Y, Erođlu C B and Bařar E. Wavelet analysis of oddball P300. ELSEVIER International Journal of Psychophysiology. 2001: 39(2-3); 221-227
- [23] Diaz F and Zurron M. Auditory evoked potentials in Down's syndrome. ELSEVIER Electroencephalography Clinical Neurophysiology. Evoked POtential Section. 1995: 96(6); 526-537.
- [24] Doyle D J. Some comments on the use of Wiener Filtering for the estimation of evoked potentials. ELSEVIER Electroencephalography Clinical Neurophysiology. 1975: 38; 533-534
- [25] Effer A, Lehnertz K, Fernandez G, Grunwald T, David P, Elger C E. Single trial analysis of event related potentials: non-linear de-noising with Wavelets. Elsevier Electroencephalography Clinical Neurophysiology 2000: 2255-2263
- [26] Heruby T, Marsalek P. Event related potentials: the P300. ACTA Neurobiologiae experimentalis. 2003: 63; 55-63.
- [27] Faghih F, Smith M. Combining spatial and scale-space techniques for edge detection to provide a spatially adaptive wavelet-based noise filtering algorithm. *IEEE Transactions on Image Processing*. 2002: 11(9); 1062-1071.
- [28] Furst M, Blau A., Optimal a posteriori time domain filter for average evoked potentials. *IEEE Transaction on Biomedical Eng.* 1991: 38(9); 827-833
- [29] Garoosi V, Jansen B H. Development and evaluation of the piecewise Prony method for evoked potential analysis. *IEEE Transactions on Biomedical Engineering*. 2000: 47(12); 1549-1554.
- [30] Georgiadis S D, Ranta-aho P O, Tarvainen M P, Karjalainen P A. Single-Trial Dynamical Estimation of Event-Related Potentials: A Kalman Filter-Based Approach. *IEEE Transactions on Biomedical Engineering*. 2005: 52(8); 1397-1406
- [31] Golub G H, Hansen P C, Óleary D P. Tikhonov Regularization and Total Least Squares. *Siam Journal Matrix Analysis Application*. 1999: 21; 185-194

- [32] Golstein R, Rodman L B. Early components of averaged evoked responses to rapidly repeated auditory stimuli. *J Speech Hearing Research* . 1967: 10; 697-705.
- [33] Grieve R, Parker P A, Hudgins B, Englehart K. Nonlinear adaptive filtering of stimulus artifact. *IEEE Transactions on Biomedical Engineering*. 2000: 47(3); 389-395
- [34] Gupta L, Molfese D L and Tammana R. An Artificial Neural-Network Approach to ERP Classification. *ELSEVIER Brain and Cognition*. 1995: 27(3); 311-330.
- [35] Golstein R, Rodman LB. Early components of averaged evoked responses to rapidly repeated auditory stimuli. *J.Speech Hearing Res.* 1967: 10; 697-705.
- [36] Golub G H. *Matrix Computation*. North Oxford Academic Press. 1983.
- [37] Golub G H, Hansen P C, Óleary D P. Tikhonov Regularization and Total Least Squares. *Siam Journal Matrix Analysis Application*. 1999: 21; 185-194
- [38] Gupta L, Molfese D L, Tammana R, Simos P G. Nonlinear alignment and averaging for estimating the evoked potential. *IEEE Transactions on Biomedical Engineering*. 1996: 43(4); 348-356.
- [39] Gupta L, Phegley J, Molfese D L. Parametric classification of multi-channel averaged event-related potentials. *IEEE Transaction on Biomedical Eng.* 2002: 49(8); 905-912
- [40] Hansen P C. *Regularization Tools: A Matlab Package for Analysis and Solution of Discrete ill-Posed Problems*. (Copenhag: UNI-C, Tech. Univ., Denmark 1992).
- [41] Hansen P C, Rasmussen ML H, Clemessen LK H. The effect of regularizing matrices and norms in Tikhonov Based mage Restorations. *Technical Report*. 2003.
- [42] Hansen P S K. *Signal subspace methods for speech enhancement*. IMM-PhD Thesis. Technical University of Denmark. 1997.

- [43] Hansson M, Gansler T, Salomonsson G. A system for tracking changes in the mid-latency evoked potential during anesthesia. *IEEE Transaction on Biomedical Engineering* 1998: 45(3); 323-334.
- [44] Haykin S *Adaptive Filter Theory* (Prentice-Hall 2nd edition)1991.
- [45] Hegerl U, Wolfgang G, Gutzman H and Ulrich G. Auditory evoked potentials as possible predictors of outcome in schizophrenic outpatients. *ELSEVIER International Journal of Psychophysiology*. 1988: 6(3); 207-214.
- [46] Hegert U, Wuff H, Mller B. Intensity dependence of auditory evoked potentials and clinical response to prophylactic lithium medication. *ELSEVIER Psychiatry research*. 1992: 181-190.
- [47] Heinrich H, Dickhaus H, Rothenberger A, Moll G H, Heinrich V. Single sweep analysis of event-related potentials by Wavelet networks-methodological basis and clinical application. *IEEE Transaction on Biomedical Engineering* 1999: 46; 7867-878.
- [48] Henning G., Husar P. Statistical detection of visually evoked potentials. *IEEE Magazine on Engineering in Medicine and Biology*. 1995: 14(4); 386-390.
- [49] Hour S, Tewfik A H. Wavelet Transform Domain Adaptive FIR Filtering. *IEEE Transaction on Signal Processing*. 1997: 45(3); 617-630.
- [50] Jacobs M H, Rao S S, Jose G V. Parametric modeling of somatosensory evoked potentials. *IEEE Transactions on Biomedical Engineering*. 1989: 36(3); 392-403.
- [51] Jaskowski P, Verleger R. Amplitudes and latencies of single-trial ERP's estimated by a maximum-likelihood method. *IEEE Transactions on Biomedical Engineering*. 1999: 46(8); 987-993.
- [52] Jaskula M and Kaszyński R. Using the Parametric Time-Varying Analog Filter to Average-Evoked Potential Signals. *IEEE Transaction on Instrumentation and Measurement*. 2004: 53(3); 709-816.
- [53] Jansen B H, Brandt M E. The effect of the phase of prestimulus alpha activity on the averaged visual evoked response. *ELSEVIER Electroencephalography Clinical Neurophysiology*. 1991: 80(4); 241-250.

- [54] Jansen B H. Nonlinear dynamics and quantitative EEG analysis. ELSEVIER Electroencephalography Clinical Neurophysiology Suppl. 1996: 45; 39-56.
- [55] Jansen B H, Agarwal G, Hegde A and Boutros N N. Phase synchronization of the ongoing EEG and auditory EP generation. ELSEVIER Clinical Neurophysiology 2003: 114; 7985.
- [56] Jung T P, Humphries C, Lee T W, Makeig S, McKeown M J, Iragui V, Sejnowski T J. Extended ICA removes artifacts from electroencephalographic recordings. Proceedings of the Conference on Advances in Neural Information Processing Systems 10, USA. 1998: 0-262-10076-2; 894-900.
- [57] Jung T P, Humphries C, Lee T W, Makeig S, McKeown M J, Iragui V, Sejnowski T J. Extended ICA Removes Artifacts from Electroencephalographic Recordings. Advances in Neural Information Processing Systems. 1997
- [58] Jung T P, Makeig S, Westerfield M, Townsend J, Courchesne E, Sejnowski T J. Analyzing and Visualizing Single-Trial Event-Related Potentials. Advances in Neural Information Processing Systems. 1999: 11; 118-24.
- [59] Jung T P, Makeig S, Humphries C, Lee T W, Mckeown M J, Iragui V, Sejnowski T J. Removing Electroencephalographic Artifacts by Blind Source Separation. Journal of Psychophysiology. 2000:37; 163-178.
- [60] Karjalainen P A, Kaipio J P, Koistinen A S and Vauhkonen M. Subspace regularization method for the single-trial estimation of evoked potential IEEE Transaction on Biomedical Engineering 1999: 46; 849-859.
- [61] Kay S. Fundamentals of Statistical Signal Processing. Vol. I - Estimation Theory Prentice Hall. 1993.
- [62] Kılıç S, Gençer N G, Baykal B. Comparison of methods for extraction of evoked potentials. 25th Annual International Conference of IEEE Engineering in Medicine and Biology Conference. 2003: 2495-2498.
- [63] Kitagawa G, Gersch W. A smoothness priors time-varying AR coefficient modeling of nonstationary covariance time series. *IEEE Transactions on Automatic Control*. 1985: 30(1); 48-56.

- [64] Klema V, Laub, A. The singular value decomposition: Its computation and some applications. *IEEE Transactions on Automatic Control*. 1980: 25(2); 164-176.
- [65] Kong X and Thakor N V. Adaptive estimation of latency changes in Evoked Potentials. *IEEE Transaction on Biomedical Engineering* 1996: 43(2); 189-197.
- [66] Kong X and Qiu T. Latency change estimation for evoked potentials via frequency selective adaptive phase spectrum analyzer. *IEEE Transaction on Biomedical Engineering* 1999: 46(8); 104-1012.
- [67] Kozma R., Freeman W J. Classification of EEG patterns using nonlinear dynamics and identifying chaotic phase transitions. *Neurocomputing*. 2002: 44-46; 1107 - 1112.
- [68] Kwong R H, Johnston E W. A variable step size LMS algorithm. *IEEE Transactions on Signal Processing*. 1992: 40(7); 1633-1642.
- [69] Laguna P, Jane R, Meste O and Poon P W. Adaptive Filter for Event-Related Bioelectric Signals using an Impulse Correlated Reference Input: Comparison with Signal Averaging Techniques. *IEEE Transaction on Biomedical Engineering* 1992: 39; 1032-1043.
- [70] Lange D H and Inbar G F. Parametric estimation of single morphologically varying evoked brain potentials. *IEEE Conference on Electrical and Electronics Engineers*. 1995: 1(2.1); 1-5.
- [71] Lange D H and Inbar G F. A robust parametric estimator for single trial movement related brain potentials. *IEEE Transaction on Biomedical Engineering* 1996: 43(4); 341-348.
- [72] Lange D H, Pratt H, Inbar G F. Modeling and Estimation of Single Evoked Brain Potential Components *IEEE Transaction on Biomedical Engineering* 1997: 44; 791-799.
- [73] Lange D H, Siegelmann H T, Pratt H, Inbar G F. Overcoming selective ensemble averaging: unsupervised identification of event-related brain potentials. *IEEE Transactions on Biomedical Engineering*. 2000: 47(6); 822-826.

- [74] Liu W Q, Qiu W, Chan F H Y, Lam F K, Poon, P W F. Estimation of evoked potentials using wavelet transform based time-frequency adaptive filtering. Proceedings of the 19th Annual International Conference of the IEEE/EMBS. 1997: 4(30); 1508-1510.
- [75] Madhavan P G. Minimal Repetition Evoked Potentials by Modified Adaptive Line Enhancement. IEEE Transaction on Biomedical Engineering 1992: 39; 760-764.
- [76] Mallat S. Zero-crossings of a wavelet transform. IEEE Transaction on Information Theory. 1991: 37(4); 1019-1033.
- [77] Mallat S and Zhong S Characterization of Signals from Multiscale Edges IEEE Transaction on Pattern Analysis and Machine Intelligence. 1992: 14; 710-720.
- [78] Mallat S and Hwang W L Singulaity Detection and Processing with Wavelets 1992: 38; 617-644.
- [79] Mallat S A Wavelet Tour of Signal Processing Academic Press UK 1998.
- [80] Makeig S, Jung T-P. Tonic, phasic, and transient EEG correlates of auditory awareness in drowsiness. Cognitive Brain Res. 1996: 4; 15-25.
- [81] Mazaheri A, Picton T W. EEG spectral dynamics during discrimination of auditory and visual targets. ELSEVIER Cognitive Brain Research. 2005: 24(1); 81-96.
- [82] Moor B D. The Singular Value Decomposition and Long and Short Spaces of Noisy Matrices. IEEE Trans. on Signal Processing 1993: 41; 2826-2838.
- [83] Nakamura M, Nishida S and, Shibasaki H. Deterioration of average Evoked Potential waveform due to asynchronous averaging and its compensation. IEEE Transaction on Biomedical Eng. 1991: 38; 309-312.
- [84] Nishida S, Nakamura M, Suwazono S, Honda M, Shibasaki H. Estimate of physiological variability of peak latency in single sweep P300. ELSEVIER Electroencephalography and Clinical Neurophysiology 1997: 104; 431-436.

- [85] Nishida S, Nakamura M, Shibasaki H. Physiological Variability of Peak Latency in Evoked Potentials: use of a Property of Asynchronous Averaging. *Medical Engineering and Physics* 1999: 21; 681-687.
- [86] Oppenheim A V, Schafer, R W. *Discrete-time signal processing*. Prentice Hall signal processing series. 1989: 599-601.
- [87] Penny W D, Kiebel S J, Kilner J M, Rugg M D. Event-related brain dynamics. *TRENDS in Neurosciences*. 2002: 25; 387-389.
- [88] Quweider M K, Farison J B. Classification of image edge blocks by orthogonal projection. *IEE Electronics Letters* 1997: 33; 1856-1857.
- [89] Pantev C, Ltkenhner B, and Elbert T., *Oscillatory Event related brain dynamics*. New York-London: Plenum Press, 1994.
- [90] Picton T W. *Handbook of Electroencephalography and Clinical Neurophysiology: Human Event-Related Potentials*. ELSEVIER Revised Series, Amsterdam-New York-Oxford 1988: 3.
- [91] Paul J S, Luft A R, Hanley D F and Thakor N V. Coherence-Weighted Wiener Filtering of Somatosensory Evoked Potentials. *IEEE Transaction on Biomedical Engineering*. 2001: 48; 1483-1488.
- [92] Pecher A, Husar P, Henning G, Roderer H. Phase estimation of visual evoked responses. *IEEE Transactions on Biomedical Engineering*. 2003: 50(3); 324-333.
- [93] Penny W D, Kiebel S J, Kilner J M, Rugg M D. Event-related brain dynamics. *TRENDS in Neurosciences*. 2002: 25; 387-389.
- [94] Raz, J. Wavelet models of event-related potentials. *Proceedings of the 16th Annual International Conference of the IEEE/EMBS: New Opportunities for Biomedical Engineers*. 1994: 1; A26-A27.
- [95] Raz J, Dickerson L and Turetsky B. A Wavelet Packet Model of Evoked Potentials. *Brain and Language*. 1999: 66(1); 61-88.
- [96] Regan D. *Evoked Potentials in Psychology, Sensory Physiology and Clinical Medicine* (Chapman and Hall, London 1972).

- [97] Ren H, Chang C I. A generalized orthogonal subspace projection approach to unsupervised multi-spectral image classification. *IEEE Transaction on Geoscience and Remote Sensing* 2000: 38; 2515-2528.
- [98] Rodinov V, Goodman C, Fisher L, Rosenstein G Z, Sohmer H. A new technique for the analysis of background and evoked EEG activity: time and amplitude distributions of the EEG deflections. 2002: 113.
- [99] Rosso O A, Blanco S, Yordanova J, Kolev V, Figliola A, Schürman M, Başar E. Wavelet entropy: a new tool for analysis of short duration brain electrical signals. *ELSEVIER Journal of Neuroscience Methods* 2001: 105; 65-75.
- [100] Robinson K and Rudge P. The use of the auditory evoked potential in the diagnosis of multiple sclerosis. *ELSEVIER Journal of the Neurological Sciences*. 1980: 45(2-3); 235-244.
- [101] Qiu W, Chan F H Y, Lam F K. Visual evoked potential estimation by eigendecomposition. *Proceedings of the 20th Annual International Conference of the IEEE/EMBS*. 1998: 6; 3192-3194.
- [102] Qiu W, Fung S M, Chan H Y, Lam F K, Poon P W F and Hamernik R P. Adaptive Filtering of Evoked Potentials with Radial Basis Function Neural Network Pre-filter. *IEEE Transaction on Biomedical Engineering* 2002: 49; 225-231.
- [103] Quiroga R Q, Garcia H. Single trial event related potentials with Wavelet de-noising. *ELSEVIER Electroencephalography Clinical Neurophysiology* 2003: 376-390.
- [104] Quweider M K, Farison J B. Classification of image edge blocks by orthogonal projection. *IEE Electronics Letters* 1997: 33; 1856-1857.
- [105] Saatchi M, Gibson C, Rowe J W K. Adaptive Multi-resolution Analysis based Evoked Potential Filtering. *Proceeding of IEE Conf. on Science Measurement and Technology*. 1997: 144; 149-155.
- [106] Salajegheh A, Link A, Elster C, Burghoff M, Sander T, Trahms L, Poeppel D. Systematic latency variation of the auditory evoked M100: from average to single-trial data. *ELSEVIER Journal of Neuroimage*. 2004: 23(1):288-95.

- [107] Sayed, A H, Kailath T A. State-space approach to adaptive RLS filtering. *IEEE Signal Processing Magazine*. 1994: 11(3); 18-60.
- [108] Singer R, Frost P. On the relative performance of the Kalman and Wiener filters. *IEEE Transactions on Automatic Control*. 1969: 14(4); 390-394.
- [109] Sita G and Ramakrishnan A G. Wavelet Domain Nonlinear filtering for evoked potential signal enhancement. *ELSEVIER Computers and Biomedical Research* 2000: 33; 431-446.
- [110] Sparacino G, Milani S, Arslan E, Cobelli C A. Bayesian Approach to estimate Evoked Potentials. *ELSEVIER Computation Methods Programs Biomedicine* 2002: 68; 233-248.
- [111] Spreckelsen M V and Bromm B. Estimation of Single-Evoked Cerebral Potentials by Means of Parametric Modeling and Kalman Filtering. *IEEE Transaction on Biomedical Engineering*: 1988; 35; 691-699.
- [112] Shyh B L, Shing B L, Wu S M, Chien J C, Chong F C. Estimation of evoked potentials using higher order statistics based adaptive filter. *Proc. 23rd IEEE/EMBS Conference* 2001: 2094-2096.
- [113] Svensson O. Tracking of changes in latency and amplitude of the evoked potential by using adaptive LMS filtera and exponential averagers. *IEEE Transaction on Biomedical Engineering*: 1993; 40(10); 1074-1080.
- [114] Tarvainen M P, Hiltunen J K, Ranta-aho P O, Karjalainen P A. Estimation of nonstationary EEG with Kalman smoother approach: an application to event-related synchronization (ERS). *IEEE Transactions on Biomedical Engineering*. 2004: 51(3); 516-524.
- [115] Thakor N V, Xin-rong G, Yi-Chun S, Hanley D F. Multiresolution wavelet analysis of evoked potentials. *IEEE Transaction on Biomedical Engineering*. 1993: 40(11); 1085-1095.
- [116] Tian J, Juhola M and Grnfors T. Latency estimation of auditory brainstem response by neural networks. *ELSEVIER Artificial Intelligence in Medicine*. 1997: 10(2); 115-128.

- [117] Tikhonov A N, Arsenin V Y. Solution of ill-posed problems. Winston and Sons Washington DC. 1977.
- [118] Truccolo W A, Ding M, Knuth K H, Nakamura R, Bressler S T Trial-to-trial variability of cortical evoked responses: implications for the analysis of functional connectivity. *ELSEVIER Electroencephalography and Clinical Neurophysiology* 2002: 113; 206-226.
- [119] Vauhkonen M, Vadász D, Karjalainen P A, Somersalo E and Kaipio J P. Tikhonov Regularization and Prior Information in Electrical Impedance Tomography. *IEEE Transaction on Medical Imaging* 1998: 17(2); 285-293.
- [120] Vasile D, Puscasu, V, Foca, E. Adaptive filter and adaptive linear Fourier combined in processing of cognitive-event-related potential. *IEEE Workshop on Signal Processing Systems*. 2000:10; 753-760.
- [121] Vaz C A and Thakor N V. Adaptive Fourier Estimation of Time-Varying Evoked Potentials. *IEEE Transaction on Biomedical Engineering* 1989: 4; 448-455.
- [122] Wang K, Begleiter H and Porjesz B. Warp-averaging event-related potentials. *ELSEVIER Clinical Neurophysiology*. 2001: 112(10); 1917-1924.
- [123] Wu Y, Zhang Z, Huang T S, Lin J Y. Multibody Grouping via Orthogonal Subspace Decomposition. *Proc. of IEEE CVPR'01* 2001: II; 252-257.
- [124] Won Y K, Park R H, Park J H, Lee B U. Variable LMS algorithms using the time constant concept. *IEEE Transactions on Consumer Electronics*. 1994: 40(3); 655-661.
- [125] Bin Yang. Projection approximation subspace tracking. *IEEE Transactions on Signal Processing*. 1995: 43(1); 95-107.
- [126] Walter D O. A posteriori Wiener Filtering of average evoked responses. In *Advances in EEG Analysis*, Walter D O and Brazier M A Edition on *ELSEVIER Electroencephalography Clinical Neurophysiology Supply*. 1969: 27; 61-70.
- [127] Xu Y, Weaver JB, Healy DM, Jian Lu. Wavelet transform domain filters: a spatially selective noise filtration technique. *IEEE Transactions on Image Processing* 1994: 3(6); 747-758

- [128] Yu X H, Zhang Y S, He Z Y. Peak component latency corrected average method for evoked potential waveform estimation. *IEEE Transaction on Biomedical Engineering* 1994: 41(11); 1072-1082.
- [129] Zhang J and Zheng C. Extracting Evoked Potentials with the Singularity Detection Technique. *IEEE Transaction on Biomedical Engineering*. 1997: 16; 155-160.
- [130] Zhao J, Xiao S. Classification of evoked potentials using wavelet coefficient features. *Proceedings of the 19th Annual International Conference of the IEEE/EMBS*. 1996: 4; 1496-1499.
- [131] Zheng Y, Tay D B H, Li L. Signal extraction and power spectrum estimation using wavelet transform scale space filtering and Bayes shrinkage *ELSEVIER Signal Proc.* 2000: 80; 1535-1549.
- [132] Zouridakis G, Jansen, B H, Boutros N N. A fuzzy clustering approach to EP estimation. *IEEE Transactions on Biomedical Engineering*. 1997: 44(8); 673-680.

VITA

The author was born in Samsun on 16 August 1971. She received her B.Sc degree in Electrical and Electronics Department from the University of Gazi, Ankara in 1993. She has been employed as a research assistant by the University of Ondokuz Mayıs in Samsun during the period 1994-1999. She worked on the model recognition and order reduction for two dimensional discrete-time systems. She received M.Sc degree from the same university in 1997. In 1999 she has joined the Electrical and Electronics Department of Middle East Technical University as a PhD student and a research assistant. Her areas of interest include signal processing, Wavelet Transform and applications, regularization techniques, model recognition for discrete-time systems.

Journal Papers

- Serap Aydın, Nevzat G. Gençer, Buyurman Baykal, Pekcan Ungan, Süha Yağcıoğlu *Comparison of Basic Linear Estimation Techniques in Extracting Template Auditory Evoked Potentials* ELSEVIER Journal of Clinical Neurophysiology (submitted)
- Serap Aydın, Nevzat G. Gençer, Buyurman Baykal *A Modified Scale Space Filter to extract single-sweep auditory EPs* ELSEVIER Journal of Clinical Neurophysiology (will be submitted)

Conference Papers

- Serap Aydın, Nevzat G. Gençer, Buyurman Baykal *Comparison of methods for extraction of evoked potentials* ,25th Annual International Conference of IEEE Engineering in Medicine and Biology Conference, pp. 2495-2498, September 2003.
- Serap Aydın, Nevzat G. Gençer, Buyurman Baykal *EB'den Uyarılmış potansiyellerin kestirimi için üç uyarlanıır süzgeç ile altuzay düzenleme yönteminin kıyaslanması* ,11th Sinyal İşleme ve İletişim Uygulamaları Kurultayı, 612-615, Haziran 2003, İstanbul

- Serap Aydın, Nevzat G. Gençer, Buyurman Baykal *Uyarılmas potansiyellerin elde edilmesinde altuzay yntemi ile birlestirilerek etkili kestirim sađlayan iki farklı Wiener süzgeç yaklaşımı*, 11th Sinyal İşleme ve İletişim Uygulamaları Kurultayı, 612-615, Haziran 2003, İstanbul
- Serap Aydın , Hatice Sezgin *İki Boyutlu Ayrılabilir Dizgeler İçin Model Tanıma ve İndirgeme Yöntemleri*, TOK-98 Otomatik Kontrol Ulusal Toplantısı, 15-16 Ekim 1998, İSTANBUL
- Melahat Toller, Elif Yapıcı, Serap Aydın, *Tempora Mandibular Eklem Seslerinin Bilgisayar Analiziyle Karşılaştırılması* Türk Oral ve Maksillofasial Cerrahi Derneđi 5th Uluslararası Bilimsel Kongresi (Turkish Association of Oral and Maxillofacial Surgeons 5th International Scientific Meeting), 27 Ekim - 3Kasım 1996, Antalya Türkiye

Thesis

- Serap Aydın, MSc Thesis, *İki Boyutlu Dizgelerde Temel Özellikler ve Ayrılabilir Dizgeler için Model Tanıma/indirgeme Yöntemleri* Department of Electrical and Electronics Engineering, University of Ondokuz Mayıs, September 1997.